

Transfer Matrices and Partition-Function Zeros for Antiferromagnetic Potts Models

V. Further Results for the Square-Lattice Chromatic Polynomial

Jesús Salas

Instituto Gregorio Millán

and

Grupo de Modelización, Simulación Numérica y Matemática Industrial

Universidad Carlos III de Madrid

Avda. de la Universidad, 30

28911 Leganés, SPAIN

JSALAS@MATH.UC3M.ES

Alan D. Sokal*

Department of Physics

New York University

4 Washington Place

New York, NY 10003 USA

SOKAL@NYU.EDU

November 9, 2007

revised February 6, 2009

Abstract

We derive some new structural results for the transfer matrix of square-lattice Potts models with free and cylindrical boundary conditions. In particular, we obtain explicit closed-form expressions for the dominant (at large $|q|$) diagonal entry in the transfer matrix, for arbitrary widths m , as the solution of a special one-dimensional polymer model. We also obtain the large- q expansion of the bulk and surface (resp. corner) free energies for the zero-temperature antiferromagnet (= chromatic polynomial) through order q^{-47} (resp. q^{-46}). Finally, we compute chromatic roots for strips of widths $9 \leq m \leq 12$ with free boundary conditions and locate roughly the limiting curves.

Key Words: Chromatic polynomial; chromatic root; antiferromagnetic Potts model; square lattice; transfer matrix; Fortuin–Kasteleyn representation; Beraha–Kahane–Weiss theorem; large- q expansion; one-dimensional polymer model; finite-lattice method.

*Also at Department of Mathematics, University College London, London WC1E 6BT, England.

Contents

1	Introduction	3
2	Preliminaries	4
2.1	Chromatic polynomials, Potts models, and all that	4
2.2	Transfer matrices	6
2.3	Beraha–Kahane–Weiss theorem	10
3	Structural properties of the square-lattice transfer matrix	11
3.1	General results	11
3.2	Free boundary conditions	14
3.3	Cylindrical boundary conditions	22
4	Large-q expansion of the leading eigenvalue	28
4.1	Overview of method and results	28
4.2	Free boundary conditions	30
4.3	Cylindrical boundary conditions	34
5	Thermodynamic limit ($m \rightarrow \infty$)	36
5.1	Generalities and finite-size-scaling theory	37
5.2	Large- q expansion for the bulk, surface and corner free energies . . .	41
5.3	Large- q expansion for the strip free energy: Free boundary conditions	46
5.4	Large- q expansion for the strip free energy: Cylindrical boundary conditions	47
5.5	Analysis of the large- q series	48
5.5.1	Differential approximants	48
5.5.2	Test cases: $m = 3_F$ and $m = 4_P$	50
5.5.3	Analysis of the series for the bulk, surface and corner free energies	52
6	Numerical results for widths $m = 9_F, 10_F, 11_F, 12_F$	57
6.1	Limiting curves and isolated limiting points	57
6.2	Value of $q_0(\text{sq})$	58
6.3	Real chromatic roots	60
7	Summary and open problems	61
A	Some combinatorial identities	63
A.1	Some preliminary lemmas	64
A.2	Proof of formula for $a_k^F(k - s)$	66
A.3	Proof of formula for $\tilde{a}_k^P(k - s)$	74
A.4	Proof of formula for $a_k^F(k)$	76
B	Upper zero-free interval for bipartite planar graphs	79

1 Introduction

The Potts model [1–4] on a regular lattice \mathcal{L} is characterized by two parameters: the number q of Potts spin states, and the nearest-neighbor coupling $v = e^{\beta J} - 1$.¹ Initially q is a positive integer and v is a real number in the interval $[-1, +\infty)$, but the Fortuin–Kasteleyn representation (reviewed in Section 2.1 below) shows that the partition function $Z_G(q, v)$ of the q -state Potts model on any finite graph G is in fact a *polynomial* in q and v . This allows us to interpret q and v as taking arbitrary real or even complex values, and to study the phase diagram of the Potts model in the real (q, v) -plane or in complex (q, v) -space.

According to the Yang–Lee picture of phase transitions [5], information about the possible loci of phase transitions can be obtained by investigating the zeros of the partition function for finite subsets of the lattice \mathcal{L} when one or more physical parameters (e.g. temperature or magnetic field) are allowed to take *complex* values; the accumulation points of these zeros in the infinite-volume limit constitute the (possible) phase boundaries. For the Potts model, therefore, by studying the zeros of $Z_G(q, v)$ in complex (q, v) -space for larger and larger pieces of the lattice \mathcal{L} , we can learn about the phase diagram of the Potts model in the real (q, v) -plane and more generally in complex (q, v) -space.

The partition function for $m \times n$ lattices can be efficiently computed using *transfer matrices*. Though the dimension of the transfer matrix (and thus the computational complexity) grows exponentially in the width m — thereby restricting us in practice to widths $m \lesssim 10$ – 30 — it is straightforward, by iterating the transfer matrix, to handle quite large lengths n . Indeed, by implementing the transfer-matrix method *symbolically* (i.e., as polynomials in q and/or v) and using the Beraha–Kahane–Weiss theorem (reviewed in Section 2.3), we can handle directly the limit $n \rightarrow \infty$ and compute the limiting curves \mathcal{B}_m of partition-function zeros. At a second stage we attempt to extrapolate these curves to $m = \infty$.

Since the problem of computing the phase diagram in complex (q, v) -space is difficult, it has proven convenient to study first certain “slices” through (q, v) -space, in which one parameter is fixed (usually at a real value) while the remaining parameter is allowed to vary in the complex plane. One very interesting special case is the chromatic polynomial ($v = -1$), which corresponds to the zero-temperature limit of the Potts antiferromagnet ($\beta J = -\infty$). In previous papers [6–10] we have used symbolic transfer-matrix methods to study the square-lattice and triangular-lattice chromatic polynomials for free, cylindrical, cyclic and toroidal boundary conditions.^{2,3} In this

¹Here we are considering only the *isotropic* model, in which each nearest-neighbor edge is assigned the same coupling v . In a more refined analysis, one could put (for example) different couplings v_1, v_2 on the horizontal and vertical edges of the square lattice, different couplings v_1, v_2, v_3 on the three orientations of edges of the triangular or hexagonal lattice, etc.

²See also the bibliographies of [6–10] for reference to the important related works of Shrock and collaborators.

³We adopt Shrock’s [11] terminology for boundary conditions: free ($m_F \times n_F$), cylindrical ($m_P \times n_F$), cyclic ($m_F \times n_P$), toroidal ($m_P \times n_P$), Möbius ($m_F \times n_{TP}$) and Klein bottle ($m_P \times n_{TP}$). Here the

paper we provide some new structural results for the transfer matrices with free and cylindrical boundary conditions. (For simplicity we restrict attention to the square lattice, but the methods could easily be adapted to handle the triangular lattice.) In particular, we shall obtain explicit closed-form expressions for the dominant (at large $|q|$) diagonal entry in the transfer matrix, for arbitrary widths m , by solving a special one-dimensional polymer gas. We shall also obtain similar but weaker results for the dominant eigenvalue. Finally, we shall obtain the large- q expansion of the bulk free energy through order q^{-47} , extending by 11 terms the previous computation of Bakaev and Kabanovich [12], and the large- q expansions of the surface and corner free energies through orders q^{-47} and q^{-46} , respectively.

This paper is organized as follows: In Section 2 we review the Fortuin–Kasteleyn representation [13, 14] of the q -state Potts model, the basic facts about transfer matrices in this representation [6, 15], and the Beraha–Kahane–Weiss theorem [16–20]. In Section 3 we prove some new structural properties of the transfer matrix for a square-lattice strip of width m and free or cylindrical boundary conditions; in particular, we obtain closed-form expressions for the dominant entry of the transfer matrix, for arbitrary widths m . In Section 4 we study the large- q expansion of the leading eigenvalue of the transfer matrix; our results are similar to those obtained for the dominant entry, but less explicit. In Section 5 we study the limit $m \rightarrow \infty$ of the strip free energy; among other things, we compute the large- q expansions of the bulk, surface and corner free energies, and we carry out a differential-approximant analysis to locate the singularities of those free energies in the complex q -plane. In Section 6 we provide some additional information concerning the chromatic roots of strips of widths $9 \leq m \leq 12$ with free boundary conditions. Finally, in Section 7 we list some open problems for future research. In Appendix A we prove some identities arising in the study of the dominant transfer-matrix entry for both boundary conditions. In Appendix B we discuss a conjecture concerning the upper zero-free interval for real chromatic roots of bipartite planar graphs.

2 Preliminaries

In this section we review briefly some needed background on chromatic and Tutte polynomials (Section 2.1), transfer matrices (Section 2.2) and the Beraha–Kahane–Weiss theorem (Section 2.3).

2.1 Chromatic polynomials, Potts models, and all that

Let $G = (V, E)$ be a finite undirected graph, and let q be a positive integer. Then the **q -state Potts-model partition function** for the graph G is defined by the

first dimension (m) corresponds to the transverse (“short”) direction, while the second dimension (n) corresponds to the longitudinal (“long”) direction. The subscripts F, P and TP denote free, periodic and twisted-periodic boundary conditions, respectively.

Hamiltonian

$$H_{\text{Potts}}(\boldsymbol{\sigma}) = - \sum_{e=ij \in E} J_e \delta(\sigma_i, \sigma_j) , \quad (2.1)$$

where the spins $\boldsymbol{\sigma} = \{\sigma_i\}_{i \in V}$ take values in $\{1, 2, \dots, q\}$, the J_e are coupling constants, and the δ is the Kronecker delta

$$\delta(a, b) = \begin{cases} 1 & \text{if } a = b \\ 0 & \text{if } a \neq b \end{cases} \quad (2.2)$$

The partition function can then be written as

$$Z_G^{\text{Potts}}(q, \mathbf{v}) = \sum_{\sigma: V \rightarrow \{1, 2, \dots, q\}} \prod_{e=ij \in E} [1 + v_e \delta(\sigma_i, \sigma_j)] , \quad (2.3)$$

where $v_e = e^{\beta J_e} - 1$. Please note, in particular, that if we set $v_e = -1$ for all edges e , then Z_G^{Potts} gives weight 1 to each proper coloring and weight 0 to each improper coloring, and so counts the proper colorings. Proper q -colorings ($v_e = -1$) thus correspond to the zero-temperature ($\beta \rightarrow +\infty$) limit of the antiferromagnetic ($J_e < 0$) Potts model.

It is far from obvious that $Z_G^{\text{Potts}}(q, \mathbf{v})$, which is defined separately for each positive integer q , is in fact the restriction to $q \in \mathbb{Z}_+$ of a *polynomial* in q . But this is in fact the case, and indeed we have:

Theorem 2.1 (Fortuin–Kasteleyn [13, 14] representation of the Potts model)

For integer $q \geq 1$,

$$Z_G^{\text{Potts}}(q, \mathbf{v}) = \sum_{A \subseteq E} q^{k(A)} \prod_{e \in A} v_e , \quad (2.4)$$

where $k(A)$ denotes the number of connected components in the subgraph (V, A) .

PROOF. In (2.3), expand out the product over $e \in E$, and let $A \subseteq E$ be the set of edges for which the term $v_e \delta(\sigma_i, \sigma_j)$ is taken. Now perform the sum over maps $\sigma: V \rightarrow \{1, 2, \dots, q\}$: in each component of the subgraph (V, A) the color σ_i must be constant, and there are no other constraints. We immediately obtain (2.4). \square

Historical Remark. The subgraph expansion (2.4) was discovered by Birkhoff [21] and Whitney [22] for the special case $v_e = -1$ (see also Tutte [23, 24]); in its general form it is due to Fortuin and Kasteleyn [13, 14] (see also [25]).

The foregoing considerations motivate defining the **multivariate Tutte polynomial** of the graph G :

$$Z_G(q, \mathbf{v}) = \sum_{A \subseteq E} q^{k(A)} \prod_{e \in A} v_e , \quad (2.5)$$

where q and $\mathbf{v} = \{v_e\}_{e \in E}$ are commuting indeterminates. If we set all the edge weights v_e equal to the same value v , we obtain a two-variable polynomial that is equivalent to

the standard Tutte polynomial $T_G(x, y)$ after a simple change of variables (see [26]). If we set all the edge weights v_e equal to -1 , we obtain the **chromatic polynomial** $P_G(q) = Z_G(q, -1)$.

Further information on the multivariate Tutte polynomial $Z_G(q, \mathbf{v})$ can be found in a recent survey article [26].

2.2 Transfer matrices

For any family of graphs $G_n = (V_n, E_n)$ consisting of n identical “layers” with identical connections between adjacent layers, the multivariate Tutte polynomials of the G_n (with edge weights likewise repeated from layer to layer) can be written in terms of a transfer matrix [6, 15]. Here we briefly summarize the needed formalism [6] specialized to the case of an $m \times n$ square lattice with free and cylindrical boundary conditions. As usual, free (resp. cylindrical) boundary conditions means free (resp. periodic) boundary conditions in the transverse (“short”) direction and free boundary conditions in the longitudinal (“long”) direction. These lattices are denoted by $m_F \times n_F$ and $m_P \times n_F$, respectively.

Consider the $m \times n$ square grid with edge weights $v_{i,i+1}$ on the horizontal edges ($1 \leq i \leq m$) and v_i on the vertical edges ($1 \leq i \leq m$). Site $m+1$ is always to be understood as a synonym for site 1. If the weight $v_{m,m+1} \equiv v_{m,1}$ is zero (resp. nonzero) we are considering free (resp. periodic) transverse boundary conditions.

We fix the “width” m and consider the family of graphs G_n obtained by varying the “length” n ; our goal is to calculate the multivariate Tutte polynomials $Z_{G_n}(q, \mathbf{v})$ for this family by building up the graph G_n layer by layer. What makes this a bit tricky is the nonlocality of the factor $q^{k(A)}$ in (2.5). At the end we will need to know the number of connected components in the subgraph (V_n, A) ; in order to be able to compute this, we shall keep track, as we go along, of which sites in the current “top” layer are connected to which other sites in that layer by a path of occupied edges (i.e. edges of A) in lower layers. Thus, we shall work in the basis of connectivities of the top layer, whose basis elements $\mathbf{e}_{\mathcal{P}}$ are indexed by partitions \mathcal{P} of the single-layer vertex set $\{1, \dots, m\}$. The elementary operators we shall need are:

- The *join operators*

$$J_{ij} \mathbf{e}_{\mathcal{P}} = \mathbf{e}_{\mathcal{P} \bullet ij}, \quad (2.6)$$

where $\mathcal{P} \bullet ij$ is the partition obtained from \mathcal{P} by amalgamating the blocks containing i and j (if they were not already in the same block). Note that all these operators commute.

- The *detach operators*

$$D_i \mathbf{e}_{\mathcal{P}} = \begin{cases} \mathbf{e}_{\mathcal{P} \setminus i} & \text{if } \{i\} \notin \mathcal{P} \\ q \mathbf{e}_{\mathcal{P}} & \text{if } \{i\} \in \mathcal{P} \end{cases} \quad (2.7)$$

where $\mathcal{P} \setminus i$ is the partition obtained from \mathcal{P} by detaching i from its block (and thus making it a singleton). Note that these operators commute as well.

Note, finally, that D_k commutes with J_{ij} whenever $k \notin \{i, j\}$.

The horizontal transfer matrix, which adds a row of horizontal edges, depends on the boundary conditions, and is given by

$$H_F = \prod_{i=1}^{m-1} (1 + v_{i,i+1} J_{i,i+1}) \quad (2.8a)$$

$$H_P = (1 + v_{m,1} J_{m,1}) H_F \quad (2.8b)$$

(note that all the operators in both products commute). The vertical transfer matrix, which adds a new row of sites along with the corresponding vertical edges, is

$$V = \prod_{i=1}^m (v_i I + D_i) \quad (2.9)$$

(note once again that all the operators commute). The multivariate Tutte polynomial for G_n is then given [6] by the formula

$$Z_{G_n}(q, \mathbf{v}) = \boldsymbol{\omega}^T H(VH)^{n-1} \mathbf{e}_{\text{id}} , \quad (2.10)$$

where “id” denotes the partition in which each site $i \in \{1, \dots, m\}$ is a singleton, and the “end vector” $\boldsymbol{\omega}^T$ is defined by

$$\boldsymbol{\omega}^T \mathbf{e}_{\mathcal{P}} = q^{|\mathcal{P}|} . \quad (2.11)$$

The transfer matrix is thus

$$T = VH . \quad (2.12)$$

In principle we are working here in the space spanned by the basis vectors $\mathbf{e}_{\mathcal{P}}$ for all partitions \mathcal{P} of $\{1, \dots, m\}$; the dimension of this space is given by the Bell number B_m [27–30]. However, it is easy to see, on topological grounds (thanks to the planarity of the G_n), that only *non-crossing* partitions can arise. (A partition is said to be *non-crossing* if $a < b < c < d$ with a, c in the same block and b, d in the same block imply that a, b, c, d are all in the same block.) The number of non-crossing partitions of $\{1, \dots, m\}$ is given by the Catalan number [28, 30]

$$C_m = \frac{(2m)!}{m!(m+1)!} = \frac{1}{m+1} \binom{2m}{m} . \quad (2.13)$$

When the horizontal couplings $v_{i,i+1}$ are all equal to 0 or -1 (which is the case for the chromatic polynomial with either free or periodic transverse boundary conditions), then the horizontal operator H is a *projection* (i.e., $H^2 = H$), so that our vector space \mathcal{V} splits up as a direct sum $\mathcal{V} = \mathcal{V}_0 \oplus \mathcal{V}_1$, where $Hv = 0$ for $v \in \mathcal{V}_0$ and $Hv = v$ for $v \in \mathcal{V}_1$. Then every vector $v \in \mathcal{V}_0$ is an eigenvector of $T = VH$ with eigenvalue 0; and for each eigenpair (λ, v) of $T = VH$ with $v \notin \mathcal{V}_0$, the pair (λ, Hv) is an eigenpair of $T' = HVH$. In this situation, therefore, we can work in the smaller vector space \mathcal{V}_1 by using the modified transfer matrix $T' = HVH$ in place of $T = VH$, and using the basis vectors

$$\mathbf{f}_{\mathcal{P}} = H\mathbf{e}_{\mathcal{P}} \quad (2.14)$$

in place of $\mathbf{e}_{\mathcal{P}}$. Indeed, if $\mathbf{T}\mathbf{e}_{\mathcal{P}} = \sum_{\mathcal{P}'} t_{\mathcal{P}\mathcal{P}'} \mathbf{e}_{\mathcal{P}'}$, then $\mathbf{T}'\mathbf{f}_{\mathcal{P}} = \sum_{\mathcal{P}'} t_{\mathcal{P}\mathcal{P}'} \mathbf{f}_{\mathcal{P}'}$, as is easily seen by applying \mathbf{H} to both sides and using $\mathbf{H}^2 = \mathbf{H}$. Please note that $\mathbf{f}_{\mathcal{P}} = 0$ if \mathcal{P} has any pair of nearest neighbors in the same block. We thus work in the space spanned by the basis vectors $\mathbf{f}_{\mathcal{P}}$ where \mathcal{P} is a non-crossing non-nearest-neighbor partition of $\{1, \dots, m\}$. The dimensionality of this space depends on the transverse boundary conditions:

- *Free transverse boundary conditions:* The number of non-crossing non-nearest-neighbor partitions of $\{1, \dots, m\}$ is given [31, Proposition 3.6] [32] by the Motzkin number M_{m-1} , where [28, 30, 33–36]⁴

$$M_n = \sum_{j=0}^{\lfloor n/2 \rfloor} \binom{n}{2j} C_j. \quad (2.15)$$

- *Periodic transverse boundary conditions:* The number of non-crossing non-nearest-neighbor partitions of $\{1, \dots, m\}$ when it is considered periodically (i.e. when 1 and m also are considered to be nearest neighbors) is given by [36, Section 3.2, family R2]

$$d_m = \begin{cases} 1 & \text{for } m = 1 \\ R_m & \text{for } m \geq 2 \end{cases} \quad (2.16)$$

where the *Riordan numbers* (or Motzkin alternating sums) R_m [33, 34, 36]⁵ are defined by $R_0 = 1$, $R_1 = 0$ and

$$R_m = \sum_{k=0}^{m-1} (-1)^{m-k-1} M_k \quad \text{for } m \geq 2 \quad (2.17)$$

Finally, spatial symmetries further restrict the subspace whenever the couplings $v_{i,i+1}$ and v_i are invariant under the symmetry. Again the symmetries depend on the transverse boundary conditions:

- *Free transverse boundary conditions:* Here the relevant symmetry is reflection in the center line of the strip. For reflection-invariant couplings, we can work in the space of equivalence classes of non-crossing non-nearest-neighbor partitions modulo reflection. The dimension $\text{SqFree}(m)$ of the transfer matrix is then given by the number of these equivalence classes. The exact expression for $\text{SqFree}(m)$ was obtained in [37, Theorem 2]:

$$\text{SqFree}(m) = \frac{1}{2} M_{m-1} + \frac{(m'-1)!}{2} \sum_{j=0}^{\lfloor m'/2 \rfloor} \frac{m' - j}{(j!)^2 (m' - 2j)!} \quad (2.18)$$

⁴ *Warning:* Several references use the notation m_n to denote what we call M_n ; and one reference [34] writes M_n to denote a *different* sequence.

⁵ In most of the literature (e.g. [33, 34]) these numbers are called γ_m . We have adopted the recent proposal of Bernhart [36] to name them after Riordan [33] and denote them R_m .

where

$$m' = \left\lfloor \frac{m+1}{2} \right\rfloor \quad (2.19)$$

and $\lfloor p \rfloor$ stands for the largest integer $\leq p$.⁶ The asymptotic behavior of $\text{SqFree}(m)$ is given by [37, Corollary 1]

$$\text{SqFree}(m) \sim \frac{\sqrt{3}}{4\sqrt{\pi}} 3^m m^{-3/2} \left[1 + O\left(\frac{1}{m}\right) \right] \quad \text{as } m \rightarrow \infty \quad (2.20)$$

- *Periodic transverse boundary conditions:* For the square lattice with periodic transverse boundary conditions, both reflections and translations are symmetries. We therefore define equivalence classes of non-crossing non-nearest-neighbor partitions modulo reflections and translations and the corresponding number $\text{SqCyl}(m)$ of equivalence classes. To our knowledge there is no known closed form for these numbers; but there is a conjectured formula [39, Conjecture 2.2]

$$\text{SqCyl}(m) = \begin{cases} \frac{1}{2} [\text{TriCyl}(m) + \frac{1}{2} N_{\text{FP}}(\frac{m}{2})] & \text{for even } m \\ \frac{1}{2} [\text{TriCyl}(m) + \frac{1}{4} N_{\text{FP}}(\frac{m+1}{2}) - \frac{1}{2} R_{\frac{m-1}{2}}] & \text{for odd } m \geq 3 \end{cases} \quad (2.21)$$

where $N_{\text{FP}}(m)$ is the number of different eigenvalues for a strip of either square or triangular lattice with cyclic boundary conditions (i.e., free transverse and periodic longitudinal boundary conditions), and $\text{TriCyl}(m)$ is the number of equivalence classes of non-crossing non-nearest-neighbor partitions modulo translations. It is known [40] that

$$N_{\text{FP}}(m) = 2(m-1)! \sum_{j=0}^{\lfloor m/2 \rfloor} \frac{(m-j)}{(j!)^2 (m-2j)!} \cdot \quad (2.22)$$

It is conjectured [39, Conjecture 2.1] that

$$\text{TriCyl}(m) = \frac{1}{m} \left[d_m + \sum_{d|m; 1 \leq d < m} \phi(m/d) t_d \right] \quad (2.23)$$

where t_d is the coefficient of z^d in the expansion of $(1+z+z^2)^d$, i.e., the central trinomial coefficient (given as sequence A002426 in [30]), and $\phi(x)$ is Euler's totient function.

The values of all these dimensions for $m \leq 16$ are displayed in Table 2 of Ref. [6].

⁶We have recently rederived this formula using a different method [38].

2.3 Beraha–Kahane–Weiss theorem

A central role in our work is played by a theorem on analytic functions due to Beraha, Kahane and Weiss [16–19] and generalized slightly by one of us [20]. The situation is as follows: Let D be a domain (connected open set) in the complex plane, and let $\alpha_1, \dots, \alpha_M, \lambda_1, \dots, \lambda_M$ ($M \geq 2$) be analytic functions on D , none of which is identically zero. For each integer $n \geq 0$, define

$$f_n(z) = \sum_{k=1}^M \alpha_k(z) \lambda_k(z)^n . \quad (2.24)$$

We are interested in the zero sets

$$\mathcal{Z}(f_n) = \{z \in D : f_n(z) = 0\} \quad (2.25)$$

and in particular in their limit sets as $n \rightarrow \infty$:

$$\liminf \mathcal{Z}(f_n) = \{z \in D : \text{every neighborhood } U \ni z \text{ has a nonempty intersection with all but finitely many of the sets } \mathcal{Z}(f_n)\} \quad (2.26)$$

$$\limsup \mathcal{Z}(f_n) = \{z \in D : \text{every neighborhood } U \ni z \text{ has a nonempty intersection with infinitely many of the sets } \mathcal{Z}(f_n)\} \quad (2.27)$$

Let us call an index k *dominant at z* if $|\lambda_k(z)| \geq |\lambda_l(z)|$ for all l ($1 \leq l \leq M$); and let us write

$$D_k = \{z \in D : k \text{ is dominant at } z\} . \quad (2.28)$$

Then the limiting zero sets can be completely characterized as follows:

Theorem 2.2 [16–20] *Let D be a domain in \mathbb{C} , and let $\alpha_1, \dots, \alpha_M, \lambda_1, \dots, \lambda_M$ ($M \geq 2$) be analytic functions on D , none of which is identically zero. Let us further assume a “no-degenerate-dominance” condition: there do not exist indices $k \neq k'$ such that $\lambda_k \equiv \omega \lambda_{k'}$ for some constant ω with $|\omega| = 1$ and such that $D_k (= D_{k'})$ has nonempty interior. For each integer $n \geq 0$, define f_n by*

$$f_n(z) = \sum_{k=1}^M \alpha_k(z) \lambda_k(z)^n .$$

Then $\liminf \mathcal{Z}(f_n) = \limsup \mathcal{Z}(f_n)$, and a point z lies in this set if and only if either

- (a) There is a unique dominant index k at z , and $\alpha_k(z) = 0$; or*
- (b) There are two or more dominant indices at z .*

Note that case (a) consists of isolated points in D , while case (b) consists of curves (plus possibly isolated points where all the λ_k vanish simultaneously). Henceforth we shall denote by \mathcal{B} the locus of points satisfying condition (b).

We shall often refer to the functions λ_k as “eigenvalues”, because that is how they arise in the transfer-matrix formalism.

3 Structural properties of the square-lattice transfer matrix

In this section we prove some structural results concerning the transfer matrices of square-lattice Potts models (and in particular chromatic polynomials) with free or cylindrical boundary conditions. We begin by proving some general results (Section 3.1) concerning the polynomial dependence in q of the transfer-matrix entries and the large- q behavior of the eigenvalues. Then we provide explicit closed-form expressions for the dominant diagonal entry of the transfer matrix with free or cylindrical boundary conditions (Sections 3.2 and 3.3).

3.1 General results

Let us begin by considering the case of the full Potts-model partition function. Indeed, we can be quite a bit more general, and consider any transfer matrix built out of operators of the form

$$\mathbf{H} = \sum_{A \subseteq \{1, \dots, m\}} c_A \prod_{i \in A} \mathbf{J}_{i, i+1} \quad (3.1a)$$

$$\mathbf{V} = \sum_{B \subseteq \{1, \dots, m\}} d_B \prod_{i \in B} \mathbf{D}_i \quad (3.1b)$$

with arbitrary coefficients $\{c_A\}$ and $\{d_B\}$. (Recall that site $m+1$ is to be understood as a synonym for site 1.) This general form includes as particular cases the square-lattice transfer matrix with free or cylindrical boundary conditions and arbitrary couplings $\{v_{i, i+1}\}$ and $\{v_i\}$.

Let us now recall that “id” denotes the partition of $\{1, \dots, m\}$ in which each element is a singleton (i.e., $\{\{1\}, \{2\}, \dots, \{m\}\}$). Let us call a partition \mathcal{P} of $\{1, \dots, m\}$ *non-trivial* if it is not “id”.

Proposition 3.1 *For any operators \mathbf{H} and \mathbf{V} of the form (3.1), where the coefficients $\{c_A\}$ and $\{d_B\}$ are numbers (i.e., independent of q), the diagonal entry $t_{\text{id}}(m)$ of the transfer matrix $\mathbf{T}(m) = \mathbf{V}\mathbf{H}$ associated to the basis element \mathbf{e}_{id} is a polynomial in q of degree at most m , of the form*

$$t_{\text{id}} = c_{\emptyset} d_{\{1, \dots, m\}} q^m + \text{terms of order at most } q^{m-1}. \quad (3.2)$$

All other entries of the transfer matrix $\mathbf{T}(m)$ are polynomials in q of degree at most $m-1$.

Remark. If \mathbf{H} is a projection, then the diagonal entry $t'_{\text{id}}(m)$ of the modified transfer matrix $\mathbf{T}'(m) = \mathbf{H}\mathbf{V}\mathbf{H}$ associated to the basis element $\mathbf{f}_{\text{id}} = \mathbf{H}\mathbf{e}_{\text{id}}$ is given by $t'_{\text{id}} = t_{\text{id}}$; indeed, *all* the entries of $\mathbf{T}'(m)$ are equal to the corresponding entries of $\mathbf{T}(m)$. This follows immediately from the fact that $\mathbf{T}\mathbf{e}_{\mathcal{P}} = \sum_{\mathcal{P}'} t_{\mathcal{P}\mathcal{P}'} \mathbf{e}_{\mathcal{P}'}$ implies $\mathbf{T}'\mathbf{f}_{\mathcal{P}} = \sum_{\mathcal{P}'} t_{\mathcal{P}\mathcal{P}'} \mathbf{f}_{\mathcal{P}'}$.

PROOF OF PROPOSITION 3.1. First of all, it is obvious that each entry in the transfer matrix $\mathsf{T}(m)$ is a polynomial in q . Indeed, from (2.7)/(2.9) it is clear that we get a factor of q every time we apply the operator D_i to a partition in which i is a singleton. We can *maximize* the number of factors of q by applying the vertical transfer matrix V to the vector \mathbf{e}_{id} that corresponds to the partition in which every site is a singleton. In particular, from (3.1b) we have

$$\mathsf{V}\mathbf{e}_{\text{id}} = \sum_{B \subseteq \{1, \dots, m\}} d_B q^{|B|} \mathbf{e}_{\text{id}} \quad (3.3a)$$

$$= (d_{\{1, \dots, m\}} q^m + \text{terms of order at most } q^{m-1}) \mathbf{e}_{\text{id}} . \quad (3.3b)$$

If we apply the vertical transfer matrix to any other partition, we get a polynomial in q of degree at most $m - 1$.

Let us now consider the quantity $\mathsf{H}\mathbf{e}_{\text{id}}$:

$$\mathsf{H}\mathbf{e}_{\text{id}} = \sum_{A \subseteq \{1, \dots, m\}} c_A \left(\prod_{i \in A} \mathsf{J}_{i, i+1} \right) \mathbf{e}_{\text{id}} \quad (3.4a)$$

$$= c_{\emptyset} \mathbf{e}_{\text{id}} + \sum_{\mathcal{P} \text{ non-trivial}} a_{\mathcal{P}} \mathbf{e}_{\mathcal{P}} , \quad (3.4b)$$

for some quantities $a_{\mathcal{P}}$ that are polynomials in $\{c_A\}$ (and of course independent of q). Using (3.3)/(3.4) it is obvious that

$$\mathsf{V}\mathsf{H}\mathbf{e}_{\text{id}} = c_{\emptyset} \sum_{B \subseteq \{1, \dots, m\}} d_B q^{|B|} \mathbf{e}_{\text{id}} + \sum_{\mathcal{P}} a'_{\mathcal{P}}(q) \mathbf{e}_{\mathcal{P}} , \quad (3.5)$$

where the coefficients $a'_{\mathcal{P}}(q)$ are polynomials in q of degree at most $m - 1$. \square

In view of Proposition 3.1, we shall henceforth refer to t_{id} (or t'_{id}) as the “dominant diagonal entry” in the transfer matrix, as it is indeed dominant at large $|q|$. Furthermore, we can deduce from Proposition 3.1 the leading large- $|q|$ behavior of the eigenvalues. We begin with a simple perturbation lemma:

Lemma 3.2 *Consider an $N \times N$ matrix $M(\xi) = (M_{ij}(\xi))_{i,j=1}^N$ whose entries are analytic functions of ξ in some disc $|\xi| < R$. Suppose that $M_{11} = 1$ and that $M_{ij} = O(\xi)$ for $(i, j) \neq (1, 1)$. Then, in some disc $|\xi| < R'$, $M(\xi)$ has a simple leading eigenvalue $\mu_{\star}(\xi)$ that is given by a convergent expansion*

$$\mu_{\star}(\xi) = 1 + \sum_{k=2}^{\infty} \alpha_k \xi^k \quad (3.6)$$

[note that $\alpha_1 = 0$] with associated eigenvector

$$\mathbf{v}_{\star}(\xi) = \mathbf{e}_1 + \sum_{k=1}^{\infty} \mathbf{v}_k \xi^k , \quad (3.7)$$

while all other eigenvalues are $O(\xi)$.

The key fact here is that the eigenvalue shift in (3.6) begins at order ξ^2 , not order ξ .

PROOF. We have

$$\det[\mu - M(\xi)] = (\mu - 1) \prod_{i=2}^N [\mu - M_{ii}(\xi)] + \xi^2 F(\mu, \xi), \quad (3.8)$$

where $F(\mu, \xi)$ is a polynomial in μ whose coefficients are analytic functions of ξ for $|\xi| < R$. The polynomial $P(\mu) = (\mu - 1) \prod_{i=2}^N [\mu - M_{ii}(\xi)]$ has, for all sufficiently small $|\xi|$, a simple root at $\mu = 1$ and roots (not necessarily simple) at $\mu = M_{ii}(\xi) = O(\xi)$. The simple root at $\mu = 1$ moves analytically [41] under the perturbation $\xi^2 F(\mu, \xi)$ — let us call this root $\mu_\star(\xi)$ — and so is given by the convergent expansion (3.6). The corresponding eigenvector also moves analytically under the perturbation $M(\xi) = \text{diag}(1, 0, \dots, 0) + O(\xi)$, which proves (3.7). To see that all other eigenvalues are $O(\xi)$, it suffices to consider the reduced matrix

$$M(\xi) - \mu_\star(\xi) \frac{\mathbf{v}_\star(\xi) \mathbf{v}_\star(\xi)^T}{\mathbf{v}_\star(\xi)^T \mathbf{v}_\star(\xi)} \quad (3.9)$$

and observe that all its entries are $O(\xi)$. \square

Remark. The “small” eigenvalues need not be analytic in ξ . For instance,

$$M(\xi) = \begin{pmatrix} 1 & 0 & 0 \\ 0 & 0 & \xi \\ 0 & \xi^2 & 0 \end{pmatrix} \quad (3.10)$$

has eigenvalues $\mu = 1$ and $\mu = \pm \xi^{3/2}$. \square

To apply Lemma 3.2 to our transfer matrix T , we set $\xi = q^{-1}$ and $M = \mathsf{T}/t_{\text{id}}$. We then have:

Corollary 3.3 *Consider operators H and V of the form (3.1) where the coefficients $\{c_A\}$ and $\{d_B\}$ are numbers (i.e., independent of q) and $c_{\emptyset d_{\{1, \dots, m\}}} \neq 0$. Then T has a simple eigenvalue λ_\star that is analytic for large $|q|$ and behaves there like $c_{\emptyset d_{\{1, \dots, m\}}} q^m$: more precisely, it has a convergent expansion*

$$\frac{\lambda_\star}{t_{\text{id}}} = 1 + \sum_{k=2}^{\infty} \alpha_k q^{-k} \quad (3.11)$$

[so that, in particular, $\lambda_\star - t_{\text{id}} = O(q^{m-2})$]. All other eigenvalues are $O(q^{m-1})$.

Let us now return to the case of main interest, in which H and V are the transfer matrices (2.8)/(2.9) for the chromatic polynomial $v_i = v_{i,j} = -1$. In this case we can sharpen (3.2) by providing explicit expressions for the lower-order terms. We must now distinguish between free and cylindrical boundary conditions, and we shall treat each case in a separate subsection.

3.2 Free boundary conditions

Let us consider a square-lattice grid of fixed width $m \geq 1$ and free boundary conditions. Let us also assume that all horizontal edges have weight v and all vertical edges have weight v' ; they need not be -1 . The horizontal transfer matrix (2.8a) is thus

$$\mathbf{H} = \prod_{i=1}^{m-1} (1 + v \mathbf{J}_{i,i+1}) \quad (3.12)$$

and the vertical transfer matrix is

$$\mathbf{V} = \prod_{i=1}^m (v' I + \mathbf{D}_i) . \quad (3.13)$$

Consider first the action of \mathbf{H} on the start vector \mathbf{e}_{id} . It generates 2^{m-1} terms, each of which corresponds to a partition \mathcal{P} in which all the blocks are sequential sets of vertices in $\{1, \dots, m\}$ (we shall call these sets “polymers”). Furthermore, each polymer of size ℓ picks up a factor $v^{\ell-1}$.

Consider next the action of \mathbf{V} on a basis vector $\mathbf{e}_{\mathcal{P}}$ corresponding to an arbitrary partition $\mathcal{P} = \{P_1, \dots, P_k\}$. If we are to end up with the partition \mathbf{e}_{id} , then for each block P_j we must either choose the delete operator \mathbf{D}_i for all $i \in P_j$ (the last deletion gives a factor q) or else choose the delete operator for all but one $i \in P_j$ and choose $v' I$ for the last site (this can be done in $|P_j|$ ways). We therefore have

$$\mathbf{V} \mathbf{e}_{\mathcal{P}} = \left[\prod_{j=1}^k (q + v' |P_j|) \right] \mathbf{e}_{\text{id}} + \text{other terms} \quad (3.14)$$

where “other terms” means terms involving $\mathbf{e}_{\mathcal{P}'}$ with $\mathcal{P}' \neq \text{id}$. We thus obtain a factor $q + \ell v'$ for each block of size $\ell = |P_j| \geq 1$.

Putting these facts together, we conclude that

$$\mathbf{V} \mathbf{H} \mathbf{e}_{\text{id}} = t_{\text{F}}(m) \mathbf{e}_{\text{id}} + \text{other terms} , \quad (3.15)$$

where $t_{\text{F}}(m)$ is the partition function for a one-dimensional m -site polymer gas (with free boundary conditions) in which each site must be occupied by exactly one polymer, and each polymer of length $\ell \geq 1$ gets a fugacity $\mu_{\ell} = v^{\ell-1}(q + \ell v')$, i.e.

$$t_{\text{F}}(m) = \sum_{k=1}^{\infty} \sum_{\substack{\ell_1, \dots, \ell_k \geq 1 \\ \ell_1 + \dots + \ell_k = m}} \prod_{j=1}^k v^{\ell_j-1} (q + \ell_j v') . \quad (3.16)$$

To solve this polymer model, let us introduce the generating function (“grand parti-

tion function")

$$\Phi_F(z) \equiv \sum_{m=1}^{\infty} z^m t_F(m) \quad (3.17a)$$

$$= \sum_{k=1}^{\infty} \sum_{\ell_1, \dots, \ell_k \geq 1} \prod_{j=1}^k z^{\ell_j} v^{\ell_j-1} (q + \ell_j v') \quad (3.17b)$$

$$= \frac{\Psi(z)}{1 - \Psi(z)} \quad (3.17c)$$

where

$$\Psi(z) \equiv \sum_{\ell=1}^{\infty} z^{\ell} v^{\ell-1} (q + \ell v') = z \left[\frac{q}{1 - zv} + \frac{v'}{(1 - zv)^2} \right] \quad (3.18)$$

is the total weight for a single polymer of arbitrary size. We therefore have

$$\Phi_F(z) = \frac{(q + v')z - qvz^2}{1 - (q + 2v + v')z + v(q + v)z^2} . \quad (3.19)$$

When $v = v' = -1$ this reduces to

$$\Phi_F(z) = \frac{(q - 1)z + qz^2}{1 - (q - 3)z - (q - 1)z^2} . \quad (3.20)$$

As a check we have expanded (3.20) in powers of z , and verified that it agrees with available dominant diagonal elements $t_F(m)$ for $1 \leq m \leq 12$ (see [6] for $m \leq 8$).

The next step is to get an explicit expression for $t_F(m)$. Using the notation $[z^m]P(z)$ for the m -th coefficient in a polynomial or power series, we have the alternate representations

$$[z^m] \frac{1}{1 - az - bz^2} = \sum_{j=0}^{\lfloor m/2 \rfloor} \binom{m-j}{j} a^{m-2j} b^j \quad (3.21a)$$

$$= 2^{-m} \sum_{j=0}^{\lfloor m/2 \rfloor} \binom{m+1}{2j+1} a^{m-2j} (a^2 + 4b)^j . \quad (3.21b)$$

The first of these comes directly from $[z^m] \sum_{k=0}^{\infty} (az + bz^2)^k$, while the second is obtained by factoring the quadratic and using partial fractions. Using (3.20) we have

$$t_F(m) = [z^m] \Phi_F(z) = (q - 1)[z^{m-1}] \frac{1}{1 - az - bz^2} + q[z^{m-2}] \frac{1}{1 - az - bz^2} \quad (3.22)$$

where $a = q - 3$ and $b = q - 1$. Inserting this into (3.21a) we have

$$\begin{aligned} t_F(m) &= \sum_{j=0}^{\lfloor (m-1)/2 \rfloor} \binom{m-1-j}{j} (q-3)^{m-1-2j} (q-1)^{j+1} \\ &\quad + q \sum_{j=0}^{\lfloor (m-2)/2 \rfloor} \binom{m-2-j}{j} (q-3)^{m-2-2j} (q-1)^j , \end{aligned} \quad (3.23)$$

which is manifestly a polynomial in q of degree at most m . Furthermore, the term of order q^m comes only from $j = 0$ in the first sum and has coefficient 1 (thereby confirming explicitly what we already knew from Proposition 3.1), so the degree is exactly m .

We may therefore write $t_F(m)$ explicitly as a polynomial in q with certain coefficients $a_k^F(m)$:

$$t_F(m) = \sum_{k=0}^m (-1)^k a_k^F(m) q^{m-k}. \quad (3.24)$$

The next step is to obtain a closed formula for the coefficients $a_k^F(m)$ with $m \geq 1$ and $0 \leq k \leq m$. We shall prove that, for each fixed $k \geq 0$, the coefficient $a_k^F(m)$ is in fact a *polynomial* in m of degree exactly k .⁷ We begin by expanding the binomials in (3.23):

$$a_k^F(m) \equiv (-1)^k [q^{m-k}] t_F(m) \quad (3.25a)$$

$$\begin{aligned} &= (-1)^k \sum_{j=0}^{\lfloor (m-1)/2 \rfloor} \sum_{\ell=0}^{\infty} \binom{m-1-j}{j} \binom{m-1-2j}{m-k-\ell} \binom{j+1}{\ell} (-3)^{k+\ell-1-2j} (-1)^{j+1-\ell} \\ &\quad + (-1)^k \sum_{j=0}^{\lfloor (m-2)/2 \rfloor} \sum_{\ell=0}^{\infty} \binom{m-2-j}{j} \binom{m-2-2j}{m-k-\ell-1} \binom{j}{\ell} (-3)^{k+\ell-1-2j} (-1)^{j-\ell} \end{aligned} \quad (3.25b)$$

$$\begin{aligned} &= \sum_{j=0}^{\lfloor (m-1)/2 \rfloor} \sum_{\ell=0}^{\infty} \binom{m-1-j}{j} \binom{m-1-2j}{k+\ell-1-2j} \binom{j+1}{\ell} (-1)^j 3^{k+\ell-1-2j} \\ &\quad - \sum_{j=0}^{\lfloor (m-2)/2 \rfloor} \sum_{\ell=0}^{\infty} \binom{m-2-j}{j} \binom{m-2-2j}{k+\ell-1-2j} \binom{j}{\ell} (-1)^j 3^{k+\ell-1-2j} \end{aligned} \quad (3.25c)$$

Let us consider the first sum in (3.25c):

$$\begin{aligned} S^{(1)}(m, k) &= \sum_{j=0}^{\lfloor (m-1)/2 \rfloor} \sum_{\ell=0}^{\infty} \binom{m-1-j}{j} \binom{m-1-2j}{k+\ell-1-2j} \binom{j+1}{\ell} (-1)^j 3^{k+\ell-1-2j} \\ &\equiv \sum_{j=0}^{\lfloor (m-1)/2 \rfloor} \sum_{\ell=0}^{\infty} S_{j,\ell}^{(1)}(m, k). \end{aligned} \quad (3.26)$$

The goal is to substitute $\sum_{j=0}^{\lfloor (m-1)/2 \rfloor}$ by something independent of m , e.g., $\sum_{j=0}^k$. Indeed, if $k = \lfloor (m-1)/2 \rfloor$, the identity is trivial. Let us consider next the case $k < \lfloor (m-1)/2 \rfloor$. Then, if we prove that the sum

$$\sum_{j=k+1}^{\lfloor (m-1)/2 \rfloor} S_{j,\ell}^{(1)}(m, k) = 0, \quad (3.27)$$

⁷More precisely, $a_k^F(m)$ is the restriction to integers $m \geq \max(k, 1)$ of such a polynomial.

then, we have not modified the result of (3.26) by changing the upper index in the sum over the variable j . The second binomial appearing in (3.26) vanishes whenever $k + \ell - 1 - 2j < 0$. On the other hand, the third binomial is *non-vanishing* only if $j \geq \ell - 1$. Therefore, if $j > k$ and $j \geq \ell - 1$, we have $k + \ell - 1 - 2j < k + \ell - 1 - k - (\ell - 1) = 0$. So, $S^{(1)}(m, k) = 0$ whenever $j > k$.⁸ Finally, let us consider the third case $k > \lfloor (m - 1)/2 \rfloor$. Then, by making this change in the upper index in the sum over j , we are adding some extra terms

$$\sum_{j=\lfloor (m-1)/2 \rfloor + 1}^k S_{j,\ell}^{(1)}(m, k). \quad (3.28)$$

In this case we have to focus on the first binomial of (3.26). This binomial is nonzero only when $0 \leq j \leq \lfloor (m - 1)/2 \rfloor$ or when $j \geq m$. The first of these do not appear in (3.28); and since $m \geq k$, the second appears only when $j = k = m$. The contribution of this extra term is 1. Thus, (3.26) reduces to

$$S^{(1)}(m, k) = \sum_{j=0}^k \sum_{\ell=0}^{\infty} \binom{m-1-j}{j} \binom{m-1-2j}{k+\ell-1-2j} \binom{j+1}{\ell} (-1)^j 3^{k+\ell-1-2j} - \delta_{km}. \quad (3.29)$$

Let us now consider the second sum in (3.25c):

$$\begin{aligned} S^{(2)}(m, k) &= \sum_{j=0}^{\lfloor (m-2)/2 \rfloor} \sum_{\ell=0}^{\infty} \binom{m-2-j}{j} \binom{m-2-2j}{k+\ell-1-2j} \binom{j}{\ell} (-1)^j 3^{k+\ell-1-2j} \\ &\equiv \sum_{j=0}^{\lfloor (m-2)/2 \rfloor} \sum_{\ell=0}^{\infty} S_{j,\ell}^{(2)}(m, k). \end{aligned} \quad (3.30)$$

The goal is now to substitute $\sum_{j=0}^{\lfloor (m-2)/2 \rfloor}$ by $\sum_{j=0}^{k-1}$. As before, the case $k - 1 = \lfloor (m - 2)/2 \rfloor$ is trivial. Let us now suppose that $k - 1 < \lfloor (m - 2)/2 \rfloor$. Then, the second binomial vanishes whenever $k + \ell - 1 - 2j < 0$, the third binomial is *non-vanishing* only if $j \geq \ell$. Therefore for $j > k - 1$ and $j \geq \ell$ we have $k + \ell - 1 - 2j < k + \ell - 1 - (k - 1) - \ell = 0$. So $S_{j,\ell}^{(2)}(m, k) = 0$ whenever $j > k - 1$. Let us finally consider the third case $k - 1 > \lfloor (m - 2)/2 \rfloor$. Then, we should consider the extra terms

$$\sum_{j=\lfloor (m-2)/2 \rfloor + 1}^{k-1} S_{j,\ell}^{(2)}(m, k). \quad (3.31)$$

In this case we have to focus on the first binomial of (3.30). This binomial is nonzero only when $0 \leq j \leq \lfloor (m - 2)/2 \rfloor$ or when $j \geq m - 1$. The first of these do not appear in (3.31); and since $m \geq k$, the second appears only when $j = k - 1 = m - 1$. The

⁸This is true even if m is treated as an algebraic indeterminate.

contribution of this extra term is again 1. Thus, (3.30) reduces to

$$S^{(2)}(m, k) = \sum_{j=0}^{k-1} \sum_{\ell=0}^{\infty} \binom{m-2-j}{j} \binom{m-2-2j}{k+\ell-1-2j} \binom{j}{\ell} (-1)^j 3^{k+\ell-1-2j} - \delta_{km} . \quad (3.32)$$

Putting together (3.29)/(3.32), we find that the two contributions δ_{km} cancel exactly, and that (3.25c) can be written as

$$\begin{aligned} a_k^F(m) &= \sum_{j=0}^k \sum_{\ell=0}^{j+1} \binom{m-1-j}{j} \binom{m-1-2j}{k+\ell-1-2j} \binom{j+1}{\ell} (-1)^j 3^{k+\ell-1-2j} \\ &\quad - \sum_{j=0}^{k-1} \sum_{\ell=0}^j \binom{m-2-j}{j} \binom{m-2-2j}{k+\ell-1-2j} \binom{j}{\ell} (-1)^j 3^{k+\ell-1-2j} , \end{aligned} \quad (3.33)$$

where the independent variable m does not appear in the summation limits. After some straightforward but lengthy algebra we can rewrite the above formula in the more compact form

$$\begin{aligned} a_k^F(m) &= \sum_{p=0}^k (-1)^p \binom{m-1-p}{p} \sum_{r=0}^{k-p} 3^r \binom{m-1-2p}{r} \binom{p+1}{k-p-r} \\ &\quad + \sum_{p=1}^k (-1)^p \binom{m-1-p}{p-1} \sum_{r=0}^{k-p} 3^r \binom{m-2p}{r} \binom{p-1}{k-p-r} . \end{aligned} \quad (3.34)$$

From (3.33) or (3.34) we see that $a_k^F(m)$ is (the restriction of) a polynomial in m of degree at most k , as m appears only in the upper index of the binomials and

$$\binom{m}{j} = \frac{m^{\underline{j}}}{j!} = \frac{m(m-1)(m-2)\cdots(m-j+1)}{j!} \quad (3.35)$$

is a polynomial in m of degree j . [Here and in what follows, we use Knuth's [42] notation for falling powers: $x^{\underline{j}} = x(x-1)(x-2)\cdots(x-j+1)$.]

The degree of the polynomial $a_k^F(m)$ is in fact exactly k . To see this, let us extract the term of order m^k from (3.34). The second sum in (3.34) does not contribute, as it is a polynomial in m of order at most $k-1$; the only contribution comes from the first sum:

$$[m^k] a_k^F(m) = \sum_{p=0}^k \frac{(-1)^p 3^{k-p}}{p!(k-p)!} = \frac{2^k}{k!} \neq 0 . \quad (3.36)$$

We can summarize all this into the following proposition:

Proposition 3.4 *Let \mathbf{H} and \mathbf{V} be the transfer matrices (2.8a)/(2.9) for the chromatic polynomial $v_i = v_{i,i+1} = -1$ with free boundary conditions. Then the dominant diagonal entry in the transfer matrix can be written as*

$$t_F(m) = \sum_{k=0}^m (-1)^k a_k^F(m) q^{m-k} \quad (3.37)$$

where each $a_k^F(m)$ is a polynomial in m of degree k given by (3.34).

For the first few values of k , we obtain

$$a_0^F(m) = 1 \quad (3.38a)$$

$$a_1^F(m) = 2m - 1 \quad (3.38b)$$

$$a_2^F(m) = 2m^2 - 3m + 1 \quad (3.38c)$$

$$a_3^F(m) = \frac{4}{3}m^3 - 4m^2 + \frac{8}{3}m \quad (3.38d)$$

$$a_4^F(m) = \frac{2}{3}m^4 - \frac{10}{3}m^3 + \frac{23}{6}m^2 + \frac{5}{6}m - 1 \quad (3.38e)$$

$$a_5^F(m) = \frac{4}{15}m^5 - 2m^4 + \frac{11}{3}m^3 + \frac{3}{2}m^2 - \frac{133}{30}m - 2 \quad (3.38f)$$

$$a_6^F(m) = \frac{4}{45}m^6 - \frac{14}{15}m^5 + \frac{23}{9}m^4 + \frac{7}{6}m^3 - \frac{733}{90}m^2 - \frac{71}{15}m + 12 \quad (3.38g)$$

We can also prove the following result concerning the polynomials $a_k^F(m)$:⁹

Proposition 3.5 *For each integer $s \geq 1$, the quantity*

$$\begin{aligned} a_k^F(k-s) &= \sum_{p=0}^k (-1)^p \binom{k-s-1-p}{p} \sum_{r=0}^{k-p} 3^r \binom{k-s-1-2p}{r} \binom{p+1}{k-p-r} \\ &\quad + \sum_{p=1}^k (-1)^p \binom{k-s-1-p}{p-1} \sum_{r=0}^{k-p} 3^r \binom{k-s-2p}{r} \binom{p-1}{k-p-r} \end{aligned} \quad (3.39)$$

is, when restricted to $k \geq s+1$, given by a polynomial in k of degree $\max(0, s-3)$, with leading coefficient

$$[k^{s-3}]a_k^F(k-s) = \frac{(-1)^{s+1}}{(s-3)!} \quad \text{for } s \geq 3 \quad (3.40)$$

and first subleading coefficient

$$[k^{s-4}]a_k^F(k-s) = \frac{(-1)^s s}{2(s-4)!} \quad \text{for } s \geq 4. \quad (3.41)$$

The proof of this Proposition can be found in Appendix A.2. For the first values

⁹This Proposition refers, however, to the regime $m < k$ that does not contribute to the sum (3.37).

of s , we have

$$a_k^F(k-1) = 0 \quad \text{for } k \geq 2 \quad (3.42a)$$

$$a_k^F(k-2) = 0 \quad \text{for } k \geq 3 \quad (3.42b)$$

$$a_k^F(k-3) = 1 \quad \text{for } k \geq 4 \quad (3.42c)$$

$$a_k^F(k-4) = -(k-2) \quad \text{for } k \geq 5 \quad (3.42d)$$

$$a_k^F(k-5) = \frac{1}{2}(k^2 - 5k - 2) \quad \text{for } k \geq 6 \quad (3.42e)$$

$$\begin{aligned} a_k^F(k-6) &= -\frac{1}{6}(k^3 - 9k^2 - 4k + 66) \\ &= -\frac{1}{6}(k-3)(k^2 - 6k - 22) \quad \text{for } k \geq 7 \end{aligned} \quad (3.42f)$$

$$a_k^F(k-7) = \frac{1}{24}(k^4 - 14k^3 - k^2 + 350k - 384) \quad \text{for } k \geq 8 \quad (3.42g)$$

$$\begin{aligned} a_k^F(k-8) &= \frac{1}{120}(k^5 - 20k^4 + 15k^3 + 1100k^2 - 3016k - 2400) \\ &= \frac{1}{120}(k-4)(k^4 - 16k^3 - 49k^2 + 904k + 600) \quad \text{for } k \geq 9 \end{aligned} \quad (3.42h)$$

In particular, we see from (3.42a,b) that $(m-k+1)(m-k+2)$ is a factor of $a_k^F(m)$ for $k \geq 3$.

We find empirically that, for each integer $s \geq 3$, the polynomial $p_s^F(k)$ that matches $(-1)^{s-1}(s-3)!a_k^F(k-s)$ for integer $k \geq s+1$ has all *integer* coefficients; and we further find empirically that for *even* integers $s \geq 4$, we have $p_s^F(s/2) = 0$, so that the polynomial $p_s^F(k)$ has $k-s/2$ as a factor.

We also find

$$a_k^F(k) = F_{2k} \quad \text{for } k \geq 1 \quad (3.43a)$$

$$a_k^F(k+1) = \frac{(2k+1)F_{2k+2} - (k-4)F_{2k+1}}{5} \quad (3.43b)$$

where

$$F_n = \frac{1}{\sqrt{5}} \left[\left(\frac{1+\sqrt{5}}{2} \right)^n - \left(\frac{1-\sqrt{5}}{2} \right)^n \right] \quad (3.44)$$

are the Fibonacci numbers: see [30, sequences A001906/A088305 and A038731]. We prove (3.43a) in Appendix A.4. We have checked (3.43b) up to $k = 100$, but do not have any proof.¹⁰ Please note that (3.43a,b) give the low-order coefficients in the polynomials $t_F(m)$:

$$a_k^F(k) = (-1)^k [q^0] t_F(k) \quad (3.45a)$$

$$a_k^F(k+1) = (-1)^k [q^1] t_F(k+1) \quad (3.45b)$$

Since we have proven that $a_k^F(m)$ is a polynomial in m of degree k , it is also of interest to obtain explicit expressions for the coefficients of this polynomial, which we

¹⁰With some more work it might be possible to find a proof of (3.43b) using the same strategy as was used for the proof of (3.43a) in Appendix A.4.

write as

$$a_k^F(m) = \sum_{\ell=0}^k \frac{(-1)^\ell 2^{k-2\ell+1}}{(k-\ell)!(\ell+2)!} a_{k,\ell}^F m^{k-\ell} ; \quad (3.46)$$

here the prefactors have been chosen to make many (though not all) of the coefficients $a_{k,\ell}^F$ integers (in fact, all of them are integers for $\ell \leq 5$, see below). Now we use the well-known expansion of the falling powers in terms of Stirling cycle numbers [42],

$$x^{\underline{r}} = \sum_{c \geq 0} \begin{bmatrix} r \\ c \end{bmatrix} (-1)^{r-c} x^c , \quad (3.47)$$

and expand all the binomials in (3.34) involving m . We arrive after some algebra at the following expression:

$$a_{k,\ell}^F \equiv \frac{(k-\ell)!(\ell+2)!}{(-1)^\ell 2^{k-2\ell+1}} [m^{k-\ell}] a_k^F(m) \quad (3.48a)$$

$$\begin{aligned} &= \frac{(k-\ell)!(\ell+2)!(-1)^k}{2^{k-2\ell+1}} \left\{ \sum_{p=0}^k \sum_{r=0}^{k-p} \binom{p+1}{k-p-r} \frac{(-3)^r}{p!r!} \right. \\ &\quad \times \sum_{a=0}^p \sum_{c=0}^r \begin{bmatrix} p \\ a \end{bmatrix} \begin{bmatrix} r \\ c \end{bmatrix} \sum_{d=0}^{k-\ell} \binom{a}{k-\ell-d} \binom{c}{d} (1+2p)^{c-d} (1+p)^{a+d-k+\ell} \\ &\quad - \sum_{p=1}^k \sum_{r=0}^{k-p} \binom{p-1}{k-p-r} \frac{(-3)^r}{(p-1)!r!} \sum_{a=0}^{p-1} \sum_{c=0}^r \begin{bmatrix} p-1 \\ a \end{bmatrix} \begin{bmatrix} r \\ c \end{bmatrix} \\ &\quad \left. \times \sum_{d=0}^{k-\ell} \binom{a}{k-\ell-d} \binom{c}{d} (2p)^{c-d} (1+p)^{a+d-k+\ell} \right\} . \quad (3.48b) \end{aligned}$$

By computing (3.48b) for integers $k \geq \ell \geq 0$, we find *empirically* that $a_{k,\ell}^F$ is in fact, for each fixed ℓ , (the restriction of) a *polynomial* in k of degree ℓ . The first few of these polynomials are:

$$a_{k,0}^F = 1 \quad (3.49a)$$

$$a_{k,1}^F = 3k + 3 \quad (3.49b)$$

$$a_{k,2}^F = 6k^2 - 14k + 52 \quad (3.49c)$$

$$a_{k,3}^F = 10k^3 - 100k^2 + 130k + 240 \quad (3.49d)$$

$$a_{k,4}^F = 15k^4 - 330k^3 + 845k^2 - 18k - 1928 \quad (3.49e)$$

$$a_{k,5}^F = 21k^5 - 805k^4 + 5005k^3 + 749k^2 + 8358k - 87360 \quad (3.49f)$$

$$\begin{aligned} a_{k,6}^F &= 28k^6 - 1652k^5 + 20020k^4 - \frac{128156}{9}k^3 + \frac{278096}{3}k^2 \\ &\quad + \frac{3141872}{9}k - \frac{3838336}{3} \end{aligned} \quad (3.49g)$$

The fact that $a_{k,0}^F = 1$ for all $k \geq 0$ is just a restatement of (3.36) [compare (3.46)].

3.3 Cylindrical boundary conditions

Let us now consider a square-lattice grid of fixed width $m \geq 1$ and cylindrical boundary conditions. (Please note that for $m = 1$ the horizontal edges are loops, and that for $m = 2$ there are *two* horizontal edges connecting the pair of sites in each row.) Let us also assume that all horizontal edges have weights v and all vertical edges have weights v' ; they need not be -1 . We proceed analogously to the preceding subsection, making the changes necessary to handle cylindrical rather than free boundary conditions.

Consider first the action of \mathbf{H} on the start vector \mathbf{e}_{id} . It generates 2^m terms, each of which corresponds to a partition \mathcal{P} in which all the blocks are sequential sets of vertices on the m -cycle (we shall call these sets “polymers”). Furthermore, each polymer of size $\ell < m$ picks up a factor $v^{\ell-1}$, while a polymer of size m picks up a factor $v^m + mv^{m-1}$ (the v^m comes from the case in which all edges are occupied, while the mv^{m-1} comes from the m cases in which all edges but one are occupied). The action of \mathbf{V} is identical to that for free boundary conditions.

The upshot is that we have

$$\mathbf{V}\mathbf{H}\mathbf{e}_{\text{id}} = t_{\text{P}}(m) \mathbf{e}_{\text{id}} + \text{other terms} , \quad (3.50)$$

where $t_{\text{P}}(m)$ is the partition function for a polymer gas on the m -cycle in which each polymer of length $\ell \geq 1$ gets a fugacity

$$\hat{\mu}_{\ell} = \begin{cases} v^{\ell-1}(q + \ell v') & \text{for } 1 \leq \ell \leq m-1 \\ v^{m-1}(v + m)(q + mv') & \text{for } \ell = m \end{cases} \quad (3.51)$$

Please note that

$$\hat{\mu}_{\ell} = \begin{cases} \mu_{\ell} & \text{for } 1 \leq \ell \leq m-1 \\ (v + m)\mu_m & \text{for } \ell = m \end{cases} \quad (3.52)$$

where μ_{ℓ} are the fugacities for free boundary conditions considered in the preceding subsection.

We can obtain the $t_{\text{P}}(m)$ by using a simple recursion relating the periodic and free cases:

$$t_{\text{P}}(m) = \sum_{k=1}^{m-1} k \mu_k t_{\text{F}}(m-k) + \hat{\mu}_m . \quad (3.53)$$

To see this, single out a site (e.g. 1) and let $k \geq 1$ be the size of the polymer placed on it. If $k \leq m-1$, we have k ways of placing this polymer such that the selected site belongs to it, with fugacity μ_k for each such placement; and for the rest of the ring, the total weight of all admissible polymer configurations is simply $t_{\text{F}}(m-k)$. Finally, if $k = m$, there is only one way of placing the polymer, and it receives fugacity $\hat{\mu}_m$. This proves (3.53).

In order to compute explicitly the $t_{\text{P}}(m)$, it is convenient to introduce the generating function

$$\Phi_{\text{P}}(z) = \sum_{m=1}^{\infty} z^m t_{\text{P}}(m) . \quad (3.54)$$

Note next that the upper limit on the sum in (3.53) can be changed to ∞ , provided that we define $t_F(\ell) = 0$ for $\ell \leq 0$ [which is anyway implicit in the definition (3.17a) of the generating function $\Phi_F(z)$]. Multiplying both sides of (3.53) by z^m and summing over m , we arrive easily at the equation

$$\Phi_P(z) = z \frac{d\Psi(z)}{dz} [1 + \Phi_F(z)] + v\Psi(z) \quad (3.55a)$$

$$= \frac{z}{1 - \Psi(z)} \frac{d\Psi(z)}{dz} + v\Psi(z) \quad (3.55b)$$

where $\Psi(z) = \sum_{\ell=1}^{\infty} z^\ell \mu_\ell$ is defined in (3.18).¹¹ When $v = v' = -1$, we obtain the final formula

$$\Phi_P(z) = \left(\frac{z}{1+z} \right)^2 \frac{q^2 - 3q + 3 + 2(q-1)^2 z + q(q-1)z^2}{1 - (q-3)z - (q-1)z^2} \quad (3.56a)$$

$$= -\frac{qz^2 + (q+1)z + 2}{(1+z)^2} + \frac{2 - (q-3)z}{1 - (q-3)z - (q-1)z^2}. \quad (3.56b)$$

By expanding this function in powers of z , we have checked that it agrees with the known dominant diagonal elements $t_P(m)$ for $m \leq 13$ [6, 7].

It is now easy to extract the partition function $t_P(m)$: using (3.21a) we get

$$\begin{aligned} t_P(m) = [z^m] \Phi_P(z) &= (-1)^m (q - m - 2) \\ &+ 2 \sum_{j=0}^{\lfloor m/2 \rfloor} \binom{m-j}{j} (q-3)^{m-2j} (q-1)^j \\ &- \sum_{j=0}^{\lfloor (m-1)/2 \rfloor} \binom{m-1-j}{j} (q-3)^{m-2j} (q-1)^j, \end{aligned} \quad (3.57)$$

which is manifestly a polynomial in q of degree m .

We can now define the coefficients $a_k^P(m)$ in the same way as for free boundary conditions:

$$t_P(m) = \sum_{k=0}^m (-1)^k a_k^P(m) q^{m-k}, \quad (3.58)$$

where k and m are integers satisfying $m \geq 1$ and $0 \leq k \leq m$. However, it is slightly more convenient to extract explicitly *part of* the term $(-1)^m (q - m - 2)$ from (3.57), and define $\tilde{a}_k^P(m)$ to be the coefficients in what remains:

$$t_P(m) = (-1)^m (q - m - 1) + \sum_{k=0}^m (-1)^k \tilde{a}_k^P(m) q^{m-k}. \quad (3.59)$$

¹¹Note that the term of order z^1 in (3.55) vanishes whenever $v = -1$ (irrespective of the values of q and v'). This reflects the fact that $t_P(1) = 0$ whenever $v = -1$ because of the loops at each vertex.

Notice that the relation between $\tilde{a}_k^P(m)$ and $a_k^P(m)$ is rather simple: for fixed $m \geq 1$ we have that

$$a_k^P(m) = \begin{cases} \tilde{a}_k^P(m) & \text{for } 0 \leq k \leq m-2 \\ \tilde{a}_k^P(m) - 1 & \text{for } k = m-1 \\ \tilde{a}_k^P(m) - (m+1) & \text{for } k = m \end{cases}. \quad (3.60)$$

Expanding the binomials in (3.57), we have

$$\begin{aligned} \tilde{a}_k^P(m) &= 2 \sum_{j=0}^{\lfloor m/2 \rfloor} \sum_{\ell=0}^{\infty} \binom{m-j}{j} \binom{m-2j}{k+\ell-2j} \binom{j}{\ell} (-1)^j 3^{k+\ell-2j} \\ &\quad - \sum_{j=0}^{\lfloor (m-1)/2 \rfloor} \sum_{\ell=0}^{\infty} \binom{m-1-j}{j} \binom{m-2j}{k+\ell-2j} \binom{j}{\ell} (-1)^j 3^{k+\ell-2j} \\ &\quad - \delta_{km} \end{aligned} \quad (3.61)$$

Again we want to substitute the m -dependent upper index in the sum over j by something independent of m : e.g., by k .

In the first sum there are two non-trivial cases: a) If $k < \lfloor m/2 \rfloor$, then the second binomial vanishes whenever $k + \ell - 2j < 0$, and the third binomial is non-vanishing only if $j \geq \ell$. Therefore for $j > k$ and $j \geq \ell$ we have that $k + \ell - 2j < k + \ell - k - \ell = 0$. So all these terms vanish. b) If $k > \lfloor m/2 \rfloor$, then the first binomial does not vanish only when $0 \leq j \leq \lfloor m/2 \rfloor$ or when $j \geq m+1$. As we are adding terms with $\lfloor m/2 \rfloor + 1 \leq j \leq k-1 \leq m-1$, none of them give rise to a non-vanishing contribution.

In the second sum we play a similar game: a) If $k < \lfloor (m-1)/2 \rfloor$, the binomials involved are the same as for the first sum, so the same result applies here too. b) If $k > \lfloor (m-1)/2 \rfloor$, then we are adding terms with $\lfloor (m-1)/2 \rfloor + 1 \leq j \leq k-1$. The first binomial does not vanish only when $0 \leq j \leq \lfloor (m-1)/2 \rfloor$ or when $j \geq m$. The first of these do not appear in the extra terms; and since $m \geq k$, the second appears only when $j = k = m$, giving rise to an extra contribution equal to 1. This contribution cancels out exactly the term $-\delta_{km}$ in (3.61).

Putting all the pieces together, we end with the following expression for $\tilde{a}_k^P(m)$:

$$\tilde{a}_k^P(m) = \sum_{j=0}^k (-1)^j \left[2 \binom{m-j}{j} - \binom{m-1-j}{j} \right] \sum_{\ell=0}^{\infty} \binom{m-2j}{k+\ell-2j} \binom{j}{\ell} 3^{k+\ell-2j}, \quad (3.62)$$

where the independent variable m does not appear in the summation limits. After some straightforward but lengthy algebra we can rewrite the above formula in a more compact form:

$$\tilde{a}_k^P(m) = 3^k \binom{m}{k} + \sum_{p=1}^k (-1)^p \frac{m}{p} \binom{m-p-1}{p-1} \sum_{r=0}^{k-p} 3^r \binom{m-2p}{r} \binom{p}{k-p-r}. \quad (3.63)$$

It is clear from (3.63) that $\tilde{a}_k^P(m)$ is (the restriction of) a polynomial in m of degree at most k . To see that its degree is exactly k , let us extract the term of order m^k :

$$[m^k]\tilde{a}_k^P(m) = \frac{3^k}{k!} + \sum_{p=1}^k \frac{(-1)^p 3^{k-p}}{p!(k-p)!} = \frac{3^k}{k!} + \frac{2^k - 3^k}{k!} = \frac{2^k}{k!} \neq 0. \quad (3.64)$$

Let us also remark that the constant term in $\tilde{a}_k^P(m)$ vanishes whenever $k \geq 1$:

$$[m^0]\tilde{a}_k^P(m) = \delta_{k0} = \begin{cases} 1 & \text{if } k = 0 \\ 0 & \text{if } k \geq 1 \end{cases} \quad (3.65)$$

We can summarize the foregoing results in the following proposition:

Proposition 3.6 *Let \mathbf{H} and \mathbf{V} be the transfer matrices (2.8b)/(2.9) for the chromatic polynomial $v_i = v_{i,i+1} = -1$ with cylindrical boundary conditions. Then the dominant diagonal entry in the transfer matrix can be written as*

$$t_P(m) = (-1)^m (q - m - 1) + \sum_{k=0}^m (-1)^k \tilde{a}_k^P(m) q^{m-k} \quad (3.66)$$

where each $\tilde{a}_k^P(m)$ is a polynomial in m of degree k given by (3.63).

The first polynomials $\tilde{a}_k^P(m)$ are given by

$$\tilde{a}_0^P(m) = 1 \quad (3.67a)$$

$$\tilde{a}_1^P(m) = 2m \quad (3.67b)$$

$$\tilde{a}_2^P(m) = 2m^2 - m \quad (3.67c)$$

$$\tilde{a}_3^P(m) = \frac{4}{3}m^3 - 2m^2 - \frac{1}{3}m \quad (3.67d)$$

$$\tilde{a}_4^P(m) = \frac{2}{3}m^4 - 2m^3 - \frac{1}{6}m^2 + \frac{3}{2}m \quad (3.67e)$$

$$\tilde{a}_5^P(m) = \frac{4}{15}m^5 - \frac{4}{3}m^4 + \frac{1}{3}m^3 + \frac{10}{3}m^2 - \frac{3}{5}m \quad (3.67f)$$

$$\tilde{a}_6^P(m) = \frac{4}{45}m^6 - \frac{2}{3}m^5 + \frac{5}{9}m^4 + \frac{7}{2}m^3 - \frac{119}{45}m^2 - \frac{23}{6}m \quad (3.67g)$$

We can also prove the following result concerning the polynomials $\tilde{a}_k^P(m)$:¹²

Proposition 3.7 *For each integer $s \geq 1$, the quantity*

$$\tilde{a}_k^P(k-s) = 3^k \binom{k-s}{k} + \sum_{p=1}^k (-1)^p \frac{k-s}{p} \binom{k-s-p-1}{p-1} \sum_{r=0}^{k-p} 3^r \binom{k-s-2p}{r} \binom{p}{k-p-r} \quad (3.68)$$

¹²This Proposition refers, however, to the regime $m < k$ that does not contribute to the sum (3.66).

is, when restricted to $k \geq s$, given by a polynomial in k of degree s , with leading coefficient

$$[k^s]\tilde{a}_k^{\text{P}}(k-s) = \frac{(-1)^{s+1}}{s!} \quad (3.69)$$

and first subleading coefficient

$$[k^{s-1}]\tilde{a}_k^{\text{P}}(k-s) = \frac{(-1)^s(s+1)}{2(s-1)!}. \quad (3.70)$$

Furthermore, $\tilde{a}_k^{\text{P}}(0) = 0$, so that the polynomial representing $\tilde{a}_k^{\text{P}}(k-s)$ for $k \geq s$ has a factor $k-s$.

The proof of this Proposition can be found in Appendix A.3. For the first values of s , we have

$$\tilde{a}_k^{\text{P}}(k-1) = k-1 \quad \text{for } k \geq 1 \quad (3.71a)$$

$$\begin{aligned} \tilde{a}_k^{\text{P}}(k-2) &= -\frac{1}{2}(k^2 - 3k + 2) \\ &= -\frac{1}{2}(k-1)(k-2) \quad \text{for } k \geq 2 \end{aligned} \quad (3.71b)$$

$$\begin{aligned} \tilde{a}_k^{\text{P}}(k-3) &= \frac{1}{6}(k^3 - 6k^2 + 5k + 12) \\ &= \frac{1}{6}(k+1)(k-3)(k-4) \quad \text{for } k \geq 3 \end{aligned} \quad (3.71c)$$

$$\begin{aligned} \tilde{a}_k^{\text{P}}(k-4) &= -\frac{1}{24}(k^4 - 10k^3 + 11k^2 + 94k - 168) \\ &= -\frac{1}{24}(k+3)(k-2)(k-4)(k-7) \quad \text{for } k \geq 4 \end{aligned} \quad (3.71d)$$

$$\begin{aligned} \tilde{a}_k^{\text{P}}(k-5) &= \frac{1}{120}(k^5 - 15k^4 + 25k^3 + 375k^2 - 1346k + 480) \\ &= \frac{1}{120}(k-5)(k^4 - 10k^3 - 25k^2 + 250k - 96) \quad \text{for } k \geq 5 \end{aligned} \quad (3.71e)$$

$$\begin{aligned} \tilde{a}_k^{\text{P}}(k-6) &= -\frac{1}{720}(k^6 - 21k^5 + 55k^4 + 1065k^3 - 6176k^2 + 3636k + 15840) \\ &= -\frac{1}{720}(k-3)(k-6)(k^4 - 12k^3 - 71k^2 + 642k + 880) \quad \text{for } k \geq 6 \end{aligned} \quad (3.71f)$$

We find empirically that, for each integer $s \geq 1$, the polynomial $p_s^{\text{P}}(k)$ that matches $(-1)^{s-1}s!\tilde{a}_k^{\text{P}}(k-s)$ for $k \geq s$ has all *integer* coefficients; and we further find empirically that for *even* integers $s \geq 2$, we have $p_s^{\text{P}}(s/2) = 0$, so that the polynomial $p_s^{\text{P}}(k)$ has $k - s/2$ as a factor.

We also find empirically

$$\tilde{a}_k^{\text{P}}(k) = F_{2k+1} + F_{2k-1} - 1 \quad (3.72a)$$

$$\tilde{a}_k^{\text{P}}(k+1) = \sum_{j=0}^{k+1} \binom{k+1}{j} j F_j \quad (3.72b)$$

where F_n are again the Fibonacci numbers (3.44): see [30, sequences A005592 and A117202]. We have checked these relationships up to $k = 100$, but do not have any

proof.¹³ Please note that (3.72a,b) give the low-order coefficients in the polynomials $t_P(m)$:

$$\tilde{a}_k^P(k) = (-1)^k [q^0] t_P(k) + (k+1) \quad (3.73a)$$

$$\tilde{a}_k^P(k+1) = (-1)^k [q^1] t_P(k+1) + 1 \quad (3.73b)$$

Since $\tilde{a}_k^P(m)$ is a polynomial in m of degree k , we are again interested in obtaining the coefficients $\tilde{a}_{k,\ell}^P$ defined by

$$\tilde{a}_k^P(m) = \sum_{\ell=0}^k \frac{(-1)^\ell 2^{k-2\ell+1}}{(k-\ell)!(\ell+2)!} \tilde{a}_{k,\ell}^P m^{k-\ell}. \quad (3.74)$$

With the help of (3.47), we obtain after some algebra the following result:

$$\begin{aligned} \tilde{a}_{k,\ell}^P = & \frac{(k-\ell)!(\ell+2)!}{2^{k-2\ell+1}} \left\{ \frac{3^k}{k!} \begin{bmatrix} k \\ k-\ell \end{bmatrix} \right. \\ & + (-1)^k \sum_{p=1}^k \sum_{r=0}^{k-p} \frac{(-3)^r}{p!r!} \binom{p}{k-p-r} \sum_{a=0}^{p-1} \sum_{c=0}^r \begin{bmatrix} p-1 \\ a \end{bmatrix} \begin{bmatrix} r \\ c \end{bmatrix} \\ & \times \sum_{d=0}^{k-\ell-1} \begin{bmatrix} c \\ d \end{bmatrix} \binom{a}{k-\ell-d-1} (2p)^{c-d} (1+p)^{a-k+\ell+d+1} \left. \right\}. \quad (3.75) \end{aligned}$$

By computing (3.75) for integers $k \geq \ell \geq 0$, we find *empirically* that $\tilde{a}_{k,\ell}^P$ is in fact, for each fixed ℓ , (the restriction of) a *polynomial* in k of degree ℓ . The first few are:

$$\tilde{a}_{k,0}^P = 1 \quad (3.76a)$$

$$\tilde{a}_{k,1}^P = 3k - 3 \quad (3.76b)$$

$$\tilde{a}_{k,2}^P = 6k^2 - 38k + 52 \quad (3.76c)$$

$$\tilde{a}_{k,3}^P = 10k^3 - 160k^2 + 390k + 0 \quad (3.76d)$$

$$\tilde{a}_{k,4}^P = 15k^4 - 450k^3 + 2405k^2 - 1450k - 7688 \quad (3.76e)$$

$$\tilde{a}_{k,5}^P = 21k^5 - 1015k^4 + 10465k^3 - 16121k^2 - 37030k - 151200 \quad (3.76f)$$

$$\begin{aligned} \tilde{a}_{k,6}^P = & 28k^6 - 1988k^5 + 34580k^4 - \frac{1100876}{9}k^3 - \frac{327376}{3}k^2 \\ & + \frac{480752}{9}k - \frac{1902976}{3} \end{aligned} \quad (3.76g)$$

The fact that $\tilde{a}_{k,0}^P = 1$ for all $k \geq 0$ is just a restatement of (3.64).

¹³With some more work it might be possible to find a proof of (3.72a,b) using the same strategy as was used for the proof of (3.43a) in Appendix A.4.

4 Large- q expansion of the leading eigenvalue

In this section we compute the large- q expansion of the leading eigenvalue $\lambda_*(m)$ for both free and cylindrical boundary conditions, and determine empirically some of its remarkable properties. In Section 5 we shall provide theoretical explanations of some (but not all!) of these empirical observations.

4.1 Overview of method and results

In the preceding section we computed in closed form the dominant diagonal entry in the transfer matrix, t_{id} , for a strip of width $m \geq 1$ with either free or cylindrical boundary conditions (denoted t_{F} and t_{P} , respectively). We found that this entry is in each case a polynomial in q of degree m :

$$t_{\text{F}}(m) = \sum_{k=0}^m (-1)^k a_k^{\text{F}}(m) q^{m-k} \quad (4.1a)$$

$$t_{\text{P}}(m) = \sum_{k=0}^m (-1)^k a_k^{\text{P}}(m) q^{m-k} \quad (4.1b)$$

$$= (-1)^m (q - m - 1) + \sum_{k=0}^m (-1)^k \tilde{a}_k^{\text{P}}(m) q^{m-k} \quad (4.1c)$$

We furthermore computed in closed form the coefficients $a_k^{\text{F}}(m)$ and $\tilde{a}_k^{\text{P}}(m)$, which are in fact polynomials in m of degree k [cf. (3.34) and (3.63)]. For instance, the leading few terms for large $|q|$ are

$$t_{\text{F}}(m) = q^m - (2m - 1)q^{m-1} + (2m^2 - 3m + 1)q^{m-2} - \left(\frac{4}{3}m^3 - 4m^2 + \frac{8}{3}m\right)q^{m-3} + \dots \quad [\text{for } m \geq 1] \quad (4.2a)$$

$$t_{\text{P}}(m) = q^m - 2mq^{m-1} + (2m^2 - m)q^{m-2} - \left(\frac{4}{3}m^3 - 2m^2 - \frac{1}{3}m\right)q^{m-3} + \dots \quad [\text{for } m \geq 5] \quad (4.2b)$$

In this section we want to carry out an analogous computation for the dominant *eigenvalue* of the transfer matrix, which we call $\lambda_*^{\text{F/P}}$. Already from Corollary 3.3 we can conclude that $\lambda_*(m)$ has, for large $|q|$, a convergent expansion in powers of q^{-1} ,

$$\lambda_*^{\text{F}}(m) = \sum_{k=0}^{\infty} (-1)^k b_k^{\text{F}}(m) q^{m-k} \quad (4.3a)$$

$$\lambda_*^{\text{P}}(m) = \sum_{k=0}^{\infty} (-1)^k b_k^{\text{P}}(m) q^{m-k} \quad (4.3b)$$

and that the first two terms in this expansion coincide with those in the dominant diagonal entry:

$$\lambda_*^{\text{F/P}}(m) - t_{\text{F/P}}(m) = O(q^{m-2}) \quad (4.4)$$

and hence

$$b_k^{\text{F/P}}(m) = a_k^{\text{F/P}}(m) \quad \text{for } k = 0, 1. \quad (4.5)$$

Here we shall go further and compute the coefficients $b_k^{\text{F/P}}(m)$ for $1 \leq m \leq 12_{\text{F}}, 13_{\text{P}}$ and $0 \leq k \leq 40$.¹⁴ Somewhat surprisingly, we shall find (for the m values we were able to study) that

$$b_k^{\text{F}}(m) = a_k^{\text{F}}(m) \quad \text{for } k = 2, 3 \quad (4.6a)$$

$$b_k^{\text{P}}(m) = a_k^{\text{P}}(m) \quad \text{for } k = 2, 3 \text{ and } m \geq k + 2 \quad (4.6b)$$

so that

$$\lambda_{\star}^{\text{F}}(m) - t_{\text{F}}(m) = O(q^{m-4}) \quad (4.7a)$$

$$\lambda_{\star}^{\text{P}}(m) - t_{\text{P}}(m) = O(q^{m-4}) \quad \text{for } m \geq 5 \quad (4.7b)$$

rather than merely $O(q^{m-2})$ as Corollary 3.3 shows. We *conjecture* that this behavior holds for larger m as well.

For some purposes it is slightly more convenient to use, in place of the coefficients $b_k^{\text{P}}(m)$, the modified coefficients $\tilde{b}_k^{\text{P}}(m)$ defined by

$$\lambda_{\star}^{\text{P}}(m) = (-1)^m(q - m - 1) + \sum_{k=0}^{\infty} (-1)^k \tilde{b}_k^{\text{P}}(m) q^{m-k} \quad (4.8)$$

[analogously to (4.1c) for $t_{\text{P}}(m)$]. Note that the relation between the coefficients $b_k^{\text{P}}(m)$ and $\tilde{b}_k^{\text{P}}(m)$ is the same as for the coefficients $a_k^{\text{P}}(m)$ and $\tilde{a}_k^{\text{P}}(m)$ [cf. (3.60)].

Most importantly, however, it is enlightening to pass from the eigenvalue $\lambda_{\star}^{\text{F/P}}(m)$ to its logarithm, which is a free energy, and define

$$\log \frac{\lambda_{\star}^{\text{F/P}}(m)}{q^m} = \sum_{k=1}^{\infty} c_k^{\text{F/P}}(m) q^{-k}. \quad (4.9)$$

For cylindrical boundary conditions it is slightly more efficient to define the modified coefficients $\tilde{c}_k^{\text{P}}(m)$ by

$$\log \frac{\lambda_{\star}^{\text{P}}(m) - (-1)^m(q - m - 1)}{q^m} = \sum_{k=1}^{\infty} \tilde{c}_k^{\text{P}}(m) q^{-k}. \quad (4.10)$$

In this section we shall see *empirically* that the coefficients $c_k(m)$ behave in a much simpler way than the $b_k(m)$: namely, while $b_k(m)$ is, for large enough m , (the restriction of) a polynomial of degree k in m , we shall find that $c_k(m)$ is, for large

¹⁴It would not be difficult to extend this computation to much larger values of k , if we really cared. Extension to larger values of m is, however, an extremely demanding computational task. The dimension of the transfer matrix for $m = 12_{\text{F}}$ is 2947; for $m = 13_{\text{F}}$ it is 7889, which is beyond the capabilities of our current computer facilities.

enough m , (the restriction of) a polynomial of degree 1 in m . In Section 5 we shall discuss the theoretical interpretation of this empirical observation.

We shall proceed as follows: Using the methods of [6, 7] we shall compute the transfer matrices for strips of width $m \leq 12$ for free boundary conditions and $m \leq 13$ for cylindrical boundary conditions.¹⁵ From these we can extract the dominant eigenvalue as a power series in q^{-1} , i.e. for each available m we can easily compute as many coefficients $b_k(m)$ and $c_k(m)$ as we please.¹⁶ We then observe *empirically* that, for each $k \geq 0$, the coefficient $b_k(m)$ [resp. $c_k(m)$] is a polynomial B_k [resp. C_k] in m of degree k [resp. degree 1] *provided that we restrict to integers $m \geq$ some $m_{\min}(k)$* .¹⁷ Assuming that this empirical observation is accurate (i.e., that the polynomial behavior persists to all larger m), we can infer the expressions for the polynomials B_k and C_k for $k \leq 31$ (resp. $k \leq 16$) for free (resp. cylindrical) boundary conditions.

4.2 Free boundary conditions

Using the methods just described, we have obtained the leading eigenvalue $\lambda_\star^F(m)$ for $0 \leq m \leq 12$ as a power series in q^{-1} [cf. (4.3a)] through order $k = 40$. The resulting coefficients $b_k^F(m)$ are displayed in Table 1, and the corresponding coefficients $c_k^F(m)$ [cf. (4.9)] are displayed in Table 2. It is interesting to note that for all (k, m) that we have computed (i.e., $1 \leq m \leq 12$ and $0 \leq k \leq 40$), the coefficients $b_k^F(m)$ and $kc_k^F(m)$ are integers. We observe *empirically* that, for each fixed k , the coefficients $b_k^F(m)$ are the restriction to integers m of a polynomial B_k^F in m of degree k , and that the coefficients $c_k^F(m)$ are the restriction to integers m of a polynomial C_k^F in m of degree 1, *provided that we restrict attention to $m \geq m_{\min}^F(k)$* with

$$m_{\min}^F(k) = \begin{cases} 1 & \text{if } 0 \leq k \leq 6 \\ \lceil \frac{k}{2} \rceil - 2 & \text{if } k \geq 7 \end{cases}. \quad (4.11)$$

Below this threshold $m_{\min}^F(k)$, the coefficients deviate from polynomial behavior. With our available data together with a few tricks described below, we are able to determine these polynomials for $0 \leq k \leq 33$.

First we start by trying to fit the coefficients $b_k^F(m)$ with $m \geq m_{\min}^F(k)$ to a polynomial B_k^F in m of degree k . As we need $k + 1$ coefficients for such a polynomial,

¹⁵In fact, this was already done in ref. [6] for $m \leq 8$ with both boundary conditions, and in ref. [7] for $9 \leq m \leq 13$ with cylindrical boundary conditions. Therefore, the only new transfer matrices we need to compute here are $m = 9, 10, 11, 12$ with free boundary conditions. See also Sections 5.2 and 6 below for further results from this computation.

¹⁶To compute the dominant eigenvalue as a power series in q^{-1} , we have applied the power method [43, Section 7.3.1] *in symbolic form* to the transfer matrix. Each iteration gives one additional term in the expansion of the dominant eigenvalue in powers of q^{-1} . We can therefore compute the *exact* expansion up to any desired order in a *finite* number of steps.

¹⁷By contrast, for the dominant diagonal entry we have *proven* that $a_k^F(m)$ and $\tilde{a}_k^P(m)$ are polynomials in m of degree k ; and in this case the polynomial form holds for *all* allowable integers m , i.e. $m \geq \max(k, 1)$.

we are able to obtain these polynomials only up to $k = 8$. Please note that in all cases we have at least one data point more than the number of unknowns, so every fit can be tested at least on one extra data point. Our results are:

$$B_0^F(m) = 1 \quad (4.12a)$$

$$B_1^F(m) = 2m - 1 \quad (4.12b)$$

$$B_2^F(m) = 2m^2 - 3m + 1 \quad (4.12c)$$

$$B_3^F(m) = \frac{4}{3}m^3 - 4m^2 + \frac{8}{3}m \quad (4.12d)$$

$$B_4^F(m) = \frac{2}{3}m^4 - \frac{10}{3}m^3 + \frac{23}{6}m^2 + \frac{11}{6}m - 3 \quad (4.12e)$$

$$B_5^F(m) = \frac{4}{15}m^5 - 2m^4 + \frac{11}{3}m^3 + \frac{7}{2}m^2 - \frac{433}{30}m + 9 \quad (4.12f)$$

$$B_6^F(m) = \frac{4}{45}m^6 - \frac{14}{15}m^5 + \frac{23}{9}m^4 + \frac{19}{6}m^3 - \frac{2263}{90}m^2 + \frac{574}{15}m - 18 \quad (4.12g)$$

$$B_7^F(m) = \frac{8}{315}m^7 - \frac{16}{45}m^6 + \frac{62}{45}m^5 + \frac{16}{9}m^4 - \frac{1144}{45}m^3 + \frac{5947}{90}m^2 - \frac{15011}{210}m + 29 \quad (4.12h)$$

$$B_8^F(m) = \frac{2}{315}m^8 - \frac{4}{35}m^7 + \frac{3}{5}m^6 + \frac{2}{3}m^5 - \frac{2131}{120}m^4 + \frac{4129}{60}m^3 - \frac{302017}{2520}m^2 + \frac{9041}{84}m - 49 \quad (4.12i)$$

Notice that the three highest-order coefficients agree with those of the corresponding polynomial $a_k^F(m)$, i.e.

$$B_k^F(m) = \begin{cases} a_k^F(m) & \text{for } 0 \leq k \leq 3 \\ a_k^F(m) + O(m^{k-3}) & \text{for } k \geq 4 \end{cases} \quad (4.13)$$

However, there is a better way of extracting the desired information from our numerical data: instead of using the coefficients $b_k^F(m)$ as our basic quantities, we can use the related coefficients $c_k^F(m)$ [cf. (4.9)]. The latter coefficients are *empirically* found to be, for each fixed k , the restriction to integer m of a polynomial C_k^F in m of degree 1, i.e.

$$C_k^F(m) = \alpha_k^F m + \beta_k^F, \quad (4.14)$$

provided that $m \geq$ the same $m_{\min}^F(k)$ defined in (4.11). As we need only *two* coefficients for such a polynomial (i.e., α_k^F and β_k^F), we are able to obtain these polynomials up to $k = 24$ (if we want at least one extra data point to test the fit) or $k = 26$ (if

we don't). Our results for $k \leq 8$ are:

$$C_1^F(m) = -2m + 1 \quad (4.15a)$$

$$C_2^F(m) = -m + \frac{1}{2} \quad (4.15b)$$

$$C_3^F(m) = \frac{1}{3}m - \frac{2}{3} \quad (4.15c)$$

$$C_4^F(m) = \frac{5}{2}m - \frac{11}{4} \quad (4.15d)$$

$$C_5^F(m) = \frac{28}{5}m - \frac{29}{5} \quad (4.15e)$$

$$C_6^F(m) = \frac{55}{6}m - \frac{28}{3} \quad (4.15f)$$

$$C_7^F(m) = \frac{89}{7}m - \frac{97}{7} \quad (4.15g)$$

$$C_8^F(m) = \frac{81}{4}m - \frac{243}{8} \quad (4.15h)$$

The polynomials C_k^F for $9 \leq k \leq 24$ are reported in the MATHEMATICA file `data_FREE.m` that is included with the preprint version of this article at arXiv.org; they can also be read off from the results of Section 5 below [cf. (5.25)/(5.33)]. Finally, the polynomials B_k^F for $9 \leq k \leq 24$ can be determined from the C_k^F using (4.9).

Actually, we can do better than this. We believe that the coefficients $c_k^F(m)$ are, for each fixed $k \geq 0$, the restriction to integers $m \geq m_{\min}^F(k)$ of a polynomial C_k^F in m of degree 1. If we compute the difference

$$\Delta_k^F(m) = c_k^F(m) - C_k^F(m) \quad (4.16)$$

between the numerical coefficients $c_k^F(m)$ and the corresponding polynomials C_k^F , we find, not surprisingly, that they are nonzero whenever $m < m_{\min}^F(k)$: see Table 3. If we could somehow guess an analytic form for at least some of these coefficients $\Delta_k^F(m)$, we could then define improved coefficients $\hat{c}_k^F(m)$ by

$$\hat{c}_k^F(m) = c_k^F(m) - \Delta_k^F(m), \quad (4.17)$$

so that these coefficients $\hat{c}_k^F(m)$ would be, for each fixed k , the restriction to integers $m \geq \hat{m}_{\min}^F(k)$ of the same polynomial C_k^F , with a *smaller* threshold $\hat{m}_{\min}^F(k) < m_{\min}^F(k)$. The important point here is that a smaller threshold $\hat{m}_{\min}^F(k)$ implies that we can obtain more polynomials C_k^F with the same raw data.

By inspecting Table 3, it is not difficult to realize that there are some patterns in $\Delta_k^F(m)$ immediately below the threshold $m_{\min}^F(k)$: for instance, for odd $k = 2p + 1$ with $3 \leq p \leq 10$, we have $\Delta_{2p+1}^F(p - 2) = 1$; and for even $k = 2p$ with $4 \leq p \leq 10$, we have $\Delta_{2p}^F(p - 3) = 3p - 2$. We then *assume* that this behavior holds true for all larger p . For other subsets of the nonzero values of $\Delta_k^F(m)$ slightly farther below the boundary $m_{\min}^F(k)$, we likewise find simple polynomial Ansätze. Our *empirical* results

are:

$$\Delta_{2p+1}^F(p-2) = 1, \quad \text{for } p \geq 3 \quad (4.18a)$$

$$\Delta_{2p+1}^F(p-3) = \frac{13}{2}p^2 - \frac{37}{2}p + 27, \quad \text{for } p \geq 4 \quad (4.18b)$$

$$\Delta_{2p+1}^F(p-4) = \frac{95}{8}p^4 - \frac{1265}{12}p^3 + \frac{2961}{8}p^2 - \frac{8515}{12}p + 917, \quad \text{for } p \geq 5 \quad (4.18c)$$

$$\Delta_{2p}^F(p-3) = 3p - 2, \quad \text{for } p \geq 4 \quad (4.18d)$$

$$\Delta_{2p}^F(p-4) = \frac{59}{6}p^3 - 66p^2 + \frac{817}{6}p - 17, \quad \text{for } p \geq 5 \quad (4.18e)$$

$$\Delta_{2p}^F(p-5) = \frac{473}{40}p^5 - \frac{2207}{12}p^4 + \frac{9023}{8}p^3 - \frac{38413}{12}p^2 + \frac{29763}{10}p + 2941, \quad \text{for } p \geq 7 \quad (4.18f)$$

We are able to test each fit on at least one additional data point. Notice that in (4.18f), the condition $p \geq 7$ does *not* follow the expected behavior from the previous correction terms (i.e., one would have expected $p \geq 6$). The new threshold $\hat{m}_{\min}^F(k)$ is given by

$$\hat{m}_{\min}^F(k) = \begin{cases} 1 & \text{if } 0 \leq k \leq 11 \\ 2 & \text{if } 12 \leq k \leq 14 \\ \left\lceil \frac{k}{2} \right\rceil - 5 & \text{if } k \geq 15 \end{cases} \quad (4.19)$$

By this method, we can obtain the polynomials C_k^F (and therefore the polynomials B_k^F) up to $k = 30$. Indeed, the fits to obtain the polynomials C_k^F with $k \leq 30$ were tested on at least one additional data point.

If we do not demand to have at least one extra data point to test the fits, we can extend this computation up to $k = 32$. We can then guess one further correction term $\Delta_k^F(m)$ (this time with an additional data point to test the fit):

$$\Delta_{2p+1}^F(p-5) = \frac{161}{16}p^6 - \frac{43693}{240}p^5 + \frac{21757}{16}p^4 - \frac{86909}{16}p^3 + \frac{110297}{8}p^2 - \frac{433772}{15}p + 42719, \quad \text{for } p \geq 8. \quad (4.20)$$

With this additional correction, the new threshold \hat{m}_{\min}^F is

$$\hat{m}_{\min}^F(k) = \begin{cases} 1 & \text{if } 0 \leq k \leq 11 \\ 2 & \text{if } 12 \leq k \leq 14 \\ 3 & \text{if } 15 \leq k \leq 17 \\ \left\lceil \frac{k}{2} \right\rceil - 5 & \text{if } k \geq 18 \end{cases} \quad (4.21)$$

so the computation of the polynomials C_k^F can be extended up to $k = 33$ (with no extra data points to test the fit). The polynomials C_k^F with $1 \leq k \leq 33$ are included in the `mathematica` file `data_FREE.m`.

4.3 Cylindrical boundary conditions

We have likewise obtained the leading eigenvalue $\lambda_\star^P(m)$ for $0 \leq m \leq 13$ as a power series in q^{-1} [cf. (4.3b)] through order $k = 40$. The resulting coefficients $b_k^P(m)$ are displayed in Table 4, and the corresponding coefficients $c_k^P(m)$ are displayed in Table 5. As for free boundary conditions, we note that for all (k, m) that we have computed (i.e., $1 \leq m \leq 13$ and $0 \leq k \leq 40$), the coefficients $b_k^P(m)$ and $kc_k^P(m)$ are integers.

We observe *empirically* that, for each fixed k , the coefficients $b_k^P(m)$ are the restriction to integers m of a polynomial B_k^P in m of degree k , and that the coefficients $c_k^P(m)$ are the restriction to integers m of a polynomial C_k^P in m of degree 1, *provided that we restrict attention to $m \geq m_{\min}^P(k)$* with

$$m_{\min}^P(k) = k + 2. \quad (4.22)$$

Below this threshold, the coefficients deviate from polynomial behavior. The polynomial behavior can be extended downwards by two steps, i.e. to $m = k$, if we use the coefficients $\tilde{b}_k^P(m)$ [cf. (4.8)] in place of $b_k^P(m)$. With our available data together with the tricks described in the preceding subsection, we are able to determine these polynomials for $0 \leq k \leq 15$. The coefficients $\tilde{b}_k^P(m)$ are displayed in Table 6.

We begin, as before, by fitting $\tilde{b}_k^P(m)$ for $m \geq k$ to a polynomial B_k^P of degree k . With our data we can do this for $0 \leq k \leq 6$; we also have, in each case, at least one extra data point to test the fit. Our results are:

$$B_0^P(m) = 1 \quad (4.23a)$$

$$B_1^P(m) = 2m \quad (4.23b)$$

$$B_2^P(m) = 2m^2 - m \quad (4.23c)$$

$$B_3^P(m) = \frac{4}{3}m^3 - 2m^2 - \frac{1}{3}m \quad (4.23d)$$

$$B_4^P(m) = \frac{2}{3}m^4 - 2m^3 - \frac{1}{6}m^2 + \frac{5}{2}m \quad (4.23e)$$

$$B_5^P(m) = \frac{4}{15}m^5 - \frac{4}{3}m^4 + \frac{1}{3}m^3 + \frac{16}{3}m^2 - \frac{28}{5}m \quad (4.23f)$$

$$B_6^P(m) = \frac{4}{45}m^6 - \frac{2}{3}m^5 + \frac{5}{9}m^4 + \frac{11}{2}m^3 - \frac{614}{45}m^2 + \frac{55}{6}m \quad (4.23g)$$

Notice that the three highest-order coefficients agree with those of the corresponding polynomial $\tilde{a}_k^P(m)$, i.e.

$$B_k^P(m) = \begin{cases} \tilde{a}_k^P(m) & \text{for } 0 \leq k \leq 3 \\ \tilde{a}_k^P(m) + O(m^{k-3}) & \text{for } k \geq 4 \end{cases} \quad (4.24)$$

Note also that the constant term vanishes in all these polynomials except B_0^P .

As in the previous subsection, we can extract the desired information more efficiently by analyzing the coefficients $c_k^P(m)$, which are found empirically to be, for each fixed k , a polynomial C_k^P in m of degree 1 for $m \geq m_{\min}^P(k) = k + 2$, i.e.

$$C_k^P(m) = \alpha_k^P m + \beta_k^P, \quad (4.25)$$

As we need only two coefficients for such a polynomial, we can obtain these polynomials up to $k = 9$ (if we want at least one extra data point to test the fit) or $k = 10$ (if we don't).

However, we can do slightly better if we consider instead of the coefficients $c_k^P(m)$ the modified coefficients $\tilde{c}_k^P(m)$ defined by (4.10). We find empirically that $k\tilde{c}_k^P(m)$ is an integer for all the computed values of (k, m) : see Table 7. We also find empirically that $\tilde{c}_k^P(m)$ is, for each fixed k , the restriction to integers $m \geq \tilde{m}_{\min}^P(k)$ of the same polynomial C_k^P with a *smaller* threshold $\tilde{m}_{\min}^P(k) = \max(k, 2) < m_{\min}^P(k)$. In this way we can obtain the polynomials C_k^P up to $k = 11$ or $k = 12$, depending on whether or not we insist on having an extra data point to test the fit. Our results for $k \leq 8$ are:

$$C_1^P(m) = -2m \quad (4.26a)$$

$$C_2^P(m) = -m \quad (4.26b)$$

$$C_3^P(m) = \frac{1}{3}m \quad (4.26c)$$

$$C_4^P(m) = \frac{5}{2}m \quad (4.26d)$$

$$C_5^P(m) = \frac{28}{5}m \quad (4.26e)$$

$$C_6^P(m) = \frac{55}{6}m \quad (4.26f)$$

$$C_7^P(m) = \frac{89}{7}m \quad (4.26g)$$

$$C_8^P(m) = \frac{81}{4}m \quad (4.26h)$$

The polynomials C_k^P for $9 \leq k \leq 12$ are reported in the MATHEMATICA file `data_CYL.m` that is included with the preprint version of this article at arXiv.org; they can also be read off from the results of Section 5 below [cf. (5.25)]. Please note that the constant term vanishes in all these polynomials, while the term linear in m is the same as for free boundary conditions [cf. (4.15)]:

$$\alpha_k^P = \alpha_k^F \quad (4.27a)$$

$$\beta_k^P = 0 \quad (4.27b)$$

in all cases that we are able to test (namely, $1 \leq k \leq 12$). Finally, the polynomials B_k^P for $7 \leq k \leq 12$ can be determined from the C_k^P using (4.10).

These results can be improved in the same way as we did in the previous subsection. First we compute the difference $\Delta_k^P(m) = \tilde{c}_k^P(m) - C_k^P(m)$: see Table 8. We then try to guess an analytic form for some of the coefficients $\Delta_k^P(m)$, and we define improved coefficients $\hat{c}_k^P(m)$ [as in (4.17)] so that the $\hat{c}_k^P(m)$ will be, for each fixed k , the restriction to integers $m \geq \hat{m}_{\min}^P(k)$ of the polynomial C_k^P , with a *smaller* threshold $\hat{m}_{\min}^P(k) < \tilde{m}_{\min}^P(k)$. As in the case of free boundary conditions, we find empirically that the coefficients $\Delta_k^P(m)$ closest to the boundary $\tilde{m}_{\min}^P(k)$ are the restriction to

integers m of certain polynomials:

$$\Delta_k^P(k-1) = (-1)^{k-1} \left(\frac{3}{2}k^2 - \frac{11}{2}k + 4 \right), \quad \text{for } k \geq 4 \quad (4.28a)$$

$$\Delta_k^P(k-2) = (-1)^{k-2} \left(\frac{11}{6}k^3 - 10k^2 + \frac{73}{6}k + 1 \right), \quad \text{for } k \geq 6 \quad (4.28b)$$

$$\Delta_k^P(k-3) = (-1)^{k-3} \left(\frac{35}{24}k^4 - \frac{199}{12}k^3 - \frac{1837}{24}k^2 - \frac{2201}{12}k + 191 \right), \quad \text{for } k \geq 8 \quad (4.28c)$$

Again, each fit can be tested on at least an extra data point. The new threshold \widehat{m}_{\min}^P is

$$\widehat{m}_{\min}^P(k) = \begin{cases} 2 & \text{if } k \leq 2 \\ \lfloor \frac{k}{2} \rfloor + 1 & \text{if } 3 \leq k \leq 8 \\ k - 3 & \text{if } k \geq 9, \end{cases} \quad (4.29)$$

By this method, we can obtain the polynomials C_k^P (and therefore the polynomials B_k^P) up to $k = 14$, with at least one extra data point to test the fit.

If we do not insist on having an extra data point to test the fit, we can extend this computation of C_k^P up to $k = 15$. We can then guess one further correction term $\Delta_k^P(m)$ (again with no additional test for the fits):

$$\Delta_k^P(k-4) = (-1)^{k-4} \left(\frac{33}{40}k^5 - \frac{115}{8}k^4 + \frac{741}{8}k^3 - \frac{1821}{8}k^2 - \frac{729}{20}k + 695 \right), \quad \text{for } k \geq 10. \quad (4.30)$$

With this correction the new threshold is

$$\widehat{m}_{\min}^P(k) = \begin{cases} 2 & \text{if } k \leq 2 \\ \lfloor \frac{k}{2} \rfloor + 1 & \text{if } 3 \leq k \leq 10 \\ k - 4 & \text{if } k \geq 11 \end{cases} \quad (4.31)$$

so the computation of the polynomials C_k^P can be extended up to $k = 16$ (with no extra data points to test the fit).

The polynomials C_k^P for $10 \leq k \leq 16$ also have a zero constant term, and the relation (4.27) between periodic and free boundary conditions continues to hold.

5 Thermodynamic limit ($m \rightarrow \infty$)

In previous sections we have dealt with semi-infinite square-lattice strips of fixed width m . In this section we will study the thermodynamic limit $m \rightarrow \infty$ of the free energy of our model.

In Section 5.1 we introduce some preliminary definitions and discuss the expected behavior of the strip free energies per unit length, $f_m^F(q)$ and $f_m^P(q)$, as a function of the strip width m . In Section 5.2 we discuss the large- $|q|$ expansion of the bulk free energy. Bakaev and Kabanovich [12] have calculated the first 36 terms of this expansion; we confirm their computation and extend it by providing 11 more terms,

i.e. through order q^{-47} . We also compute the large- $|q|$ expansion of the surface (resp. corner) free energy through order q^{-47} (resp. q^{-46}). These computations are based on the finite-lattice method [44–49].

In Section 5.3 we obtain (using the polynomials C_k^F) a large- $|q|$ expansion for the limiting free energy $f_m^F(q)$ of a semi-infinite strip of width m and free boundary conditions. We find that this expansion contains two terms: a bulk term (independent of m) and a surface term (linear in $1/m$). This computation gives an independent check of the first 33 terms of the series expansions for the bulk and surface free energies for the square lattice. In Section 5.4 we repeat the computation with cylindrical boundary conditions. We find that the bulk contribution is the same as for free boundary conditions and that there is *no* surface contribution. These results provide a theoretical interpretation for some aspects of the behavior found in the preceding section for C_k^F and C_k^P [cf. (4.15)/(4.26) and (4.27)].

Finally, in Section 5.5 we perform a series-extrapolation analysis of the large- $|q|$ series for the bulk, surface and corner free energies, in an effort to locate their singular points in the complex q -plane.

5.1 Generalities and finite-size-scaling theory

Corollary 3.3 shows that, for each width m and each boundary condition (free or cylindrical), the transfer matrix has, for sufficiently large $|q|$, a *single* dominant eigenvalue $\lambda_*(q)$ that moreover is an analytic function of q (in fact, it is q^m times an analytic function of q^{-1}). However, Corollary 3.3 gives no information about *how large* $|q|$ has to be for this behavior to occur; in particular, there is no guarantee that this large- q domain is uniform in m . However, the uniformity in m can be proven by invoking the following theorem:

Theorem 5.1 [50, Corollary 5.3 and Proposition 5.4] *Let $G = (V, E)$ be a loopless¹⁸ finite undirected graph of maximum degree Δ . Then all the zeros of the chromatic polynomial $P_G(q)$ lie in the disc $|q| < 7.963907\Delta$.*

Let us remark that this theorem has been recently improved by Fernández and Procacci [51, Corollary 2]: they showed that the constant 7.963907 in Theorem 5.1 can be replaced by 6.907652.¹⁹

For the square lattice with any of the standard boundary conditions (free, cylindrical, cyclic or toroidal) we have $\Delta = 4$, so we can conclude that all chromatic roots

¹⁸**Warning:** We are here using the graph theorists’ terminology, in which a *loop* is an edge connecting a vertex to itself. Obviously, if G has a loop, then $P_G(q)$ is identically zero. What physicists often call “loops” — particularly when referring to Feynman diagrams — are called “cycles” or “circuits” by graph theorists. Thus, a “3-loop Feynman diagram” is a graph with with cyclomatic number 3; it may or may not have loops.

¹⁹Jackson, Procacci and Sokal [52] have recently observed that the Fernández–Procacci constant is in fact

$$K^* = W(e/2)/[1 - W(e/2)]^2 \approx 6.907\,651\,697\,774\,449\,218 \dots$$

where W is the Lambert W function [53], i.e. the inverse function to $x \mapsto xe^x$.

lie inside the disc $|q| < 7.963907 \times 4 = 31.855628$. Actually, by [50, Corollary 5.3 and Table 1], we have for $\Delta = 4$ the slightly stronger bound $|q| < C(4) \leq 29.081607$. With the improved result of Fernández and Procacci, we get $|q| < 6.907652 \times 4 = 27.630607$; and for the particular case $\Delta = 4$ these authors [51, Corollary 1] obtained the slightly better bound $|q| < C^*(4) \leq 24.443218$.

It follows that the limiting curves \mathcal{B}_m must also lie inside the disc $|q| \leq 24.443218$ for all widths m : for if part of the limiting curve were to lie outside the (closed) disc, then the Beraha–Kahane–Weiss theorem (Theorem 2.2) would imply that chromatic roots would also lie outside the disc for $m \times n$ strips of all sufficiently large lengths n . Furthermore, using again the Beraha–Kahane–Weiss theorem we can conclude that, outside this disc, the transfer matrix for each width m must have one and only one eigenvalue of largest modulus. Since this dominant eigenvalue cannot collide with any other eigenvalue, it must be an analytic function of q outside the given disc.

In summary, the transfer matrix for a square-lattice strip of width m and with free or cylindrical boundary conditions has a single dominant eigenvalue $\lambda_{*,m}^{\text{F/P}}(q)$ that is an analytic function of q (in fact, q^m times an analytic function of q^{-1}) whenever $|q| > 24.443218$.

Let us now introduce the free energy per site for a finite strip with free or cylindrical boundary conditions,

$$f_{m,n}^{\text{F/P}}(q) = \frac{1}{mn} \log P_{G_{m_{\text{F/P}} \times n_{\text{F}}}}(q) , \quad (5.1)$$

and its limiting value for a semi-infinite strip,

$$f_m^{\text{F/P}}(q) = \lim_{n \rightarrow \infty} \frac{1}{mn} \log P_{G_{m_{\text{F/P}} \times n_{\text{F}}}}(q) . \quad (5.2)$$

Finally, let us introduce the free energy per site for the infinite lattice,

$$f^{\text{F/P}}(q) = \lim_{m,n \rightarrow \infty} \frac{1}{mn} \log P_{G_{m_{\text{F/P}} \times n_{\text{F}}}}(q) . \quad (5.3)$$

Here we are assuming that the indicated limits exist and that in (5.3) the limit is independent of the way that m and n tend to infinity. Furthermore, it is natural to expect that in (5.3) the limiting free energy is independent of boundary conditions, in which case we can omit the superscripts F or P and write simply $f(q)$.

In fact, some of these assumptions can be proven. Indeed, the above discussion guarantees that at least for $|q| > 24.443218$, the limiting strip free energy $f_m(q)$ exists for all m and is given by

$$f_m^{\text{F/P}}(q) = \frac{1}{m} \log \lambda_{*,m}^{\text{F/P}}(q) , \quad (5.4)$$

which in particular is an analytic function of q in the indicated domain. Moreover, Procacci *et al.* [54, Theorem 2] have proven that, when $|q|$ is large enough (namely, $|q| > 8e^3 \approx 160.684295$), the infinite-volume limiting free energy $f(q)$ exists and is analytic in $1/q$ and is the same for all reasonable sequences of graphs $G_{m \times n}$ (in

particular, it is the same for free, cylindrical, cyclic and toroidal boundary conditions and is independent of the way that m and n tend to infinity). In this paper we will take $n \rightarrow \infty$ first and then take $m \rightarrow \infty$, so that

$$f(q) = \lim_{m \rightarrow \infty} f_m^{\text{F/P}}(q). \quad (5.5)$$

Finite-size-scaling theory [55, Section 2.5] gives a rather precise prediction for the form of the free energy (5.1)/(5.2) for a finite or semi-infinite system away from a critical point (and in the absence of soft modes). In particular, for an $m \times n$ strip with free or cylindrical boundary conditions and bulk correlation length $\xi_{\text{bulk}} \ll m, n$, the predicted behavior is

$$f_{m,n}^{\text{F}} = f_{\text{bulk}} + \frac{m+n}{mn} f_{\text{surf}} + \frac{1}{mn} f_{\text{corner}} + O(e^{-\min(m,n)/\xi_{\text{bulk}}}) \quad (5.6a)$$

$$f_{m,n}^{\text{P}} = f_{\text{bulk}} + \frac{1}{n} f_{\text{surf}} + O(e^{-\min(m,n)/\xi_{\text{bulk}}}) \quad (5.6b)$$

where $f_{\text{bulk}} = f$, f_{surf} and f_{corner} are, respectively, the bulk, surface and corner free energies. (More precisely, f_{surf} is the free energy for *two* units of surface, and f_{corner} is the free energy for *four* corners.) For a semi-infinite strip $m \times \infty$ with free or cylindrical boundary conditions, we have

$$f_m^{\text{F}} = f_{\text{bulk}} + \frac{1}{m} f_{\text{surf}} + O(e^{-m/\xi_{\text{bulk}}}) \quad (5.7a)$$

$$f_m^{\text{P}} = f_{\text{bulk}} + O(e^{-m/\xi_{\text{bulk}}}) \quad (5.7b)$$

The relations (5.7) of course hold for the chromatic polynomials at *fixed* large q . But we can also argue heuristically what they should imply for the series expansion in powers of $1/q$. It is not difficult to see that, for large q , we have

$$e^{-1/\xi_{\text{bulk}}(q)} = \frac{1}{q} + O\left(\frac{1}{q^2}\right) \quad (5.8)$$

(just as for a *one-dimensional* Potts antiferromagnet at zero temperature).²⁰ We can therefore interpret $O(e^{-m/\xi_{\text{bulk}}(q)})$ as meaning $O(q^{-m})$. Therefore, we expect that

$$f_m^{\text{F}} = f_{\text{bulk}} + \frac{1}{m} f_{\text{surf}} + O(q^{-m}) \quad (5.9a)$$

$$f_m^{\text{P}} = f_{\text{bulk}} + O(q^{-m}) \quad (5.9b)$$

²⁰Let $G = (V, E)$ be a finite graph (let us suppose for simplicity that it has no loops or multiple edges) with n vertices and m edges; then one sees immediately from the Fortuin–Kasteleyn representation (2.4) that its Potts-model partition function has the large- q expansion

$$Z_G(q, v) = q^n + mq^{n-1} + \frac{m(m-1)}{2} q^{n-2} + O(q^{n-3}).$$

When G is a finite piece of a regular lattice, the corresponding expansion for $|V|^{-1} \log Z_G(q, v)$ gives in the infinite-volume limit the large- q expansion for the bulk free energy $f(q, v)$.

Now let i, j be vertices of G ; then the unnormalized 2-point correlation function $Z_G \langle \sigma_i \cdot \sigma_j \rangle = Z_G \langle (q \delta_{\sigma_i, \sigma_j} - 1)/(q - 1) \rangle$ is given by a representation like (2.4) but with the constraint that i and j must belong to the same connected component. The dominant terms of the large- q expansion are the ones in which this component has the minimal number of vertices and all other components are

This explains why the coefficients $c_k^{\text{F/P}}(m)$ in the expansion of $\log \lambda_{*,m}^{\text{F/P}} = m f_m^{\text{F/P}}$ [cf. (4.9)] are polynomials of *degree 1* in m for large enough m , i.e. $m \geq m_{\min}^{\text{F/P}}(k)$, and consequently why the coefficients $b_k^{\text{F/P}}(m)$ in the expansion of $\lambda_{*,m}^{\text{F/P}}$ [cf. (4.3)] are polynomials of degree k in m . It also explains why, for cylindrical boundary conditions, $c_k^{\text{P}}(m)$ is strictly proportional to m , i.e. the constant term vanishes [cf. (4.26)/(4.27b)]. The error term $O(q^{-m})$ in (5.9) furthermore suggests that $m_{\min}^{\text{F/P}}(k) = k+1$. Of course, we should not take too seriously the “+1” here, since the *amplitude* of the correction term in (5.7) could be proportional to a positive or negative power of q . But we do predict that $m_{\min}^{\text{F/P}}(k) = k + O(1)$ as $k \rightarrow \infty$. This is indeed what we found for cylindrical boundary conditions, where we have $m_{\min}^{\text{P}}(k) = k + 2$ [cf. (4.22)]. For free boundary conditions, however, we found the *faster* convergence $m_{\min}^{\text{F}}(k) \approx k/2$ [cf. (4.11)], for which we lack at present any theoretical explanation.

In the next subsection we will use our transfer matrices to compute the large- q expansion for the bulk, surface and corner free energies, using the finite-lattice method [44–49]. In the subsequent two subsections we will compute the large- q expansion of the strip free energy $f_m(q)$ for free and cylindrical boundary conditions, respectively,

isolated vertices; one therefore gets

$$Z_G\langle \sigma_i \cdot \sigma_j \rangle = Q_G(v; i, j) \left(\frac{v}{q}\right)^{d_G(i, j)} q^n [1 + O(q^{-1})]$$

where $d_G(i, j)$ is the length of the shortest path in G from i to j , and $Q_G(v; i, j)$ is a polynomial in v that enumerates the connected subgraphs of G that contain i and j and have exactly $d_G(i, j) + 1$ vertices [with a weight v for each edge beyond the minimum number $d_G(i, j)$]. In particular, if G is triangle-free, these subgraphs are simply shortest paths from i to j . In general $Q_G(v; i, j)$ can grow exponentially in $d_G(i, j)$ [when e.g. G is an infinite regular lattice]; but if G is a piece of the square lattice and $i - j$ lies *along an axis direction*, then $Q_G(v; i, j) = 1$. It follows that the exponential decay rate of correlations along an axis is

$$e^{-1/\xi_{\text{bulk}}(q, v)} = \left| \frac{v}{q} \right| + O\left(\frac{1}{|q|^2}\right).$$

For $v = -1$ this gives (5.8).

It is instructive to ask how these results would be seen in the transfer-matrix formalism. Ordinarily one has $e^{-1/\xi_{\text{bulk}}} = |\lambda_2/\lambda_*|$, where λ_* is the dominant eigenvalue and λ_2 is the first subleading eigenvalue. But when one performs the computation using our transfer matrices, one finds $\lambda_2/\lambda_* = \alpha_m^{\text{F/P}}(v)/q^2 + O(1/q^3)$ for suitable polynomials $\alpha_m^{\text{F/P}}$ — *not* the predicted v/q . (Indeed, for width $m = 1$ — i.e., a one-dimensional Potts model — the transfer matrix is of size 1×1 , i.e. there is *no* subleading eigenvalue at all.) What is going on here?

The point is that the exponential decay rate in the correlation function $\langle \sigma_0 \cdot \sigma_x \rangle$ is controlled by a “colored” intermediate state, i.e. the state obtained by applying the field σ_0 to the vacuum. The corresponding eigenvalue λ_2 would be seen in a transfer matrix in the *spin representation* [6, Section 3.1]; but it is not seen in our transfer matrix in the *Fortuin–Kasteleyn representation*, which represents only “colorless” states (i.e., states invariant under the Potts global symmetry group S_q). Rather, the first subleading eigenvalue of the latter transfer matrix corresponds to a “colorless” two-particle state, hence has λ_2/λ_* of order $1/q^2$. More precisely, for square-lattice strips of widths $m \geq 4$ (resp. $m \geq 3$) with cylindrical (resp. free) boundary conditions, we find (at least up to $m = 9_{\text{P}}, 7_{\text{F}}$) that there are *at least two* subleading eigenvalues of order $1/q^2$. Some of these satisfy $\lambda_2/\lambda_* = (v/q)^2 + O(q^{-3})$, and the others satisfy $\lambda_2/\lambda_* = (1+v)(v/q)^2 + O(q^{-3})$; note that the latter ones vanish at order $1/q^2$ for the chromatic polynomial $v = -1$. All other eigenvalues are $O(q^{-3})$.

using our polynomials C_k^F and C_k^P .

5.2 Large- q expansion for the bulk, surface and corner free energies

First of all, as we are interested in the large- q limit, it is convenient to explicitly remove the leading term $\log q$ in the free energy by considering the modified chromatic polynomial \tilde{P}_G for a loopless graph $G = (V, E)$:

$$\tilde{P}_G(q) = q^{-|V|} P_G(q). \quad (5.10)$$

Using the Fortuin–Kasteleyn representation (2.4) we get

$$\tilde{P}_G(q) = \sum_{A \subseteq E} (-1)^{|E|} q^{k(A) - |V|} \quad (5.11a)$$

$$= \sum_{A \subseteq E} (-1)^{|E|} (1/q)^{|A| - c(A)}, \quad (5.11b)$$

where $c(A) = |A| - |V| + k(A)$ is the cyclomatic number of the subgraph (V, A) .

It is instructive to begin by computing “by hand” the first few terms of the large- q expansion for the bulk, surface and corner free energies. To do this, let us first consider an $m \times n$ square lattice with *free* boundary conditions: it has $|V| = mn$ sites, $|E| = 2mn - m - n$ edges, and $|F| = (m-1)(n-1)$ square faces (“plaquettes”). We can compute the first few first terms in the large- q expansion for the modified chromatic polynomial $\tilde{P}_{m_F \times n_F}(q)$ by using (5.11b) and explicitly identifying the subsets A having a given small value of $|A| - c(A)$:

$|A| - c(A) = 0$: Only $A = \emptyset$.

$|A| - c(A) = 1$: $A =$ any single edge.

$|A| - c(A) = 2$: $A =$ two distinct edges.

$|A| - c(A) = 3$: $A =$ three distinct edges *or* four edges forming a plaquette.

$|A| - c(A) = 4$: $A =$ four distinct edges not forming a plaquette *or* four edges forming a plaquette together with one additional edge.

We therefore have

$$\begin{aligned} \tilde{P}_{m_F \times n_F}(q) &= 1 - \frac{|E|}{q} + \frac{|E|(|E| - 1)}{2q^2} - \left[\frac{|E|(|E| - 1)(|E| - 2)}{6} - |F| \right] \frac{1}{q^3} \\ &\quad + \left[\frac{|E|(|E| - 1)(|E| - 2)(|E| - 3)}{24} - |F|(|E| - 3) \right] \frac{1}{q^4} \\ &\quad + O(q^{-5}). \end{aligned} \quad (5.12)$$

Taking the logarithm, dividing by $|V|$, and putting back the leading term $\log q$, one finds the large- q expansion for the free energy

$$\begin{aligned} f_{m,n}^F(q) = & \log q - \frac{2}{q} - \frac{1}{q^2} + \frac{1}{3q^3} + \frac{5}{2q^4} + \left[\frac{1}{q} + \frac{1}{2q^2} - \frac{2}{3q^3} - \frac{11}{4q^4} \right] \left(\frac{1}{m} + \frac{1}{n} \right) \\ & + \left[\frac{1}{q^3} + \frac{3}{q^4} \right] \frac{1}{mn} + O(q^{-5}). \end{aligned} \quad (5.13)$$

Comparing to the finite-size-scaling Ansatz (5.6), we obtain

$$f_{\text{bulk}}(q) = \log q - \frac{2}{q} - \frac{1}{q^2} + \frac{1}{3q^3} + \frac{5}{2q^4} + O(q^{-5}) \quad (5.14a)$$

$$f_{\text{surf}}(q) = \frac{1}{q} + \frac{1}{2q^2} - \frac{2}{3q^3} - \frac{11}{4q^4} + O(q^{-5}) \quad (5.14b)$$

$$f_{\text{corner}}(q) = \frac{1}{q^3} + \frac{3}{q^4} + O(q^{-5}) \quad (5.14c)$$

Now consider an $m \times n$ square lattice with *cylindrical* boundary conditions: we have $|V| = mn$, $|E| = 2mn - m$, and $|F| = m(n - 1)$. For small m we have to worry about terms A that wind horizontally around the lattice using the periodic boundary conditions; such terms start at order $q^{-(m-1)}$. But we can avoid such terms simply by assuming that m is large enough, i.e. $m \geq k + 2$ if we want an expansion valid through order q^{-k} . Therefore, we can obtain the expansion through order q^{-4} by assuming that $m \geq 6$; then the contributing terms are exactly the same as those for free boundary conditions, and we obtain the same expansion (5.12) but with the modified values of $|E|$ and $|F|$. A simple computation shows that

$$f_{m,n}^P(q) = f_{\text{bulk}}(q) + f_{\text{surf}}(q) \frac{1}{n} + O(q^{-5}) \quad (5.15)$$

where f_{bulk} and f_{surf} are the *same* as those given in (5.14), in agreement with the finite-size-scaling prediction (5.6).

Unfortunately, this elementary graphical method for generating the large- q expansion is not very efficient if one wants to go to high order. To obtain long expansions we will use a more sophisticated procedure: the *finite-lattice method* pioneered by Enting and collaborators [44–49]. Indeed, Bakaev and Kabanovich [12] used this method to obtain, already in 1994, the large- q expansion of the bulk free energy through order q^{-36} .²¹ Their results can be summarized as follows: as $|q| \rightarrow \infty$, the exponential of the bulk free energy per site for the zero-temperature Potts antiferromagnet (i.e., chromatic polynomial) on the square lattice is given by the series expansion

$$\begin{aligned} e^{f(q)} = & \frac{(q-1)^2}{q} \left[1 + z^3 + z^7 + 3z^8 + 4z^9 + 3z^{10} + 3z^{11} + 11z^{12} + 24z^{13} + 8z^{14} \right. \\ & \left. - 91z^{15} - 261z^{16} - 290z^{17} + \dots - 3068121066z^{36} + O(z^{37}) \right] \end{aligned} \quad (5.16)$$

²¹For relevant earlier work on obtaining large- q series for the infinite-volume limit of the chromatic polynomial, see Kim and Enting [46] and the references cited therein.

(the full series is given in Table 9), where z is defined as

$$z = \frac{1}{q-1} . \quad (5.17)$$

Before presenting our extensions of this result, let us first briefly review the finite-lattice method.

In the finite-lattice method [44–49], the large- q expansion of the infinite-volume free energy through a given order in $z = 1/(q-1)$ is written as a linear combination of free energies for rectangles of various sizes $r \times s$:

$$f(q) - \log q \equiv \lim_{m,n \rightarrow \infty} \frac{1}{mn} \log \tilde{P}_{m_F \times n_F}(z) \quad (5.18a)$$

$$= \sum_{(r,s) \in B(k)} \alpha_k(r,s) \log \tilde{P}_{r_F \times s_F}(z) + O(z^{2k-3}), \quad (5.18b)$$

where we have used the variable $z = 1/(q-1)$ instead of $q = 1 + 1/z$, and the modified partition function $\tilde{P}_{m_F \times n_F}$ [see (5.10)]. The sum in (5.18) is taken over all rectangles $r \times s$ belonging to the set

$$B(k) = \{(r,s) : r \leq s \text{ and } r+s \leq k\} . \quad (5.19)$$

The weights $\alpha_k(r,s)$ are defined as

$$\alpha_k(r,s) = \begin{cases} 2W_k(r,s) & \text{for } r < s \\ W_k(r,r) & \text{for } r = s \end{cases} \quad (5.20)$$

where

$$W_k(r,s) = \begin{cases} 1 & \text{for } r+s = k \\ -3 & \text{for } r+s = k-1 \\ 3 & \text{for } r+s = k-2 \\ -1 & \text{for } r+s = k-3 \\ 0 & \text{otherwise} \end{cases} \quad (5.21)$$

The error term in (5.18) is given by a particular subclass of connected graphs that do not fit into any of the rectangles in $B(k)$ [44] [56, Chapter 12]. In our case, these graphs are [12] the convex polygons²² of perimeter $2k-2$ having the property that any pair of nearest-neighbor sites belonging to the polygon must be connected by an edge of the polygon.²³ Since any polygon of perimeter $2k-2$ has $|A| - c(A) = (2k-2) - 1 = 2k-3$, we deduce that the error term in (5.18) is of order $q^{-(2k-3)} \sim z^{2k-3}$.

Now suppose that we are somehow able to compute the transfer matrices for widths $L \leq L_{\max}$ with free boundary conditions. We can then use these transfer matrices to

²²We recall [57] that a *convex polygon* (in the square lattice) is a self-avoiding polygon whose length equals the perimeter of its minimal bounding rectangle.

²³This condition excludes, for instance, polygons containing a “bottleneck” of width 1 or a “protuberance” of width 1.

compute the partition functions $\tilde{P}_{r_F \times s_F}$ for $r \leq L_{\max}$ and s arbitrary. This means that if we set the cut-off k equal to $2L_{\max} + 1$, we will be able to compute the partition function for all pairs $(r, s) \in B(k)$. It follows that formula (5.18) gives the bulk-free-energy series correct through order $z^{4L_{\max}-2}$. We have empirically checked (by doing computations for different values of L_{\max} and checking to what order they agree) that this formula is correct. In our case $L_{\max} = 12$, so we expect to obtain the free-energy series correct up to order z^{46} .

If we compare the results coming from different values of L_{\max} , we find empirically that the first incorrect term (of order $z^{4L_{\max}-1}$) is given by the generating function of the aforementioned subclass of convex polygons, which is [12]

$$\sum_{k=4}^{\infty} \mu_k x^{2k} = x^8 \frac{2 - 2x^2 - x^2 \sqrt{1 - 4x^2}}{(1 - 4x^2)(2 + x^2)} + x^{12} \frac{3 - 4x^2 - 4\sqrt{1 - 4x^2}}{(1 - 4x^2)^2}. \quad (5.22)$$

If we add the term $\mu_{2L_{\max}} z^{4L_{\max}-1}$ to the series obtained with a given value of L_{\max} , we get a series correct up to (and including) $z^{4L_{\max}-1}$. In our case $L_{\max} = 12$, so we obtain a series expansion correct up to order z^{47} . The idea of adding this correction term is due to Bakaev and Kabanovich [12] and was used by them to improve their own series by one term.²⁴

In this way, we confirm the expansion (5.16) found by Bakaev and Kabanovich [12] and extend it by 11 terms:

$$e^{f(q)} = \frac{(q-1)^2}{q} [1 + z^3 + z^7 + 3z^8 + 4z^9 + 3z^{10} + 3z^{11} + 11z^{12} + 24z^{13} + 8z^{14} - 91z^{15} - 261z^{16} - 290z^{17} + \dots - 598931311074z^{47} + O(z^{48})], \quad (5.23)$$

where the full series is given in Table 9. In terms of the variable $1/q$, we obtain

$$e^{f(q)} = q [1 - 2q^{-1} + q^{-2} + q^{-3} + q^{-4} + q^{-5} + q^{-6} + 2q^{-7} + 9q^{-8} + 38q^{-9} + 130q^{-10} + 378q^{-11} + 987q^{-12} + \dots + 1311159363081366872q^{-47} + O(q^{-48})]. \quad (5.24)$$

Finally, for the bulk free energy $f(q)$ itself (rather than its exponential) in terms of the variable $1/q$, we obtain

$$f(q) = \log q - \frac{2}{q} - \frac{1}{q^2} + \frac{1}{3q^3} + \frac{5}{2q^4} + \frac{28}{5q^5} + \frac{55}{6q^6} + \frac{89}{7q^7} + \frac{81}{4q^8} + \frac{505}{9q^9} + \frac{1029}{5q^{10}} + \frac{7742}{11q^{11}} + \frac{25291}{12q^{12}} + \frac{73552}{13q^{13}} + \frac{197755}{14q^{14}} + \dots + \frac{190018276619486037135}{47q^{47}} + O(q^{-48}). \quad (5.25)$$

Clearly, $e^{f(q)}$ has a much simpler expansion than $f(q)$; in particular, its coefficients are integers (at least through the order calculated thus far).²⁵ A further simplification is obtained by using the variable $z = 1/(q-1)$ in place of $1/q$: the integer coefficients

²⁴They actually went farther and improved their series by a second term, by enumerating a more complicated class of contributing graphs that we refrain from considering here.

²⁵The coefficients of $f(q)$ are not integers, but $k[q^{-k}]f(q)$ is an integer (at least through the order calculated thus far). Indeed, it is not hard to show that if $F(z)$ is a power series with integer coefficients and constant term 1, then $k[z^k] \log F(z)$ is always an integer.

become much smaller. Finally, a slight extra simplification arises from extracting the prefactor $(q-1)^2/q$ in (5.23).

The finite-lattice method can be used for computing series expansions, not only of the bulk free energy, but also of the surface and corner free energies [cf. (5.6)]. The main ideas were introduced by Enting [45] three decades ago and have been further developed by him [48, 49]. To our knowledge, however, no one has yet applied this technique to the large- q expansions of chromatic polynomials, so the all the results to be presented below are new.

As for the bulk case, the large- q expansions of the surface and corner free energies through a given order in $z = 1/(q-1)$ are written as certain linear combinations of free energies for rectangles of various sizes $r \times s$ [cf. (5.18)]:

$$f_{\text{surf}}(q) = \sum_{(r,s) \in B(k)} \beta_k(r,s) \log \tilde{P}_{r_F \times s_F}(z) + O(z^{2k-3}) \quad (5.26a)$$

$$f_{\text{corner}}(q) = \sum_{(r,s) \in B(k)} \gamma_k(r,s) \log \tilde{P}_{r_F \times s_F}(z) + O(z^{2k-3}), \quad (5.26b)$$

where the set $B(k)$ is the same as for the bulk case [cf. (5.19)]. The weights for the surface free energy are given by [45]

$$\beta_k(r,s) = \begin{cases} S_k(r,s) + S_k(s,r) & \text{for } r < s \\ S_k(r,r) & \text{for } r = s \end{cases} \quad (5.27)$$

where

$$S_k(r,s) = \begin{cases} 1-r & \text{for } r+s = k \\ 3r-1 & \text{for } r+s = k-1 \\ -3r-1 & \text{for } r+s = k-2 \\ r+1 & \text{for } r+s = k-3 \\ 0 & \text{otherwise} \end{cases} \quad (5.28)$$

The weights for the corner free energy are given by [45]

$$\gamma_k(r,s) = \begin{cases} 2V_k(r,s) & \text{for } r < s \\ V_k(r,r) & \text{for } r = s \end{cases} \quad (5.29)$$

where

$$V_k(r,s) = \begin{cases} (r-1)(s-1) & \text{for } r+s = k \\ 1+r+s-3rs & \text{for } r+s = k-1 \\ 3rs+r+s-1 & \text{for } r+s = k-2 \\ -(r+1)(s+1) & \text{for } r+s = k-3 \\ 0 & \text{otherwise} \end{cases} \quad (5.30)$$

The error term in (5.26a,b) is given by the same reasoning as for the bulk case, i.e. it is $O(z^{2k-3})$. Therefore, by considering strips up to a maximum width L_{max} , we

can use (5.26a,b) to obtain the series for the surface and corner free energies correct through order $z^{4L_{\max}-2}$. We have empirically checked (by doing computations for different values of L_{\max} and checking to what order they agree) that this formula is correct. In our case we have $L_{\max} = 12$, hence series valid through order z^{46} .

For the surface free energy we can conjecturally extend the series by one term by comparing the series for different values of L_{\max} and noticing empirically that the needed correction for the term of order $z^{4L_{\max}-1}$ is simply a multiple of the correction term (5.22) for the bulk-free-energy series. More precisely, if we add the term $-L_{\max}\mu_{2L_{\max}}z^{4L_{\max}-1}$ to the series obtained with a given value of L_{\max} , we get a series correct through order $z^{4L_{\max}-1}$. In our case $L_{\max} = 12$, so we obtain a series expansion for f_{surf} correct (conjecturally) through order z^{47} . Unfortunately, we have not yet succeeded in figuring out an analogous correction for the corner free energy.

The results for the series expansions are given by

$$e^{f_{\text{surf}}} = 1 + z - z^3 - z^4 + z^6 - z^7 - 8z^8 - 16z^9 - 16z^{10} - 12z^{11} - 41z^{12} - 138z^{13} + \dots - 130312353695974z^{47} + O(z^{48}) \quad (5.31)$$

$$e^{f_{\text{corner}}} = 1 + z^3 + 4z^7 + 12z^8 + 20z^9 + 28z^{10} + 67z^{11} + 208z^{12} + 484z^{13} + 753z^{14} + \dots + 448320847685638z^{46} + O(z^{47}), \quad (5.32)$$

where the full list of coefficients is displayed in Table 9. In terms of the variable $1/q$ we get

$$f_{\text{surf}} = \frac{1}{q} + \frac{1}{2q^2} - \frac{2}{3q^3} - \frac{11}{4q^4} - \frac{29}{5q^5} - \frac{28}{3q^6} - \frac{97}{7q^7} - \frac{243}{8q^8} - \frac{1019}{9q^9} - \frac{4489}{10q^{10}} - \frac{17280}{11q^{11}} - \frac{14654}{3q^{12}} - \frac{183143}{13q^{13}} + \dots - \frac{1103009229135728011786}{47q^{47}} + O(q^{-48}) \quad (5.33)$$

$$f_{\text{corner}} = \frac{1}{q^3} + \frac{3}{q^4} + \frac{6}{q^5} + \frac{19}{2q^6} + \frac{16}{q^7} + \frac{101}{2q^8} + \frac{685}{3q^9} + \frac{948}{q^{10}} + \frac{3409}{q^{11}} + \frac{44399}{4q^{12}} + \frac{34558}{q^{13}} + \dots + \frac{280315319437238591517}{2q^{46}} + O(q^{-47}) \quad (5.34)$$

5.3 Large- q expansion for the strip free energy: Free boundary conditions

We can check the results (5.25)/(5.33) for the bulk and surface free energies by computing the large- $|q|$ expansion of the limiting free energy for a semi-infinite strip with free boundary conditions:

$$\begin{aligned} f_m^{\text{F}}(q) &= \frac{1}{m} \log \lambda_{*,m}^{\text{F}}(q) \\ &= \log q + \frac{1}{m} \log \left[\sum_{k=0}^{\infty} (-1)^k b_k^{\text{F}}(m) q^{-k} \right] \\ &= \log q + \frac{1}{m} \sum_{k=1}^{\infty} (-1)^k c_k^{\text{F}}(m) q^{-k} \end{aligned} \quad (5.35)$$

If $m \geq m_{\min}^{\text{F}}(k)$, we can replace the coefficients $c_k^{\text{F}}(m)$ by the corresponding polynomials $C_k^{\text{F}}(m)$ [cf. (4.15)]. These polynomials C_k^{F} are of degree 1 in m for $1 \leq k \leq 33$,

and we have conjectured that this behavior holds for all values of $k \geq 1$. Thus, $f_m^F(q)$ contains [as predicted in (5.9a)] only two terms: a bulk term $f_{\text{bulk}}(q) = f(q)$ that is independent of m , and a surface free energy $f_{\text{surf}}^F(q)$ that is of order $1/m$:

$$f_m^F(q) \cong f_{\text{bulk}}(q) + \frac{1}{m} f_{\text{surf}}(q) . \quad (5.36)$$

Here \cong denotes that the two sides agree at each order q^{-k} of the expansion in powers of q^{-1} , but we require this only for $m \geq m_{\text{min}}^F(k)$. This computation using the polynomials C_k^F thus provides an independent check of the first 33 terms of the series (5.25) and (5.33). Conversely, the finite-lattice computation of the preceding subsection provides an independent confirmation of the empirically observed regularities in the behavior of the polynomials C_k^F [cf. (4.16)–(4.21)].

We can slightly extend the check for the surface-free-energy series by using the series (5.25) for f_{bulk} as an *input*: in this case, each polynomial C_k^F contains a single unknown coefficient to be determined (rather than two unknown coefficients). We then obtain the coefficient of the term z^{34} in f_{surf} , which agrees with the result from the finite-lattice method displayed in Table 9.

5.4 Large- q expansion for the strip free energy: Cylindrical boundary conditions

The large- $|q|$ expansion of the free energy for a semi-infinite strip with cylindrical boundary conditions is

$$\begin{aligned} f_m^P(q) &= \frac{1}{m} \log \lambda_{*,m}^P(q) \\ &= \log q + \frac{1}{m} \log \left[\sum_{k=0}^{\infty} (-1)^k b_k^P(m) q^{-k} \right] \\ &= \log q + \frac{1}{m} \sum_{k=1}^{\infty} (-1)^k c_k^P(m) q^{-k} \end{aligned} \quad (5.37)$$

Once again, if m is large enough (depending on k), we can replace the coefficients $c_k^P(m)$ by the corresponding polynomials $C_k^P(m)$ [cf. (4.26)]. These polynomials C_k^P are of degree 1 in m with a zero constant term for $1 \leq k \leq 16$, and we conjecture that this behavior holds for every $k \geq 1$. Thus, $f_m^P(q)$ contains [as predicted in (5.9b)] only a single m -independent term $f_{\text{bulk}}(q) = f(q)$; there is no surface contribution. Of course this result is to be expected, as an infinitely long cylinder has no boundary. This computation using the polynomials C_k^P yields a series for f_{bulk} that is the *same*, up to the order we are able to compute (namely, q^{-16}), as for free boundary conditions; in particular, it provides an independent check of the first 16 terms of the series (5.25). Conversely, the finite-lattice computation of the preceding subsection provides an independent confirmation of the empirically observed regularities in the behavior of the polynomials C_k^P [cf. (4.28)–(4.31)].

If we use the bulk free-energy series (5.25) as input, we can compute the term of order q^{-17} in the surface free energy: as expected, we find that it vanishes.

5.5 Analysis of the large- q series

In this subsection we shall perform a series-extrapolation analysis of the large- q series (5.23) ff. for the bulk free energy, (5.31) ff. for the surface free energy, and (5.32) ff. for the corner free energy. As a warm-up, we shall first perform an analogous analysis for the large- q series of the strip free energy $f_m(q)$ for two selected cases, $m = 3_F$ and $m = 4_P$. In these cases we can easily generate long large- q series (up to 100 terms or more) using the symbolic power method (see footnote 16 above) and can compare the predicted location and nature of singularities with the exactly known answers [6]. In this way, we can learn how many terms in the large- q series are likely to be needed in order to extract specific features of the singularity structure.

Before beginning this analysis, it is useful to know what types of singularities we are expecting. For statistical-mechanical models with only one dimension tending to infinity (i.e., finite-width strips), the answer is clear: the free energy $f_m(q)$ [cf. (5.4)] is an analytic function of q except at branch points arising from the collision of two eigenvalues. Therefore, the limiting curve \mathcal{B}_m is *not* a curve of singularities of the free energy; only its endpoints are singularities.

For statistical-mechanical models with two or more dimensions tending to infinity, as in our infinite-width limit $m \rightarrow \infty$, the situation is much less clear. It is well established in a variety of cases [58–61] that the infinite-volume free energy has a “soft” essential singularity (i.e., one in which the free energy is infinitely differentiable but not analytic) at a first-order phase transition in the physical region. What is less clear, however, is how the free energy behaves on *complex* phase boundaries (such as our limiting curve \mathcal{B}_∞). For instance, the point $h = 0$ is known rigorously to be an essential singularity for the free energy of a low-temperature Ising ferromagnet in dimension $d \geq 2$ [58, 59, 61]: it is not possible to analytically continue *through* this point, because the derivatives at $h = 0$ grow too fast (the Taylor series has zero radius of convergence). But might it be possible to analytically continue *around* this point in the complex h -plane? If so, then the imaginary axis $\text{Re } h = 0, \text{Im } h \neq 0$ would be merely the curve where two analytic functions *defined in a neighborhood of that curve* — namely, the free energies that are initially defined for $\text{Re } h > 0$ and for $\text{Re } h < 0$ but are analytically continuable to at least part of the opposite half-plane, the point $h = 0$ excluded — have equal real part. By contrast, the alternative scenario is that these two analytic functions *cannot* be continued into any part of the opposite half-plane: that is, they would have the full imaginary axis $\text{Re } h = 0$ as a *natural boundary*. It does not seem to be known, even heuristically, which of these two scenarios is correct.²⁶

5.5.1 Differential approximants

To perform the series-extrapolation analysis of our large- q series, we shall use the *differential-approximant (DA) method*: see the review [64] and the references cited therein. The idea is simple: The K th-order approximant $[N_0, N_1, \dots, N_K; M]$ to a power series $F(z) = \sum_{k=0}^{\infty} f_k z^k$ is built by choosing polynomials Q_0, Q_1, \dots, Q_K

²⁶See also [62, 63] for related work on complex phase boundaries and partition-function zeros.

and P of degrees N_0, N_1, \dots, N_K and M , respectively, so that the solution \tilde{F} of the inhomogenous linear differential equation

$$\sum_{j=0}^K Q_j(z) \left(z \frac{d}{dz} \right)^j \tilde{F}(z) = P(z) \quad (5.38)$$

agrees with the initial coefficients of the series $F(z)$ through order z^N , where $N = \sum_{i=0}^K (N_i + 1) + M$ (notice that we fix the overall normalization with $Q_K(0) = 1$). The singularities of $\tilde{F}(z)$ are located at the zeros $\{z_\ell\}$ of the polynomial Q_K (and possibly also at $z = 0$ and $z = \infty$), and the critical exponent associated to a *simple* zero z_ℓ of Q_K is given by

$$\lambda_\ell = K - 1 - \frac{Q_{K-1}(z_\ell)}{z_\ell Q'_K(z_\ell)}, \quad (5.39)$$

in the sense that $\tilde{F}(z) \sim (z - z_\ell)^{\lambda_\ell}$ as $z \rightarrow z_\ell$.

In practice, we have used a MATHEMATICA code to obtain the polynomials Q_j *exactly* (i.e., with exact rational arithmetic) from the coefficients $\{f_k\}$, and then used the program MPSOLVE [65, 66] to compute the N_K zeros of the polynomial Q_K to very high precision (i.e., 100 digits). Our code and the numerical accuracy of its results were checked in a previous work [67] with the help of an independent C++ program written by Y. Chan, A.J. Guttmann and A. Rechnitzer.

In many cases, one is principally interested in the singularities that are located on the real axis. This assumption simplifies a bit the practical procedure, as one needs to search only on a one-dimensional space. However, in our case we want to locate all the singularities (real or complex) of the approximants. In fact, we expect from the sign pattern of the series coefficients (5.23)–(5.25) [cf. Table 9] that the leading singularity of the bulk free energy is *not* on the real z -axis. Therefore, we need to slightly change the usual definition of a non-defective approximant (i.e., those that are taken into account in the computation) [64, 67]. Roughly speaking, we want to consider an approximant $[N_0, N_1, \dots, N_K; M]$ to be non-defective if there is a zero of Q_K sufficiently near to the expected (complex) singularity, and this zero is sufficiently well separated from all other zeros of Q_K .

Of course, this definition needs to be made more precise; and things are made more difficult by the fact that we do not know even roughly the position of the singularities in the complex z -plane. In order to find a rough estimate of these positions, we first make a histogram of all the “well-separated” complex zeros $\{z_\ell\}$ coming from all computed approximants $[N_0, N_1, \dots, N_K; M]$. A pair of complex zeros z_1, z_2 of Q_K is defined to be well-separated if $|z_1 - z_2| > R$ for some (small) free parameter R ; a zero z_1 is then defined to be well-separated if it is well-separated from all other zeros (in particular, it is required to be simple). Given a fixed value of R , we select from each polynomial Q_K the well-separated zeros and make the corresponding histogram, using square cells of side $R' = 0.04$. This histogram is expected to display peaks at the singularities of the function F . We further expect that the final result should not depend strongly on the chosen value of R . In practice, we started with $R = 0.2$ and then compared the histogram to those obtained with smaller values of $R =$

0.1, 0.05, 0.02, etc. We considered that the procedure had converged when the number and positions of the peaks did not vary when “halving” the value of R . Usually, the choice $R = 0.05$ was optimal.

Each peak displayed in the histogram corresponds to a cell in the complex z -plane: $\text{Re } z \in [A_1, A_2]$ and $\text{Im } z \in [B_1, B_2]$ with $A_2 - A_1 = B_2 - B_1 = R' = 0.04$. Therefore, for a given singularity z_ℓ , we consider an approximant $[N_0, N_1, \dots, N_K; M]$ to be non-defective if there is a (simple) zero of Q_K inside the above cell, and there is no other zero of Q_K inside the larger region $\text{Re } z \in [A_1 - 0.05, A_2 + 0.05]$ and $\text{Im } z \in [B_1 - 0.05, B_2 + 0.05]$.²⁷ Then we perform the analysis explained by Guttman in his review article [64]. Taking all the non-defective approximants of a given order N corresponding to a given singularity z_ℓ , we form the mean and standard deviation for each of the three quantities $\text{Re } z$, $\text{Im } z$ and λ . Of course, this standard deviation is only pseudo-statistical; for brevity we term it the “error bar”, but it is not necessarily indicative of the accuracy of the estimate.

Our initial goals are twofold: to test that the above-described procedure gives the right answers in exactly soluble cases, and to determine how the estimates for the positions $\{z_\ell\}$ and critical exponents $\{\lambda_\ell\}$ of the singularities vary with the available order N of the series.²⁸ In order to achieve these goals, we have chosen two simple examples for which we know the position and type of all the singularities, and for which we can easily obtain many terms of the corresponding free energies (say, 100 terms): namely, the strip free energies $m = 3_F$ and $m = 4_P$. As in Ref. [67], we have computed the approximants of first and second order ($K = 1, 2$) satisfying $|N_i - N_j| \leq 1$. There are four free parameters in this computation: the maximum degree $N_{0,\max}$ of the polynomial Q_0 , the maximum degree M_{\max} of the inhomogeneous term P , the minimum number of series coefficients used in the analysis N_{\min} , and the number of available coefficients N . We have chosen the first three parameters in terms of N in the following way: $N_{0,\max} = 0.8N$, $M_{\max} = 0.5N$, and $N_{\min} = 0.3N$. Thus, the only free parameter in the computation is N . In our test cases, we have chosen N to range between 30 and 100 in steps of 10. The two test cases are described in the next subsection.

5.5.2 Test cases: $m = 3_F$ and $m = 4_P$

The eigenvalues for the case $m = 3_F$ are the solutions of the quadratic equation [6]

$$\lambda^2 - (q^3 - 5q^2 + 11q - 10)\lambda + (q^4 - 7q^3 + 19q^2 - 24q + 11) = 0. \quad (5.40)$$

Therefore, the only singularities are those corresponding to the six endpoints of the limiting curve \mathcal{B}_3 , where the discriminant of the quadratic vanishes. In the complex

²⁷For real singularities, we used a slightly different definition: namely, for zeros near $z = 0.5$ (resp. $z = -1$) we asked that there should be no other zero in the region $|\text{Im } z| \leq 0.1$ and $\text{Re } z \in [0, 1.2]$ (resp. $\text{Re } z \in [-1.8, 0]$).

²⁸That is, we assume that we know the coefficients of the series $F(z)$ through order z^N . Sometimes we shall refer loosely to N as the “number of available coefficients” even though, strictly speaking, the number of available coefficients (including the constant term) is $N + 1$.

plane of $z = 1/(q - 1)$, they are located at

$$z_1 \approx -0.2811172691 \pm 0.7752009092 i \quad (5.41a)$$

$$z_2 \approx 0.4477839366 \pm 0.5382490441 i \quad (5.41b)$$

$$z_3 = \frac{3 + \sqrt{3}i}{6} \approx 0.5 \pm 0.2886751346 i \quad (5.41c)$$

In Figures 1(a,b) we plot the histograms obtained with $N = 50$ and $N = 100$, respectively, using $R = 0.05$. The number of zeros contained in each square cell of linear size 0.04 is indicated with a gray scale of 16 tones: those cells with the maximum number of zeros are depicted in black, while those with the smallest number of zeros (i.e., less than 7% of that maximum number) are depicted in white. We have labelled the peaks with $\text{Im } z \geq 0$ as z_1, \dots, z_7 . We observe several empirical properties: as N is increased, the number of peaks increases (e.g. z_6 and z_7 appear for $N = 100$ but not for $N = 50$) and some of the peaks become sharper (e.g. z_4); furthermore, we find more peaks than the actual number of singularities (we expect three pairs of complex-conjugate peaks z_1, z_2, z_3 , but we also find two further pairs z_4, z_7 of complex-conjugate peaks and two peaks z_5, z_6 on the real axis).²⁹ For each of the seven peaks, we have performed the analysis described in the preceding subsection, in order to estimate the position of the singularity and the corresponding exponent. In Tables 10 and 11 we display the results.

We indeed find the three “correct” singularities associated to each of three endpoints of the limiting curve in the upper half-plane (see Table 10). As the number of coefficients is increased, the accuracy of the results increase: with $N = 100$ we attain a maximum accuracy of order 10^{-7} (resp. 10^{-5}) for the position of the singularity (resp. the critical exponent), and in all cases the estimate agrees with the known exact value within 3 times the claimed error bar (and usually much less).

In Table 11, we show the “singularities” found in the series analysis that do *not* correspond to any of the endpoints of the limiting curve. Once again, as we increase the number of coefficients N in the analysis, the claimed error bars decrease. Let us stress that the exponents of the first three singularities (z_4, z_5, z_6) are consistent with $\lambda = 0$; therefore, the DA analysis is asserting (correctly) that there is no true singularity at these points. The same conclusion holds for the point z_7 , for which estimated exponent is very close to the positive-integer value $\lambda = 2$. Finally, it seems that $z_5 = -1$ (i.e., $q = 0$). For this example, at least, the DA method has itself told us (correctly) that the only true singularities are those shown in Table 10.

In Figure 2(a) we plot the limiting curve for $m = 3_F$ in the complex z -plane together with the singularities found by the series analysis. For comparison, we have also estimated the radius of convergence of the series from the formula $r_{\text{conv}} = \liminf_{n \rightarrow \infty} |a_n|^{-1/n}$: despite some oscillations, we are able to obtain the estimate $r_{\text{conv}} \approx 0.5982$, which is close to (and slightly larger than) the modulus $|z_3| \approx 0.5774$ of the singularity closest to the origin (see Table 10).

²⁹In some cases, we find a “broad” peak that has large counts in two (or more) neighboring cells. These peaks are counted as one peak; but we have always looked carefully to see whether they have a finer structure or not (i.e., if they correspond to two nearby singularities).

The case $m = 4_P$ is more involved from a numerical point of view because, even though the free-energy singularities are of the same type as for $m = 3_F$ (namely, square-root branch points with $\lambda = 1/2$), two of them lie extremely close to one another. The eigenvalues for this strip are given by the solutions of the quadratic equation [6]

$$\lambda^2 - (q^4 - 8q^3 + 29q^2 - 55q + 46)\lambda + (q^6 - 12q^5 + 61q^4 - 169q^3 + 269q^2 - 231q + 85) = 0. \quad (5.42)$$

The eight endpoints of the corresponding limiting curve are located in the z -plane at

$$z_1 \approx 0.3316354418 \pm 0.2371152471 i \quad (5.43a)$$

$$z_2 \approx -0.0681712693 \pm 0.4798609413 i \quad (5.43b)$$

$$z_3 \approx 0.2814289723 \pm 0.4521062477 i \quad (5.43c)$$

$$z_4 \approx 0.7398155434 \quad (5.43d)$$

$$z_5 \approx 0.7978491474 \quad (5.43e)$$

In Tables 12 and 13 we display our results as a function of N . (For brevity we refrain from showing the histograms.) The three complex singularities (z_1, z_2, z_3) and their corresponding exponents are well determined with small error bars. However, the determination of the two closely-separated real singularities (z_4, z_5) is (not surprisingly) rather poor: these singularities can be seen only if we have at least 80 coefficients, and even with 90 coefficients we obtain only a single singularity located in-between the two endpoints. Only for $N = 100$ do we start seeing a (noisy) signal of the second endpoint.

In this case the analysis also gives two singularities that do not correspond to any of the endpoints of the limiting curve (see Table 13). One is located at $z = -1$ (i.e. $q = 0$) and the other at $z \approx 0.285 \pm 0.518 i$. In both cases, the critical-exponent estimate is consistent with $\lambda = 0$. Therefore, the DA analysis is itself telling us that they are not true singularities.

In Figure 2(b) we plot the limiting curve for $m = 4_P$ in the complex z -plane together with the singularities found by the series analysis. We have also estimated the radius of convergence of the series using $r_{\text{conv}} = \liminf_{n \rightarrow \infty} |a_n|^{-1/n}$: the result is $r_{\text{conv}} \approx 0.4216$, which is close to (and slightly larger than) the modulus $|z_1| \approx 0.4077$ of the singularity closest to the origin (see Table 12).

5.5.3 Analysis of the series for the bulk, surface and corner free energies

We are now ready to analyze the large- q series (5.23) ff. for the bulk free energy, (5.31) ff. for the surface free energy, and (5.32) ff. for the corner free energy. We began by analyzing the series expansions for the exponential of the free energy $e^{f_i(z)}$ [$i = \text{bulk, surface, corner}$] using the variable $z = 1/(q - 1)$. Later we tried analogous analyses for the free energy $f_i(z)$ itself, and analyses using $1/q$ as the variable instead of z .

For the bulk free energy, we have $N = 47$ coefficients. The histograms for the $K = 1$ and $K = 2$ approximants are displayed in Figure 3(a,b), using the gray-scale

coding described earlier. If we compare these histograms to that of the test case of Figure 1(a) with a similar number of coefficients ($N = 50$), we see that the zeros do not accumulate on small regions on the complex z -plane as they did for the test case; rather, we find a complex-conjugate pair of broad peaks z_1 , a broad peak z_2 on the real axis, and for $K = 1$ a rather sharp peak $z_3 \approx -1$. It is unclear (at least to us) what this behavior of the differential approximants is telling us about the singularity structure of the function $e^{f_{\text{bulk}}(z)}$; suffice it to say that we do not expect to obtain terribly accurate estimates for the locations and exponents of the singularities.

For the point z_1 using the second-order ($K = 2$) approximants, our protocol gives the estimates

$$z_1 = 0.25(4) \pm 0.40(4) i \quad (5.44a)$$

$$\lambda_1 = -2.4(6) \quad (5.44b)$$

For the first-order ($K = 1$) approximants, the estimates are

$$z_1 = 0.28(7) \pm 0.44(7) i \quad (5.45a)$$

$$\lambda_1 = -1.6(6) \quad (5.45b)$$

For the broad peak z_2 on the real axis, all the non-defective zeros are precisely real (if they weren't, they would come in complex-conjugate pairs so close to the real axis that they would fail to be well-separated), and for $K = 2$ our protocol gives the estimates

$$z_2 = 0.60(8) \quad (5.46a)$$

$$\lambda_2 = -1.5(14) \quad (5.46b)$$

For $K = 1$, the estimates are

$$z_2 = 0.64(7) \quad (5.47a)$$

$$\lambda_2 = -1.7(6) \quad (5.47b)$$

The peak z_3 is seen only in the $K = 1$ approximants, and we estimate

$$z_3 = -1.00(2) \quad (5.48a)$$

$$\lambda_3 = 1.0(1) \quad (5.48b)$$

The exponent $\lambda_3 \approx 1$ suggests that z_3 may not be a singularity of $e^{f_{\text{bulk}}(z)}$, but rather a simple zero; if so, it would be a logarithmic singularity of the free energy $f_{\text{bulk}}(z)$.

We also analyzed the series expansion (5.25) of the bulk free energy $f_{\text{bulk}}(z)$ [as opposed to its exponential (5.23), which we have discussed until now]. In Figure 4 we show the histogram for the $K = 2$ approximants of $f_{\text{bulk}}(z)$. For z_1 and z_2 the picture is roughly similar to what was seen in Figure 3(b); but for z_3 we see a much sharper peak. Our protocol gives the estimates

$$z_3 = -1.02(2) \quad (5.49a)$$

$$\lambda_3 = -0.6(5) \quad (5.49b)$$

The estimate $\lambda = -0.6(5)$ in (5.49b) is barely compatible with the value $\lambda = 0$ corresponding to a logarithmic singularity in f_{bulk} , which is what we would expect if $e^{f_{\text{bulk}}}$ has a singularity or zero of finite order [e.g. the estimate (5.48b) that suggests a simple zero].

For the surface free energy, we have $N = 47$ coefficients (assuming the correctness of the conjectural last coefficient). The histograms for $K = 1$ and $K = 2$ approximants are displayed in Figure 5, and they look even broader than those for the bulk free energy. Using second-order ($K = 2$) differential approximants we are able to reliably locate only one singularity, namely

$$z_1 = 0.25(4) \pm 0.39(4) i \quad (5.50a)$$

$$\lambda_1 = -2.0(8) \quad (5.50b)$$

(The estimate for z_2 is

$$z_2 = -1.02(2) \quad (5.51a)$$

$$\lambda_2 = -1.9(15), \quad (5.51b)$$

which we disregard because the error bar on λ_2 is so large.) For first-order ($K = 1$) approximants, we find two singularities

$$z_1 = 0.25(5) \pm 0.43(9) i \quad (5.52a)$$

$$z_2 = 0.7(1) \quad (5.52b)$$

with exponents $\lambda_1 = -1.3(5)$ and $\lambda_2 = -1.6(11)$, respectively.

Finally, for the corner free energy, we have $N = 46$ coefficients, and the corresponding histograms are displayed in Figure 6(a,b). In this case, we find a fairly sharp peak around $z_2 \approx 0.5$ (it is especially sharp for $K = 1$), and a complex-conjugate pair of broad peaks around $z \approx 0.2 \pm 0.4 i$ (they are, in fact, slightly less broad than for the bulk and surface free energies). As these peaks are close to those found for the other two free energies, let us try to locate them carefully. Using second-order ($K = 2$) differential approximants we locate two singularities:

$$z_1 = 0.22(4) \pm 0.36(5) i \quad (5.53a)$$

$$z_2 = 0.51(1) \quad (5.53b)$$

with associated critical exponents $\lambda_1 = -1.9(9)$ and $\lambda_2 = -1.1(3)$. These error bars are smaller than those found for the bulk and surface free energies (this is especially so for z_2), reflecting the sharper peaks in the histogram. For first-order ($K = 1$) approximants, we find the singularities

$$z_1 = 0.23(3) \pm 0.36(2) i \quad (5.54a)$$

$$z_2 = 0.509(10) \quad (5.54b)$$

with exponents $\lambda_1 = -1.8(7)$ and $\lambda_2 = -1.0(1)$. As for bulk case, the analysis of series for $f_{\text{corner}}(z)$ [rather than its exponential] leads to a new singularity $z_3 \approx -1$,

with a quite sharp peak: see Figure 6(c) for the histogram corresponding to the $K = 2$ approximants. Our analysis of this peak yields

$$z_3 = -1.007(8), \quad (5.55)$$

with exponent $\lambda_3 = -0.8(2)$. The error bar here is about half of that found in (5.48a)/(5.49a) for the bulk and surface free energies, reflecting the sharper peak in the histogram.

One possible reason for the better behavior of the corner-free-energy series, at least as concerns the real zeros z_2 and z_3 , comes from the empirical fact that the series for $f_{\text{corner}}(q)$, written in powers of $1/q$, has all *nonnegative* coefficients (as does, therefore, the series for its exponential). By contrast, all the other series analyzed here have coefficients of both signs, with no clear sign pattern.

In order to obtain more realistic error bars, we have repeated the analysis using the following variations (in addition to the order of the differential approximant $K = 1, 2$):

- Using the free energy f_i instead of its exponential e^{f_i} .
- Using the variable $1/q$ instead of the variable $z = 1/(q - 1)$.
- “Truncating” the series expansions of $e^{f_i(z)}$ by deleting the terms of order z^0, \dots, z^9 and then dividing by z^{10} . This truncation ought to have little influence on the estimates of the singularities, as the relevant information is encoded in the higher-order terms.

Alas, the estimates obtained with these procedures deviate among themselves by about twice the error bars provided by each method. For instance, the position of the singularity z_1 for the bulk free energy takes values ranging from $0.23(3) \pm 0.39(3) i$ [for the truncated series expansion of $e^{f_{\text{bulk}}(z)}$ with $K = 2$] to $0.30(4) \pm 0.51(5) i$ [for the series expansion of $f_{\text{bulk}}(1/q)$ with $K = 1$].

Taking all this information into account, our final estimates for the location of the singularities are

$$\text{Bulk} \Rightarrow \begin{cases} z_1 = 0.26(4) \pm 0.42(4) i \\ z_2 = 0.63(10) \\ z_3 = -1.01(2) \end{cases} \quad (5.56a)$$

$$\text{Surface} \Rightarrow \begin{cases} z_1 = 0.24(4) \pm 0.39(5) i \\ z_2 = 0.67(14) \end{cases} \quad (5.56b)$$

$$\text{Corner} \Rightarrow \begin{cases} z_1 = 0.23(4) \pm 0.37(4) i \\ z_2 = 0.51(1) \\ z_3 = -1.01(1) \end{cases} \quad (5.56c)$$

(We refrain from further discussion of the exponents λ_i , because the error bars are so large.)

We see from (5.56) that the estimated locations of the singularities associated to the three free energies are (as expected) compatible within errors. Combining these estimates, we obtain

$$z_1 = 0.24(4) \pm 0.39(4) i \quad [q_1 = 2.14(19) \pm 1.86(19) i] \quad (5.57a)$$

$$z_2 = 0.51(2) \quad [q_2 = 2.96(8)] \quad (5.57b)$$

$$z_3 = -1.01(1) \quad [q_3 = 0.01(1)] \quad (5.57c)$$

The absolute values are therefore $|z_1| = 0.46(5)$, $|z_2| = 0.51(2)$ and $|z_3| = 1.01(1)$.

In Figure 7(a,b,c) we compare the estimates (5.56) for z_1, z_2, z_3 with the two best currently available approximations to the square-lattice limiting curve \mathcal{B}_∞ (namely, the curves \mathcal{B}_m coming from $m = 7$ with toroidal boundary conditions [10] and $m = 11$ with cylindrical boundary conditions [7]). We also show a circle with radius $r_{\text{conv}} \approx 0.4290$ [resp. $r_{\text{conv}} \approx 0.4225$, $r_{\text{conv}} \approx 0.4139$] indicating the radius of convergence obtained by estimating $r_{\text{conv}} = \liminf_{n \rightarrow \infty} |a_n|^{-1/n}$.

Let us discuss the three singularities in order.

The singularity of smallest modulus is the complex point z_1 , given by (5.57a). From Figure 7 we see that the estimated location z_1 lies fairly close to the most prominent T point of the limiting curve $\mathcal{B}_{7\text{tor}}$ (solid black line), namely [10, sec. 3.6]

$$z_{\text{T},7\text{tor}} = 0.26158090412 \pm 0.3162213774 i \quad [q_{\text{T},7\text{tor}} = 2.5531414480 \pm 1.8775702667 i], \quad (5.58)$$

and one can conjecture that this is not an accident. On the other hand, this singularity lies rather far from the T point of the limiting curve $\mathcal{B}_{11\text{cyl}}$ (dashed green curve), namely [7, sec. 3.3]

$$z_{\text{T},11\text{cyl}} = 0.409 \pm 0.218 i \quad [q_{\text{T},11\text{cyl}} = 2.902 \pm 1.015 i]. \quad (5.59)$$

Thus, we are unable to draw any firm conclusion about the physical nature of this singularity. It does, however, seem likely that this singularity lies somewhere on the limiting curve \mathcal{B}_∞ — possibly (but not necessarily) at a “special” point of \mathcal{B}_∞ such as a T point.

The two singularities on the real axis are given by (5.57b,c). The estimate for z_2 is compatible within errors with $q_2 = 3$, which is the physical critical point $q_c(\text{sq}) = 3$ of the square-lattice zero-temperature Potts antiferromagnet [68–75] and is expected to be the uppermost real crossing point of the limiting curve \mathcal{B}_∞ (see Section 6.2 below). The estimate for z_3 is compatible with $q_3 = 0$, which is expected to be the lowermost real crossing point of the limiting curve \mathcal{B}_∞ .

In conclusion, the analysis of the free-energy series expansions has led to the location of four singularities in the complex q -plane: two of them are the real points $q = 0$ and $q = 3$, which correspond to the transitions between the disordered and critical phases, while the other two are a pair of complex-conjugate points that presumably lie somewhere on the limiting curve \mathcal{B}_∞ , *possibly* at a “special” point such as a T point.

Our difficulties in locating the singularities of the free energies — in particular, the wide dispersion of estimates visible in the histograms (Figures 3–6), which contrasts strongly with the behavior observed in our test cases 3_F and 4_P (Figure 1) — suggest that the singularity structure of the infinite-volume free energies may be quite different from that of the finite-width strips that we used as test cases. In particular, it is possible that the entire limiting curve \mathcal{B}_∞ is a natural boundary for the infinite-volume free energies — possibly with a very soft singularity — and that the differential approximants are trying, with limited success, to mimic this behavior. In this interpretation, the points z_1 , z_2 and z_3 would simply be approximations to the places on \mathcal{B}_∞ where the free energies are most strongly singular; and one would furthermore expect that as the number N of series coefficients increases, the number of peaks in the histograms will increase, and the zeros will gradually condense on the whole of the curve \mathcal{B}_∞ (perhaps with high density on some parts of the curve and low density on others). It would be interesting to try further numerical tests of this scenario; but they will probably require fairly radical extensions of our large- q series, e.g. to order $N \approx 100$.

6 Numerical results for widths $m = 9_F, 10_F, 11_F, 12_F$

As part of this work, we have computed the transfer matrices for square-lattice strips with free boundary conditions and widths $m = 9, 10, 11, 12$. (Widths $m \leq 8$ were computed in a previous paper [6].) In this section we use these newly-computed transfer matrices to study the real and complex roots of the chromatic polynomials $P_{m_F \times n_F}(q)$ for $m = 9, 10, 11, 12$, focusing on the behavior in the infinite-length limit ($n \rightarrow \infty$). In Section 6.1 we discuss the limiting curve \mathcal{B}_m and the isolated limiting points for each width m . In Section 6.2 we study the behavior of the real crossing points $q_0(m)$ and attempt to extract $q_0(\text{sq}) = \lim_{m \rightarrow \infty} q_0(m)$. In Section 6.3 we discuss the *real* chromatic roots for finite lattices $m_F \times n_F$.

6.1 Limiting curves and isolated limiting points

Having computed the transfer matrices for $m = 9_F, 10_F, 11_F, 12_F$, we can analyze them as in [6–10] to extract the chromatic roots for finite-length lattices ($n < \infty$) as well as the limiting curves and isolated limiting points in the infinite-length limit ($n \rightarrow \infty$). Unfortunately, we have not been able to compute the full limiting curves \mathcal{B}_m , as this would have required a major computational effort. However, we have tried to locate the most important points on each of them, i.e. crossings of the real axis and endpoints near the real axis, using the direct-search method [6]. These results are summarized in Table 14.³⁰ (Furthermore, the chromatic roots for $n = 5m$ and $n = 10m$ shown in Figures 8(a)–(d) give a fairly good idea of the general shape of

³⁰For widths $m \leq 11$, we implemented the direct-search method in MATHEMATICA, using 100-digit internal precision. For width $m = 12$, we used the double-precision FORTRAN subroutines in the ARPACK package [76]. We also checked our results for $7 \leq m \leq 11$ using ARPACK; the results are consistent with those obtained using MATHEMATICA but are less precise.

the curve \mathcal{B}_m .) Finally, for all these strips there are real isolated limiting points at the Beraha numbers $q = 0, 1, 2, B_5$, and for $m = 9, 11, 12$ there also appear to be complex isolated limiting points (we cannot, however, guarantee that we have found all of them). In Figures 8(a)–(d) these points are marked with a \times sign.

For $m = 9$, the dimension of the transfer matrix is 179. In Figure 8(a) we have plotted the chromatic zeros in the complex q -plane for the strips $9_F \times 45_F$ and $9_F \times 90_F$. The limiting curve crosses the real q -axis at a single point:

$$q_0(9) \approx 2.70165995678. \quad (6.1)$$

Figure 8(a) also suggests that there is a complex-conjugate pair of isolated limiting points at $q \approx 2.5946 \pm 0.5963 i$.

For $m = 10$, the dimension of the transfer matrix is 435. In Figure 8(b) we have plotted the chromatic zeros for the strips $10_F \times 50_F$ and $10_F \times 100_F$. In this case the limiting curve does not cross the real q -axis; rather, there is a pair of complex-conjugate endpoints very close to the real q -axis, at

$$q_0(10) \approx 2.7343903604 \pm 0.0003924978 i. \quad (6.2)$$

For $m = 11$, the dimension of the transfer matrix is 1142. In Figure 8(c) we have plotted the chromatic zeros for the strips $11_F \times 55_F$ and $11_F \times 110_F$. The limiting curve crosses the real q -axis at

$$q_0(11) \approx 2.7608973951. \quad (6.3)$$

Figure 8(c) also suggests that there are two complex-conjugate pairs of isolated limiting points at $q \approx 2.6555 \pm 0.4978 i$ and $q \approx 2.4648 \pm 1.1380 i$.

Finally, for $m = 12$, the dimension of the transfer matrix is 2947. In Figure 8(d) we have plotted the chromatic zeros for the strips $12_F \times 60_F$ and $12_F \times 120_F$. In this case the limiting curve does not seem to cross the real q -axis; rather, there is a pair of complex-conjugate endpoints very close to the real q -axis, at

$$q_0(12) \approx 2.782817590 \pm 0.00018700 i. \quad (6.4)$$

Figure 8(d) also suggests that there is a complex-conjugate pair of isolated limiting points at $q \approx 2.6172 \pm 0.7562 i$.

In view of the results reported in Table 14, we conjecture that the limiting curve \mathcal{B}_m crosses the real axis for all odd m and has a complex-conjugate pair of endpoints very near the real axis for all even $m \geq 8$.

6.2 Value of $q_0(\text{sq})$

We can try to use the results reported in Table 14 to obtain the value of $q_0(\text{sq}) = \lim_{m \rightarrow \infty} q_0(m)$. Of course, we expect $q_0(\text{sq}) = 3$ [68–75], but it will be interesting to see with what accuracy this result can be obtained.

Let us also warn the reader that the value for $m = 8$ reported in [6] is wrong; the correct value is displayed here in Table 14.

As just discussed, there are clear parity effects in $q_0(m)$: the limiting curve \mathcal{B}_m crosses the real q -axis for odd m but not for even m . We have therefore split the data into two sets according to the parity of m , and analyzed each set separately. Please note that the data for $q_0(m)$ are essentially exact: there is a tiny *non-statistical* error of order 10^{-10} in their numerical estimates. In order to keep to the standard notation in finite-size-scaling theory, we here denote the strip width by L instead of m .

For each data set we have considered several Ansätze, and for a given Ansatz with k free parameters, we have taken into account the points with $L = L_{\min}, L_{\min} + 2, \dots, L_{\min} + 2(k - 1)$. So in each fit there are no degrees of freedom. From the variation of the estimates as L_{\min} is increase, we can roughly estimate the error bar.

If we use the power-law Ansatz

$$q_0(L) = q_0(\text{sq}) + BL^{-\Delta} \quad (6.5)$$

for the data coming from odd L , we obtain the following estimates using $L_{\min} = 7$

$$q_0(\text{sq}) = 2.999(5) \quad (6.6a)$$

$$\Delta = 1.108(16) \quad (6.6b)$$

where the error bars are defined to be twice the distance between these estimates and those obtained with $L_{\min} = 5$.

If we play the same game for the quantity $\text{Re } q$ for even L , we arrive at the estimates for $L_{\min} = 8$

$$q_0(\text{sq}) = 3.00(7) \quad (6.7a)$$

$$\Delta = 1.10(29) \quad (6.7b)$$

where again the error bars are twice the difference from the estimates for $L_{\min} = 6$. The convergence in this case is not very good, so we cannot trust these results too much.

The results (6.6)/(6.7) are consistent with the behavior

$$q_0(\text{sq}) = 3 \quad (6.8a)$$

$$\Delta = 1 \quad (6.8b)$$

Of course, we expect that $q_0(\text{sq}) = q_c(\text{sq}) = 3$; moreover, the correction exponent $\Delta = 1$ is to be expected for *free* b.c. because of the surface effect. For cylindrical boundary conditions [7, Section 4], the estimates are less well converged but are consistent with $q_0(\text{sq}) = 3$ and suggest that $\Delta \gtrsim 1.7$ (e.g. perhaps $\Delta = 2$). Finally, very recent work [10, Section 5.1] gives strong evidence that $q_0(\text{sq}) = 3$ holds also for toroidal boundary conditions.³¹

³¹The authors of Ref. [10] found that for toroidal square-lattice strips of *odd* widths $3 \leq L \leq 11$, the value of $q_0(L)$ is *exactly* equal to the expected limiting value $q_0(\text{sq}) = 3$, while for toroidal strips of *even* widths $2 \leq L \leq 12$, the fits of the numerical data to the Ansatz (6.5) gave $q_0(\text{sq}) = 2.999 \pm 0.012$ and $\Delta = 2.04 \pm 0.08$, in agreement with the conjectured behavior (6.8a) but suggesting that here $\Delta = 2$.

Better fits can in principle be obtained by imposing the values (6.8). In particular, we expect the following Ansatz to describe better the data points:

$$q_0(L) = 3 - BL^{-1} - CL^{-2}. \quad (6.9)$$

However the results are not very stable: for odd L we find that for $L_{\min} = 7$, $B \approx 2.436$, and $C \approx 2.243$, while for $L_{\min} = 9$, $B \approx 2.283$, and $C \approx 2.719$. A similar behavior is found for even L : for $L_{\min} = 8$, $B \approx 2.409$, and $C \approx 2.473$, while for $L_{\min} = 10$, $B \approx 2.357$, and $C \approx 2.994$. We conclude that our numerical data are not accurate enough to be able to accurately determine corrections to scaling to the behavior of $q_0(L)$.

For odd L , we can also look at $\text{Im } q_0(L)$. In Ref. [7, Conjecture 4.2] it was conjectured that for square-lattice strips with cylindrical boundary conditions $\text{Im } q_0(L) \sim B_5^{-L/2} = \tau^{-L}$ where $\tau = (1 + \sqrt{5})/2$ is the golden ratio. We have fitted our numerical results for $\text{Im } q_0(L)$ with $L = 8, 10, 12$ to check whether this conjecture holds or not also for free boundary conditions. A 3-parameter fit to a power-law Ansatz $\text{Im } q_0(L) = A + BL^{-\Delta}$ shows that $A \approx -0.00042$ is indeed a small number. We also obtain that $B \approx 0.033$ and $\Delta \approx 1.606$. As we have only three data points, there are no degrees of freedom in the fit and the error bars cannot be reliably estimated. In conclusion, we expect that $\text{Im } q_0(L)$ decays to zero exponentially fast. Thus, we use the improved Ansatz: $\text{Im } q_0(L) = A \times B^L$. The results for $L_{\min} = 10$ are $A = 0.16(13)$ and $B = 0.690(75)$. The error bars are computed as twice the difference between the estimates for $L_{\min} = 10$ and $L_{\min} = 8$. If we compare $B^{-1} = 1.44(16)$ to $\tau \approx 1.6180339887$, we see that they are barely compatible within errors. As the error bar for B^{-1} is 20 times larger than the corresponding error for cylindrical boundary conditions [7, Section 4], we cannot draw any firm conclusion about the validity of the above conjecture for square-lattice strips with free boundary conditions.

6.3 Real chromatic roots

It is also of interest to study the real chromatic roots for lattices of finite length n . For every length n there are, of course, roots at $q = 0$ and $q = 1$; and there are also roots converging (exponentially rapidly) as $n \rightarrow \infty$ to the isolated limiting point at $q = 2$. Here we shall concentrate on the roots converging to the isolated limiting point at $q = B_5 = (3 + \sqrt{5})/2$ and, for $m = 9$ and 11 , to the real crossing point $q_0(m)$.

For width $m = 10, 12$, the real roots converging to B_5 do so monotonically from below; we refrain from presenting the details. There are no real roots above B_5 .

For widths $m = 9$ and 11 , by contrast, two interesting things happen (see Tables 15 and 16). On the one hand, the real roots converging to B_5 do so with parity $(-1)^{n+1}$, i.e. alternating from above and below (starting from $n = 39$ and $n = 23$, respectively). On the other hand, for odd lengths n , there are also real roots converging to $q_0(m)$ from below. We conjecture that these behaviors will persist for all larger odd widths m .

These results for $m = 9, 11$ provide a (presumably infinite) family of counterexamples to a conjecture made in [6] concerning the real chromatic roots of bipartite planar graphs. For further discussion and for a revised conjecture, see Appendix B.

An important question is the rate of convergence of these real zeros towards the limiting values B_5 and $q_0(m)$. For B_5 we expect an exponentially rapid convergence (as with all isolated limiting points in the Beraha–Kahane–Weiss theorem); for $q_0(m)$, by contrast, we expect a $1/n$ convergence. We have tested these predictions by fitting the given real roots q_n to a power-law Ansatz

$$q = q_\infty + An^{-\Delta}, \quad (6.10)$$

using the data points $n \geq$ a variable threshold n_{\min} . For the sequences of zeros converging to B_5 , the estimates of the power Δ appear to increase without bound as n_{\min} is increased (e.g. $\Delta \gtrsim 45$), suggesting that the convergence is indeed exponentially fast. For the sequences converging to $q_0(m)$, by contrast, we obtain powers $\Delta \approx 1.1$ for small values of n_{\min} , which slowly decrease toward 1 as we increase n_{\min} . In particular, for $n_{\min} = 99$ we obtain $\Delta \approx 1.023$ for $m = 9$ and $\Delta \approx 1.037$ for $m = 11$. This is consistent with the $1/n$ behavior expected from the Beraha–Kahane–Weiss theorem.

7 Summary and open problems

In this paper we have derived some new structural results for the transfer matrix of square-lattice Potts models with free and cylindrical boundary conditions. In particular, we have obtained explicit closed-form expressions for the dominant (at large $|q|$) diagonal entry in the transfer matrix, for arbitrary widths m , as the solution of a special one-dimensional polymer model. We have also obtained the first 47 (resp. 46) terms in the large- q expansion of the bulk and surface (resp. corner) free energies for the zero-temperature antiferromagnet (= chromatic polynomial). Finally, we have computed chromatic roots for strips of width $m = 9, 10, 11, 12$ with free boundary conditions and located roughly the limiting curves.

Let us end by listing some open problems for future research. The first group of such problems would be to understand theoretically (and ideally to prove rigorously) some of the regularities that were observed empirically in Sections 4 and 5, for instance:

- 1) The empirically observed property that the polynomials $p_s^F(k)$ and $p_s^P(k)$ arising in (3.42)/(3.71) ff. have for even $s \geq 2$ a factor $k - s/2$.
- 2) The formulae (3.43b) and (3.72a,b) relating the coefficients $a_k^F(k+s)$ and $\tilde{a}_k^P(k+s)$ for $s = 1$ and $s = 0, 1$, respectively, to Fibonacci numbers (and possible extensions of these formulae to higher values of s).
- 3) The fact that $a_{k,\ell}^F$ and $\tilde{a}_{k,\ell}^P$ [defined in (3.48) and (3.75)] are, for each fixed $\ell \geq 0$, the restriction to integers $k \geq \ell$ of a *polynomial* in k of degree ℓ .
- 4) The behavior (4.6)/(4.7) relating the leading eigenvalue $\lambda_\star^{F/P}(m)$ to the dominant diagonal entry $t_{F/P}(m)$.
- 5) The fact that the coefficients $c_k^{F/P}(m)$ in the large- q expansion of $\log \lambda_\star^{F/P}(m)$ [cf. (4.9)] are the restriction to integers $m \geq m_{\min}^{F/P}(k)$ of a polynomial of degree 1 in m . Finite-size-scaling theory (Section 5.1) gives a nonrigorous (but physically intuitive)

explanation of why the $c_k^{\text{F/P}}(m)$ are polynomials of degree 1 in m for *large enough* m . But we do not really understand why the cutoffs $m_{\min}^{\text{F/P}}(k)$ take the values they do; even less do we understand the improvements found empirically in Sections 4.2 and 4.3. And of course we lack a rigorous proof for all of this.

6) The correction term of order $z^{4L_{\max}-1}$ found empirically for the surface free energy [cf. the paragraph preceding (5.31)].

Among the more fundamental extensions of this work, we would like to propose the following:

1. *Obtain longer large- q series.* It is natural to ask whether our large- q series for the bulk, surface and corner free energies (Section 5.2) can be extended to higher order. Modest extensions are no doubt possible over the next few years, with increased computer power; but the memory and CPU-time requirements are heavy, even for width $m = 12$ or 13 . It seems to us that radical algorithmic improvements in the implementation of the transfer-matrix method will be required in order to go to significantly larger widths m . Unfortunately, our results from the series analysis (Section 5.5.3) suggest that these series are badly behaved, and that it will be necessary to obtain *many* more terms — for instance, doubling the length of our series from $N = 47$ to $N \approx 100$ — in order to improve significantly our understanding of the analytic structure.

2. *Extend this work to the triangular lattice.* Extension of this work to the triangular lattice is particularly interesting in view of Baxter’s [77, 78] conjectured exact solution for the bulk free energy of the triangular-lattice chromatic polynomial (see also [8, Section 6] for a critical discussion). It ought to be fairly easy to obtain exact formulae for the dominant transfer-matrix entry, analogous to those obtained here in Section 3 for the square lattice. Likewise, the transfer-matrix calculations in Sections 4 and 5 can easily be extended to the triangular lattice, as discussed in [8], albeit possibly for slightly smaller widths. The main trouble arises in the use of the finite-lattice method: using transfer matrices of widths up to L_{\max} , we obtain the large- q series through order $4L_{\max} - 2$ on the square lattice (Section 5.2) but only order $\approx 2L_{\max}$ on the triangular lattice [67, Section 3.1].

But the calculation of the large- q series for the *bulk* free energy is expected to be superfluous, as Baxter [77, 78] has an exact expression

$$g_1(q) = -\frac{1}{x} \prod_{j=1}^{\infty} \frac{(1 - x^{6j-3})(1 - x^{6j-2})^2(1 - x^{6j-1})}{(1 - x^{6j-5})(1 - x^{6j-4})(1 - x^{6j})(1 - x^{6j+1})} \quad (7.1)$$

(where $q = 2 - x - x^{-1}$ and $|x| < 1$) that is claimed to represent the exponential of the bulk free energy at large enough $|q|$ (namely, outside the limiting curve \mathcal{B}_{∞}). The finite-lattice calculations would thus serve only to check (7.1) through order $x^{\approx 20}$ (and also to compute the series for the surface and corner free energies). Assuming that this check confirms (7.1) — as we expect that it will³² — we will learn nothing

³²See also the numerical confirmations in [8, Section 6.3].

new! One could equally well carry out a differential-approximant analysis like that of Section 5.5.3 directly on the series obtained by expanding (7.1), for which it is easy to obtain 1000 or more terms.

On the other hand, there is little point in carrying out such a differential-approximant analysis, since we already know the analytic structure of (7.1): namely, it is analytic and nonvanishing in the disc $|x| < 1$, or equivalently in the complex q -plane with a cut along the real interval $0 \leq q \leq 4$. It follows that, if Baxter’s formula (7.1) is correct at large $|q|$, then the limiting curve \mathcal{B}_∞ for the triangular-lattice chromatic polynomial is *not* a natural boundary for the bulk free energy — contrary to what we suspect to be the case for the square-lattice chromatic polynomial (see the discussion at the end of Section 5.5.3).

When all is said and done, our lack of understanding of the triangular-lattice chromatic polynomial concerns *small* $|q|$ — namely, the region *inside* the limiting curve \mathcal{B}_∞ — and not large $|q|$ (see [8, Section 6] for discussion). This issue is probably best addressed by trying to understand better the structure of Baxter’s [77, 78] Bethe-Ansatz solution for finite widths m , including the effect of boundary conditions.

3. *Carry out transfer-matrix calculations for the diced lattice.* The discussion in Appendix B and in [79] suggests that it would be very interesting to carry out transfer-matrix calculations analogous to those of [6–10] and the present paper for the *diced lattice* (namely, the dual of the kagomé lattice). We have established in [79] that $q_c(\text{diced}) > 3$, but we do not know whether the limiting curves \mathcal{B}_m intersect the real axis at some value $q_0(m) > 3$, or merely have complex-conjugate endpoints that tend to $q_c(\text{diced})$ as $m \rightarrow \infty$.

4. *Understand the analytic nature of complex phase boundaries.* As discussed at the beginning of Section 5.5, it is proven in some cases, and expected in general for statistical-mechanical models in dimension $d \geq 2$, that the infinite-volume free energy has a “soft” essential singularity (where it is infinitely differentiable but not analytic) whenever a first-order-phase-transition point in the physical region is approached. But it is unclear whether the *complex* phase boundaries are natural boundaries of the free energies defined in each phase. (In our case, we are uncertain whether the limiting curve \mathcal{B}_∞ is a natural boundary for the bulk free energy of the square-lattice chromatic polynomial.) It would be useful to resolve this question in at least one model (for instance, the analyticity or nonanalyticity at pure-imaginary magnetic field of the low-temperature Ising ferromagnet), ideally by a mathematically rigorous proof.

A Some combinatorial identities

In this appendix we will prove Propositions 3.5 and 3.7 concerning the quantities $a_k^{\text{F}}(k-s)$ and $\tilde{a}_k^{\text{P}}(k-s)$, respectively. We will also prove eq. (3.43a) for the quantity $a_k^{\text{F}}(k)$.

We shall use Knuth’s notation for falling powers [42]

$$x^{\underline{n}} = x(x-1) \cdots (x-n+1) . \tag{A.1}$$

We also use the standard convention [42] for the definition of binomial coefficients:

$$\binom{x}{k} = \begin{cases} x^{\underline{k}}/k! & \text{for integer } k \geq 0 \\ 0 & \text{for integer } k < 0 \end{cases} \quad (\text{A.2})$$

where x can be a real or complex number (or more generally an algebraic indeterminate) while k is always an integer. Finally, we adopt the convention that $k! = \Gamma(k+1) = \infty$ for integer $k < 0$, so that (A.2) could be written simply as $\binom{x}{k} = x^{\underline{k}}/k!$.

A.1 Some preliminary lemmas

Let us start with a simple lemma that will make the analysis easier:

Lemma A.1 *For any integers $s, a \geq 0$, let us define the polynomial*

$$T_{s,a}(\lambda) = \sum_{r=0}^s \lambda^r \frac{r^a}{r!(s-r)!}. \quad (\text{A.3})$$

Then

$$T_{s,a}(\lambda) = \frac{\lambda^a (\lambda+1)^{s-a}}{(s-a)!} \quad (\text{A.4})$$

(hence in particular $T_{s,a}(\lambda) = 0$ for $a > s$).

PROOF. Expanding r^a in (A.3) and using the fact that $r^a = 0$ for $a > r$, we obtain

$$T_{s,a}(\lambda) = \sum_{r=a}^s \lambda^r \frac{r(r-1)(r-2)\dots(r-a+1)}{r!(s-r)!}. \quad (\text{A.5})$$

If $a > s$, then the sum is empty, so let us suppose that $a \leq s$. Then we can rearrange the factorials to obtain

$$\begin{aligned} T_{s,a}(\lambda) &= \sum_{r=a}^s \lambda^r \frac{1}{(r-a)!(s-r)!} \\ &= \frac{1}{(s-a)!} \sum_{r=a}^s \lambda^r \binom{s-a}{r-a} \\ &= \frac{\lambda^a}{(s-a)!} \sum_{r'=0}^{s-a} \lambda^{r'} \binom{s-a}{r'} \\ &= \frac{\lambda^a}{(s-a)!} (\lambda+1)^{s-a}. \end{aligned} \quad (\text{A.6})$$

□

The next lemma will allow us to perform the inner sums in (3.34) and (3.63):

Lemma A.2 *For any integers $\ell, a, b \geq 0$, let us define the polynomial*

$$F_{\ell,a,b}(\lambda) = \sum_{r=0}^{\ell} \lambda^r \binom{\ell-a-b-1}{r} \binom{b}{\ell-r}. \quad (\text{A.7})$$

Then

$$F_{\ell,a,b}(\lambda) = \frac{(-1)^\ell b!}{\ell! (a+b-\ell)!} Q_{\ell,a}(b, \lambda), \quad (\text{A.8})$$

where

$$Q_{\ell,a}(b, \lambda) = \sum_{m=0}^{\min(a,\ell)} \binom{a}{m} (a+b-\ell)^{\overline{a-m}} \ell^{\overline{m}} \lambda^m (\lambda-1)^{\ell-m} \quad (\text{A.9})$$

is a polynomial in b, λ that is of degree a in the variable b and of degree ℓ in λ , with leading coefficient

$$[b^a] Q_{\ell,a}(b, \lambda) = (\lambda-1)^\ell \quad (\text{A.10})$$

and hence $[b^a \lambda^\ell] Q_{\ell,a}(b, \lambda) = 1$.

PROOF. Let us first consider the case $\ell - a - b - 1 \geq 0$. Then $\binom{\ell-a-b-1}{r} = 0$ whenever $r > \ell - a - b - 1$. On the other hand, $\binom{b}{\ell-r} = 0$ whenever $\ell - r > b$, i.e. $r < \ell - b$. But these two conditions on r involve all possible cases, as $a \geq 0$. Therefore, $F_{\ell,a,b}(\lambda) = 0$ for $\ell - a - b - 1 \geq 0$.

Let us now consider the nontrivial case $\ell - a - b - 1 < 0$. As the upper index in $\binom{\ell-a-b-1}{r}$ is now negative, it is convenient to rewrite (A.7) as

$$F_{\ell,a,b}(\lambda) = \sum_{r=0}^{\ell} (-\lambda)^r \binom{r-\ell+b+a}{r} \binom{b}{\ell-r}, \quad (\text{A.11})$$

where now all the indexes are nonnegative. We can then rewrite the binomial coefficients in terms of factorials as follows:

$$\begin{aligned} F_{\ell,a,b}(\lambda) &= \sum_{r=0}^{\ell} (-\lambda)^r \frac{(r-\ell+b+a)!}{r! (a+b-\ell)!} \frac{b!}{(\ell-r)! (b-\ell+r)!} \\ &= \frac{b!}{(a+b-\ell)!} \sum_{r=0}^{\ell} \frac{(-\lambda)^r}{r! (\ell-r)!} \prod_{m=1}^a (r+b-\ell+m). \end{aligned} \quad (\text{A.12})$$

The product in (A.12) can be written as a sum using the “binomial theorem” for falling powers [42, Exercise 5.37]. Defining $x = b - \ell$, we have

$$\prod_{m=1}^a (r+x+m) = (r+x+a)^{\underline{a}} \quad (\text{A.13a})$$

$$= \sum_{m=0}^a \binom{a}{m} r^{\overline{m}} (x+a)^{\overline{a-m}} \quad (\text{A.13b})$$

and therefore

$$F_{\ell,a,b}(\lambda) = \frac{b!}{(a+b-\ell)!} \sum_{m=0}^a \binom{a}{m} (a+b-\ell)^{\overline{a-m}} \sum_{r=0}^{\ell} \frac{(-\lambda)^r r^{\overline{m}}}{r! (\ell-r)!} \quad (\text{A.14a})$$

$$= \frac{b!}{(a+b-\ell)!} \sum_{m=0}^a \binom{a}{m} (a+b-\ell)^{\overline{a-m}} \frac{(-1)^{\ell} \lambda^m (\lambda-1)^{\ell-m}}{(\ell-m)!} \quad (\text{A.14b})$$

$$= \frac{b!}{(a+b-\ell)!} \frac{(-1)^{\ell}}{\ell!} Q_{\ell,a}(b, \lambda), \quad (\text{A.14c})$$

where we have used Lemma A.1 and the definition (A.9) of $Q_{\ell,a}(b, \lambda)$ [note that the sum in (A.9) can be stopped at $m = \ell$ because $\ell^{\overline{m}} = 0$ for $m > \ell$]. Clearly, $Q_{\ell,a}(b, \lambda)$ is a polynomial in b, λ that is of degree at most a in the variable b and of degree at most ℓ in λ . Indeed, this is its exact degree, as the leading coefficient is $[b^a]Q_{\ell,a}(b, \lambda) = (\lambda-1)^{\ell}$ [from the $m = 0$ term in (A.9)] and hence $[b^a \lambda^{\ell}]Q_{\ell,a}(b, \lambda) = 1$. \square

Remarks. 1. When $\lambda = 1$, (A.7) reduces to the Vandermonde convolution

$$F_{\ell,a,b}(1) = \binom{\ell-a-1}{\ell}, \quad (\text{A.15})$$

while (A.9) reduces to

$$Q_{\ell,a}(b, 1) = \binom{a}{\ell} (a+b-\ell)^{\overline{a-\ell}} \ell! = \frac{a!}{(a-\ell)!} \frac{(a+b-\ell)!}{b!}, \quad (\text{A.16})$$

so that (A.8) gives

$$F_{\ell,a,b}(1) = (-1)^{\ell} \binom{a}{\ell} = \binom{\ell-a-1}{\ell}. \quad (\text{A.17})$$

2. In our applications we will always take $\ell = k - p \geq 0$ and $\lambda = 3$. In addition, in Theorem A.4 we will take $(a, b) = (s-1, p+1)$ with $p \geq 0$, and $(a, b) = (s, p-1)$ with $p \geq 1$; finally in Theorem A.6, we will take $(a, b) = (s-1, p-1)$ with $p \geq 1$.

A.2 Proof of formula for $a_k^{\text{F}}(k-s)$

The next lemma deals with the outer sums we find in (3.34):

Lemma A.3 *Let $\alpha = 0$ or 1. Then, for any integers $s \geq 1 - \alpha$ and $k \geq s + \alpha$, let us define*

$$A_{\alpha,s,k}(\lambda) = \sum_{p=\alpha}^k (-1)^p \binom{k-s-p-1}{p-\alpha} F_{k-p,s+\alpha-1,p+1-2\alpha}(\lambda), \quad (\text{A.18})$$

where $F_{\ell,a,b}(\lambda)$ is defined by (A.7). We then have

$$A_{\alpha,s,k}(\lambda) = \begin{cases} \sum_{q=0}^s \frac{(-1)^q (k+1-q)}{q! (s-q)!} Q_{q,s-1}(k+1-q, \lambda) & \text{if } \alpha = 0 \\ \sum_{q=0}^s \frac{(-1)^{q+1}}{q! (s-q)!} Q_{q,s}(k-1-q, \lambda) & \text{if } \alpha = 1 \end{cases} \quad (\text{A.19})$$

where the polynomial $Q_{\ell,a}(b, \lambda)$ is defined by (A.9). In particular, $A_{\alpha,s,k}(\lambda)$ is the restriction to integers $k \geq s + \alpha$ of a polynomial in k, λ that is of degree s in k and λ separately, with leading coefficient

$$[k^s] A_{\alpha,s,k}(\lambda) = \frac{(-1)^\alpha}{s!} (2-\lambda)^s \quad (\text{A.20})$$

and hence $[k^s \lambda^s] A_{\alpha,s,k}(\lambda) = (-1)^{s+\alpha}/s!$. The next subleading coefficients are given by

$$[k^{s-1}] A_{\alpha,s,k}(\lambda) = \frac{(2-\lambda)^{s-1}}{2(s-1)!} \times \begin{cases} (4-\lambda-2s+\lambda s) & \text{if } \alpha = 0 \\ (2-\lambda)(s+1) & \text{if } \alpha = 1 \end{cases} \quad (\text{A.21a})$$

$$[k^{s-2}] A_{\alpha,s,k}(\lambda) = \frac{(2-\lambda)^{s-1}}{24(s-2)!} \times \begin{cases} -(3\lambda s^2 - 6s^2 - 7\lambda s + 2s + 2\lambda - 4) & \text{if } \alpha = 0 \\ 3\lambda s^2 - 6s^2 + 5\lambda s - 34s + 2\lambda - 4 & \text{if } \alpha = 1 \end{cases} \quad (\text{A.21b})$$

$$[k^{s-3}] A_{\alpha,s,k}(\lambda) = \frac{(2-\lambda)^{s-2}}{48(s-3)!} \times \begin{cases} (-48 + 80s - 10\lambda s - 3\lambda^2 s - 20s^2 \\ \quad + 2\lambda s^2 + 4\lambda^2 s^2 - 4s^3 + 4\lambda s^3 - \lambda^2 s^3) & \text{if } \alpha = 0 \\ (2-\lambda)s(s+1)(26-\lambda+2s-\lambda s) & \text{if } \alpha = 1 \end{cases} \quad (\text{A.21c})$$

$$[k^{s-4}] A_{\alpha,s,k}(\lambda) = \frac{(2-\lambda)^{s-2}}{5760(s-4)!} \times \begin{cases} (2-\lambda)(-16 + 8\lambda + 924s + 18\lambda s \\ \quad - 1310s^2 - 125\lambda s^2 + 420s^3 \\ \quad + 90\lambda s^3 + 30s^4 - 15\lambda s^4) & \text{if } \alpha = 0 \\ 32 - 32\lambda + 8\lambda^2 + 1032s + 888\lambda s \\ \quad + 18\lambda^2 s - 5300s^2 + 1220\lambda s^2 \\ \quad - 5\lambda^2 s^2 - 1560s^3 + 840\lambda s^3 \\ \quad - 30\lambda^2 s^3 - 60s^4 + 60\lambda s^4 - 15\lambda^2 s^4 & \text{if } \alpha = 1 \end{cases} \quad (\text{A.21d})$$

PROOF. In (A.18) let us insert the result (A.8) of Lemma A.2 for $F_{k-p, s+\alpha-1, p+1-2\alpha}(\lambda)$,³³ we get

$$A_{\alpha, s, k}(\lambda) = \sum_{p=\alpha}^k \binom{k-s-p-1}{p-\alpha} \frac{(-1)^k (p+1-2\alpha)!}{(2p+s-k-\alpha)! (k-p)!} \times Q_{k-p, s+\alpha-1}(p+1-2\alpha, \lambda). \quad (\text{A.22})$$

First of all, we notice that all terms with $p \leq k-s-1$ vanish: for if $0 \leq k-s-p-1 < p-\alpha$, then $\binom{k-s-p-1}{p-\alpha} = 0$, while if $2p+s-k-\alpha < 0$, then $1/(2p+s-k-\alpha)! = 0$; and these two cases cover all values of p satisfying $p \leq k-s-1$. So the only nonzero contributions to the sum (A.22) come from $p \geq k-s \geq \alpha$. Using the variable $q = k-p$, we can rewrite (A.22) as

$$\begin{aligned} A_{\alpha, s, k}(\lambda) &= \sum_{q=0}^s \binom{q-s-1}{k-q-\alpha} \frac{(-1)^k (k+1-q-2\alpha)!}{(k+s-2q-\alpha)! q!} \\ &\quad \times Q_{q, s+\alpha-1}(k+1-q-2\alpha, \lambda) \\ &= \sum_{q=0}^s \binom{k+s-2q-\alpha}{k-q-\alpha} \frac{(-1)^{q+\alpha} (k+1-q-2\alpha)!}{(k+s-2q-\alpha)! q!} \\ &\quad \times Q_{q, s+\alpha-1}(k+1-q-2\alpha, \lambda) \\ &= \sum_{q=0}^s \frac{(-1)^{q+\alpha} (k-q-2\alpha+1)!}{q! (s-q)!} \frac{1}{(k-q-\alpha)!} \\ &\quad \times Q_{q, s+\alpha-1}(k+1-q-2\alpha, \lambda). \end{aligned} \quad (\text{A.23})$$

Evaluating this for $\alpha = 0, 1$ yields (A.18). This expression for $A_{\alpha, s, k}(\lambda)$ is manifestly a polynomial in k and λ of degree at most s in each of the variables separately. Indeed, using (A.10) and performing a binomial sum over q , we obtain (A.20).

The computation of the subleading terms (A.21) is more involved. Let us start with the case $\alpha = 0$. Our goal is to extract the leading powers of k in (A.19), so our first task is to convert the falling power $(k+s-2q)^{\underline{s-1-m}}$ that appears in the definition of $Q_{q, s-1}(k+1-q, \lambda)$ [cf. (A.9)] to a regular power using the Stirling cycle numbers [42]. The key formula is obtained from (3.47) and the binomial theorem:

$$(k+x)^{\underline{m}} = \sum_{r=0}^m k^{m-r} \sum_{p=0}^r (-1)^p \begin{bmatrix} m \\ m-p \end{bmatrix} \binom{m-p}{r-p} x^{r-p}. \quad (\text{A.24})$$

³³Please note that the hypotheses of Lemma A.3 ($\alpha \in \{0, 1\}$, $s \geq 1-\alpha$ and $k \geq s+\alpha$) together with the summation limits $\alpha \leq p \leq k$ imply that the three subscripts in $F_{k-p, s+\alpha-1, p+1-2\alpha}$ are nonnegative; this justifies the use of Lemma A.2.

Using this formula in the definition of $Q_{q,s-1}(k+1-q, \lambda)$ allows us to obtain the first five leading terms in the expansion of the summand in (A.19):

$$\begin{aligned}
& (k+1-q) Q_{q,s-1}(k+1-q, \lambda) \\
&= (k+1-q) \sum_{m=0}^q \binom{s-1}{m} (k+s-2q)^{\overline{s-1-m}} q^{\overline{m}} \lambda^m (\lambda-1)^{q-m} \\
&= \sum_{i=0}^4 k^{s-i} a_i^{(0)} + O(k^{s-5}) , \tag{A.25}
\end{aligned}$$

where the coefficients $a_i^{(0)}$ are given by

$$a_0^{(0)} = (\lambda - 1)^q \quad (\text{A.26a})$$

$$a_1^{(0)} = (\lambda - 1)^{q-1} \left[-q(1 - 2s + \lambda s) + \frac{(\lambda - 1)}{2} s(s + 1) \right] \quad (\text{A.26b})$$

$$\begin{aligned} a_2^{(0)} = (\lambda - 1)^{q-2} \binom{s-1}{1} & \left[q^2 \frac{(\lambda - 2)}{2} (2 - 2s + \lambda s) \right. \\ & - q \frac{(\lambda - 1)}{2} (-2 + 3s - 2s^2 + \lambda s^2) \\ & \left. + \frac{(\lambda - 1)^2}{24} s(s + 1)(2 + 3s) \right] \end{aligned} \quad (\text{A.26c})$$

$$\begin{aligned} a_3^{(0)} = (\lambda - 1)^{q-3} \binom{s-1}{2} & \left[-q^3 \frac{(\lambda - 2)^2}{3} (3 - 2s + \lambda s) \right. \\ & + q^2 \frac{(\lambda - 1)}{2} (16 - 6\lambda - 16s + 10\lambda s - \lambda^2 s + 4s^2 - 4\lambda s^2 + \lambda^2 s^2) \\ & - q \frac{(\lambda - 1)^2}{12} (12 - 25s + 17s^2 - \lambda s^2 - 6s^3 + 3\lambda s^3) \\ & \left. + \frac{(\lambda - 1)^3}{24} s^2(1 + s)^2 \right] \end{aligned} \quad (\text{A.26d})$$

$$\begin{aligned} a_4^{(0)} = (\lambda - 1)^{q-4} \binom{s-1}{3} & \left[q^4 \frac{(\lambda - 2)^3}{4} (4 - 2s + \lambda s) \right. \\ & - q^3 \frac{(\lambda - 1)(\lambda - 2)}{2} (36 - 12\lambda - 26s + 17\lambda s - 2\lambda^2 s + 4s^2 - 4\lambda s^2 + \lambda^2 s^2) \\ & + q^2 \frac{(\lambda - 1)^2}{8} (-208 + 56\lambda s + 236s - 102\lambda s + 4\lambda^2 s - 88s^2 + 58\lambda s^2 \\ & \quad - 7\lambda^2 s^2 + 12s^3 - 12\lambda s^3 + 3\lambda^2 s^3) \\ & - q \frac{(\lambda - 1)^3}{8} (s - 1)(8 - 14s + 7s^2 - 2s^3 + \lambda s^3) \\ & \left. + \frac{(\lambda - 1)^4}{960} s(s + 1)(-8 - 10s + 15s^2 + 15s^3) \right] \end{aligned} \quad (\text{A.26e})$$

In the derivation of these formulae we have used the following special values of the Stirling cycle numbers [80, Chapter 5, Exercise 16] (see also [30, 42]):

$$\begin{bmatrix} n \\ n-1 \end{bmatrix} = \binom{n}{2} \quad (\text{A.27a})$$

$$\begin{bmatrix} n \\ n-2 \end{bmatrix} = \binom{n}{3} \frac{3n-1}{4} \quad (\text{A.27b})$$

$$\begin{bmatrix} n \\ n-3 \end{bmatrix} = \binom{n}{4} \binom{n}{2} \quad (\text{A.27c})$$

$$\begin{bmatrix} n \\ n-4 \end{bmatrix} = \binom{n}{5} \frac{15n^3 - 30n^2 + 5n + 2}{48} \quad (\text{A.27d})$$

The second task is to perform the sum over q in (A.19). It is clear from (A.26) that the coefficients $a_i^{(0)}$ are polynomials in q ; and we have chosen to write them in terms of the falling powers $q^{\underline{m}}$ in order to facilitate the use of Lemma A.1 to perform the sum over q in (A.19). Each coefficient $a_i^{(0)}$ in (A.26) contributes only to the coefficient $[k^{s-i}]A_{0,s,k}(\lambda)$:

$$[k^{s-i}]A_{0,s,k}(\lambda) = \sum_{q=0}^s \frac{(-1)^q}{q!(s-q)!} a_i^{(0)} \quad \text{for } i \geq 0. \quad (\text{A.28})$$

Using the definition (A.3) of $T_{s,a}(\lambda)$, we can rewrite (A.26) as

$$[k^s]A_{0,s,k}(\lambda) = T_{s,0}(1-\lambda) \quad (\text{A.29a})$$

$$\begin{aligned} [k^{s-1}]A_{0,s,k}(\lambda) &= (\lambda-1)^{-1} \left[-(1-2s+\lambda s)T_{s,1}(1-\lambda) \right. \\ &\quad \left. + \frac{(\lambda-1)}{2}s(s+1)T_{s,0}(1-\lambda) \right] \end{aligned} \quad (\text{A.29b})$$

along with similar formulae for $[k^{s-i}]A_{0,s,k}(\lambda)$ with $i = 2, 3, 4$. From these equations together with Lemma A.1 we can derive after some algebra the results (A.20)/(A.21) for $\alpha = 0$.

The computation for $\alpha = 1$ is similar. The five leading terms for $Q_{q,s}(k-1-q, \lambda)$ can be written as

$$\begin{aligned} Q_{q,s}(k-1-q, \lambda) &= \sum_{m=0}^q \binom{s}{m} (k+s-2q-1)^{\underline{s-m}} q^{\underline{m}} \lambda^m (\lambda-1)^{q-m} \\ &= \sum_{i=0}^4 k^{s-i} a_i^{(1)} + O(k^{s-5}), \end{aligned} \quad (\text{A.30})$$

where the coefficients $a_i^{(1)}$ are given by

$$a_0^{(1)} = (\lambda - 1)^q \quad (\text{A.31a})$$

$$a_1^{(1)} = (\lambda - 1)^{q-1} \binom{s}{1} \left[q(2 - \lambda) + \frac{(\lambda - 1)}{2}(s - 1) \right] \quad (\text{A.31b})$$

$$a_2^{(1)} = (\lambda - 1)^{q-2} \binom{s}{2} \left[q^2(2 - \lambda)^2 - q(\lambda - 1)(6 - 2\lambda - 2s + \lambda s) + \frac{(\lambda - 1)^2}{12}(s - 2)(3s - 1) \right] \quad (\text{A.31c})$$

$$a_3^{(1)} = (\lambda - 1)^{q-3} \binom{s}{3} \left[q^3(2 - \lambda)^3 - q^2 \frac{3(2 - \lambda)(\lambda - 1)}{2}(10 - 3\lambda - 2s + \lambda s) - q \frac{(\lambda - 1)^2}{4}(s - 3)(20 - 4\lambda - 6s + 3\lambda s) + \frac{(\lambda - 1)^3}{8}s(s - 1)(s - 3) \right] \quad (\text{A.31d})$$

$$a_4^{(1)} = (\lambda - 1)^{q-4} \binom{s}{4} \left[q^4(2 - \lambda)^4 - 2q^3(2 - \lambda)^2(\lambda - 1)(14 - 4\lambda - 2s + \lambda s) + q^2 \frac{(\lambda - 1)^2}{2}(328 - 208\lambda + 28\lambda^2 - 124s + 100\lambda s - 19\lambda^2 s + 12s^2 - 12\lambda s^2 + 3\lambda^2 s^2) - q \frac{(\lambda - 1)^3}{2}(s - 4)(-18 + 2\lambda + 12s - 3\lambda s - 2s^2 + \lambda s^2) + \frac{(\lambda - 1)^4}{240}(s - 4)(2 + 5s - 30s^2 + 15s^3) \right] \quad (\text{A.31e})$$

We now perform the sum over q in (A.19). Again, each coefficient $a_i^{(1)}$ in (A.31) contributes only to the coefficient $[k^{s-i}]A_{1,s,k}(\lambda)$:

$$[k^{s-i}]A_{1,s,k}(\lambda) = - \sum_{q=0}^s \frac{(-1)^q}{q!(s-q)!} a_i^{(1)} \quad \text{for } i \geq 0. \quad (\text{A.32})$$

Using the definition (A.3) of $T_{s,a}(\lambda)$, we can rewrite (A.31) as

$$[k^s]A_{1,s,k}(\lambda) = -T_{s,0}(1 - \lambda) \quad (\text{A.33a})$$

$$[k^{s-1}]A_{1,s,k}(\lambda) = -(\lambda - 1)^{-1} \binom{s}{1} \left[(2 - \lambda)T_{s,1}(1 - \lambda) + \frac{(\lambda - 1)}{2}(s - 1)T_{s,0}(1 - \lambda) \right] \quad (\text{A.33b})$$

along with similar formulae for $[k^{s-i}]A_{1,s,k}(\lambda)$ with $i = 2, 3, 4$. These equations lead via Lemma A.1 to (A.20)/(A.21) for $\alpha = 1$. \square

We now proceed to prove the main result of this subsection:

Theorem A.4 (= Proposition 3.5) *For each integer $s \geq 1$, the quantity*

$$\begin{aligned} a_k^F(k-s) &= \sum_{p=0}^k (-1)^p \binom{k-s-1-p}{p} \sum_{r=0}^{k-p} 3^r \binom{k-s-1-2p}{r} \binom{p+1}{k-p-r} \\ &\quad + \sum_{p=1}^k (-1)^p \binom{k-s-1-p}{p-1} \sum_{r=0}^{k-p} 3^r \binom{k-s-2p}{r} \binom{p-1}{k-p-r} \end{aligned} \quad (\text{A.34})$$

is, when restricted to $k \geq s+1$, given by a polynomial in k of degree $\max(0, s-3)$, with leading coefficient

$$[k^{s-3}]a_k^F(k-s) = \frac{(-1)^{s+1}}{(s-3)!} \quad \text{for } s \geq 3 \quad (\text{A.35})$$

and first subleading coefficient

$$[k^{s-4}]a_k^F(k-s) = \frac{(-1)^s s}{2(s-4)!} \quad \text{for } s \geq 4. \quad (\text{A.36})$$

PROOF. Using Lemma A.3 we can rewrite (A.34) as

$$a_k^F(k-s) = A_{0,s,k}(3) + A_{1,s,k}(3), \quad (\text{A.37})$$

where each of the two terms is, for integers $k \geq s+1$, the restriction of a polynomial in k of degree s . Moreover, it follows from (A.20)/(A.21) that for a general value of λ we have

$$[k^s][A_{0,s,k}(\lambda) + A_{1,s,k}(\lambda)] = 0 \quad (\text{A.38a})$$

$$[k^{s-1}][A_{0,s,k}(\lambda) + A_{1,s,k}(\lambda)] = \frac{(2-\lambda)^{s-1}}{(s-1)!} (3-\lambda) \quad (\text{A.38b})$$

$$[k^{s-2}][A_{0,s,k}(\lambda) + A_{1,s,k}(\lambda)] = \frac{s(2-\lambda)^{s-1}}{2(s-2)!} (3-\lambda) \quad (\text{A.38c})$$

$$\begin{aligned} [k^{s-3}][A_{0,s,k}(\lambda) + A_{1,s,k}(\lambda)] &= \frac{(2-\lambda)^{s-2}}{24(s-3)!} (3\lambda^2 s^2 - 15\lambda s^2 + 18s^2 - \lambda^2 s \\ &\quad - 19\lambda s + 66s - 24) \end{aligned} \quad (\text{A.38d})$$

$$\begin{aligned} [k^{s-4}][A_{0,s,k}(\lambda) + A_{1,s,k}(\lambda)] &= -\frac{(2-\lambda)^{s-2} s}{48(s-4)!} (\lambda^2 s^2 - 5\lambda s^2 + 6s^2 - \lambda^2 s \\ &\quad - 19\lambda s + 66s - 24) \end{aligned} \quad (\text{A.38e})$$

Specializing to $\lambda = 3$, we see that the first three coefficients vanish, while the next two coefficients are nonzero and given by (A.35)/(A.36). Therefore, $a_k^F(k-s)$ is the restriction to integers $k \geq s+1$ of a polynomial in k of degree exactly $\max(0, s-3)$. \square

A.3 Proof of formula for $\tilde{a}_k^P(k-s)$

In this subsection we shall carry out an analogous analysis for the case of periodic transverse boundary conditions. It is convenient to prove first a technical lemma (analogous to Lemma A.3) that deals with the outer sums we find in (3.63):

Lemma A.5 *For any integers $s \geq 1$ and $k \geq s$, let us define*

$$B_{s,k}(\lambda) = (k-s) \sum_{p=1}^k \frac{(-1)^p}{p} \binom{k-s-p-1}{p-1} F_{k-p,s-1,p}(\lambda), \quad (\text{A.39})$$

where $F_{\ell,a,b}(\lambda)$ is defined by (A.7). We then have

$$B_{s,k}(\lambda) = (k-s) \sum_{q=0}^s \frac{(-1)^{q+1}}{q!(s-q)!} Q_{q,s-1}(k-q, \lambda), \quad (\text{A.40})$$

where the polynomial $Q_{\ell,a}(b, \lambda)$ is defined by (A.9). In particular, $B_{s,k}(\lambda)$ is the restriction to integers $k \geq s$ of a polynomial in k, λ that is of degree s in k and λ separately with leading coefficient

$$[k^s] B_{s,k}(\lambda) = -\frac{1}{s!} (2-\lambda)^s \quad (\text{A.41})$$

and hence $[k^s \lambda^s] B_{s,k}(\lambda) = (-1)^{s+1}/s!$. The next subleading coefficient is given by

$$[k^{s-1}] B_{s,k}(\lambda) = \frac{s+1}{2(s-1)!} (2-\lambda)^s. \quad (\text{A.42})$$

PROOF. In (A.39) let us insert the result (A.8) of Lemma A.2 for $F_{k-p,s-1,p}(\lambda)$; we get

$$\begin{aligned} B_{s,k}(\lambda) &= (k-s) \sum_{p=1}^k \binom{k-s-p-1}{p-1} \frac{(-1)^k (p-1)!}{(2p+s-k-1)! (k-p)!} \\ &\quad \times Q_{k-p,s-1}(p, \lambda). \end{aligned} \quad (\text{A.43})$$

First of all, we see that for $k = s$, the sum is finite, and therefore $B_{k,k}(\lambda) = 0$. So, we can restrict ourselves to the nontrivial cases $k \geq s+1$. Secondly, we notice, as in the proof of Lemma A.3, that all terms with $p \leq k-s-1$ vanish. So the only nonzero contributions to the sum (A.43) come from $p \geq k-s \geq 1$. Using the variable $q = k-p$, we can rewrite (A.43) as

$$\begin{aligned} B_{s,k}(\lambda) &= (k-s) \sum_{q=0}^s \binom{q-s-1}{k-q-1} \frac{(-1)^k (k-q-1)!}{(k+s-2q-1)! q!} Q_{q,s-1}(k-q, \lambda) \\ &= (k-s) \sum_{q=0}^s \binom{k+s-2q-1}{k-q-1} \frac{(-1)^{q+1} (k-q-1)!}{(k+s-2q-1)! q!} Q_{q,s-1}(k-q, \lambda) \\ &= (k-s) \sum_{q=0}^s \frac{(-1)^{q+1}}{q!(s-q)!} Q_{q,s-1}(k-q, \lambda). \end{aligned} \quad (\text{A.44})$$

This expression for $B_{s,k}(\lambda)$ is manifestly a polynomial in k and λ of degree at most s in each of the variables separately. Indeed, using (A.10) and performing a binomial sum over q , we obtain (A.41).

The computation of the subleading term (A.42) is similar to the one in Lemma A.3. Using the expansion (A.24) in the definition of $Q_{q,s-1}(k-q, \lambda)$ that appears in (A.44), we obtain the two leading terms:

$$\begin{aligned} Q_{q,s-1}(k-q, \lambda) &= \sum_{m=0}^{s-1} \binom{s-1}{m} (k+s-2q-1)^{\overline{s-1-m}} q^{\overline{m}} \lambda^m (\lambda-1)^{q-m} \\ &= k^{s-1} a_1^{(2)} + k^{s-2} a_2^{(2)} + O(k^{s-3}), \end{aligned} \quad (\text{A.45})$$

where the coefficients $a_k^{(2)}$ are given by

$$a_1^{(2)} = (\lambda-1)^q \quad (\text{A.46a})$$

$$a_2^{(2)} = (\lambda-1)^{q-1} (s-1) \left[\frac{s(\lambda-1)}{2} + q(2-\lambda) \right] \quad (\text{A.46b})$$

The second task is to perform the sum over q in (A.40). Because of the prefactor $k-s$, each coefficient $a_i^{(2)}$ in (A.46) gives a nonzero contribution to both $[k^{s-i+1}]B_{s,k}(\lambda)$ and $[k^{s-i}]B_{s,k}(\lambda)$. After some algebra we find

$$\begin{aligned} [k^s]B_{s,k}(\lambda) &= \sum_{q=0}^s \frac{(-1)^q}{q!(s-q)!} (-a_1^{(2)}) \\ &= T_{s,0}(1-\lambda) \end{aligned} \quad (\text{A.47a})$$

$$\begin{aligned} [k^{s-1}]B_{s,k}(\lambda) &= \sum_{q=0}^s \frac{(-1)^q}{q!(s-q)!} [-a_2^{(2)} + s a_1^{(2)}] \\ &= \frac{s(3-s)}{2} T_{s,0}(1-\lambda) - \frac{(s-1)(2-\lambda)}{\lambda-1} T_{s,1}(1-\lambda) \end{aligned} \quad (\text{A.47b})$$

where the $T_{s,a}$ are given in (A.4). From these equations we can derive after some algebra the results (A.41)/(A.42). \square

Now we are ready to prove the main result of this subsection:

Theorem A.6 (= Proposition 3.7) *For each integer $s \geq 1$, the quantity*

$$\tilde{a}_k^P(k-s) = 3^k \binom{k-s}{k} + \sum_{p=1}^k (-1)^p \frac{k-s}{p} \binom{k-s-p-1}{p-1} \sum_{r=0}^{k-p} 3^r \binom{k-s-2p}{r} \binom{p}{k-p-r} \quad (\text{A.48})$$

is, when restricted to $k \geq s$, given by a polynomial in k of degree s , with leading coefficient

$$[k^s] \tilde{a}_k^P(k-s) = \frac{(-1)^{s+1}}{s!} \quad (\text{A.49})$$

and first subleading coefficient

$$[k^{s-1}]\tilde{a}_k^{\text{P}}(k-s) = \frac{(-1)^s(s+1)}{2(s-1)!}. \quad (\text{A.50})$$

Furthermore, $\tilde{a}_k^{\text{P}}(0) = 0$, so that the polynomial representing $\tilde{a}_k^{\text{P}}(k-s)$ for $k \geq s$ has a factor $k-s$.

PROOF. The term $3^k \binom{k-s}{k}$ in (A.48) vanishes for integers $s \geq 1$ and $k \geq s$, so we have

$$\tilde{a}_k^{\text{P}}(k-s) = B_{s,k}(3). \quad (\text{A.51})$$

Therefore, the main assertions of Theorem A.6 are an immediate consequence of Lemma A.5. Finally, it is known from (3.65) that $\tilde{a}_k^{\text{P}}(0) = 0$ for $k \geq 1$; and this corresponds to the case $k = s$, which lies within the regime $k \geq s$ where $\tilde{a}_k^{\text{P}}(k-s)$ is given by a polynomial in k . \square

A.4 Proof of formula for $a_k^{\text{F}}(k)$

Our last goal is to prove (3.43a). Let us start by proving two lemmas similar to Lemmas A.3 and A.5.

Lemma A.7 *For any integer $k \geq 1$, let $a_{1,k}(\lambda)$ be defined as*

$$a_{1,k}(\lambda) = \sum_{p=0}^k (-1)^p \binom{k-1-p}{p} \sum_{r=0}^{k-p} \lambda^r \binom{k-2p-1}{r} \binom{p+1}{k-p-r}. \quad (\text{A.52})$$

Then

$$a_{1,k}(\lambda) = 1 + \sum_{p=0}^{k-1} (-1)^p \binom{k-1-p}{p} \lambda^{k-2p-1}. \quad (\text{A.53})$$

PROOF. The inner sum in (A.52),

$$S_{k,p}(\lambda) = \sum_{r=0}^{k-p} \lambda^r \binom{k-2p-1}{r} \binom{p+1}{k-p-r}, \quad (\text{A.54})$$

can be performed analogously to the proof of Lemma A.2: If $k-2p-1 \geq 0$, then $\binom{k-1-2p}{r} = 0$ for all $r > k-2p-1 \geq 0$. Moreover, $\binom{p+1}{k-p-r} = 0$ whenever $k-p-r > p+1 \geq 1$, i.e. for all $r < k-2p-1$. Thus, when $k-2p-1 \geq 0$ there is a single nonzero term coming from $r = k-2p-1$ and whose contribution is λ^{k-2p-1} . On the other hand, if $k-2p-1 < 0$, then following similar steps to those of the proof of Lemma A.2, we obtain a finite sum. Putting these two contributions together we get

$$\begin{aligned} S_{k,p}(\lambda) &= \frac{(p+1)!}{(2p-k)!} \sum_{r=0}^{k-p} \frac{(-\lambda)^r}{r! (k-p-r)! (2p+r+1-p)} \\ &\quad + \lambda^{k-2p-1} I[k \geq 2p+1], \end{aligned} \quad (\text{A.55})$$

where $I[A]$ is the indicator function of the event A , and in the first term it is not necessary to add $I[k < 2p + 1]$ because of the factor $1/(2p - k)!$.

The outer sum in (A.52) is easy:

$$\begin{aligned} a_{1,k}(\lambda) &= \sum_{p=0}^k (-1)^p \binom{k-1-p}{p} \frac{(p+1)!}{(2p-k)!} \sum_{r=0}^{k-p} \frac{(-\lambda)^r}{r! (k-p-r)! (2p+r+1-p)} \\ &\quad + \sum_{p=0}^k (-1)^p \binom{k-1-p}{p} \lambda^{k-2p-1} I[k \geq 2p+1], \end{aligned} \quad (\text{A.56})$$

as the only nonzero contribution of the second term corresponds to $p = k$. (The contributions of the terms with $0 \leq p \leq k-1$ vanish because Euler's reflection formula.) We then obtain,

$$a_{1,k}(\lambda) = 1 + \sum_{p=0}^{\lfloor (k-1)/2 \rfloor} (-1)^p \binom{k-1-p}{p} \lambda^{k-2p-1}. \quad (\text{A.57})$$

Notice that the upper limit $\lfloor (k-1)/2 \rfloor$ comes from the condition $k \geq 2p+1$; but we can replace it by the simpler term $k-1$, as $\binom{k-1-p}{p} = 0$ whenever $p > k-1-p$ (i.e., $2p > k-1$). We then obtain the claimed formula (A.53). \square

Lemma A.8 *For any integer $k \geq 1$, let $a_{2,k}(\lambda)$ be defined as*

$$a_{2,k}(\lambda) = \sum_{p=0}^k (-1)^p \binom{k-1-p}{p-1} \sum_{r=0}^{k-p} \lambda^r \binom{k-2p}{r} \binom{p-1}{k-p-r}. \quad (\text{A.58})$$

Then

$$a_{2,k}(\lambda) = -1. \quad (\text{A.59})$$

PROOF. By inspection it is clear that $a_{2,k}(\lambda) = A_k(1, 0; \lambda)$ [cf. (A.18)]. Then Lemma A.3 ensures that for any $k \geq 1$

$$A_k(1, 0; \lambda) = -Q_{0,0}(k-1, \lambda) = -1, \quad (\text{A.60})$$

where we have also used (A.9). \square

Now the strategy is to show that the quantities $C_k(\lambda) = a_{1,k}(\lambda) + a_{2,k}(\lambda)$ satisfy a second-order linear recursion, which reduces to that of the Fibonacci numbers F_{2k} when $\lambda = 3$. In particular we prove the following lemma:

Lemma A.9 *For any integer $k \geq 1$, let $C_k(\lambda)$ be defined as*

$$C_k(\lambda) = a_{1,k}(\lambda) + a_{2,k}(\lambda), \quad (\text{A.61})$$

where the quantities $a_{i,k}(\lambda)$ are defined in (A.52)/(A.58). Then, for any $k \geq 3$, the quantity

$$f_k(\lambda) = C_k(\lambda) - \lambda C_{k-1}(\lambda) + C_{k-2}(\lambda) \quad (\text{A.62})$$

vanishes identically (i.e., $f_k(\lambda) = 0$ for all $k \geq 3$).

PROOF. From Lemmas A.7 and A.8 it is clear that

$$C_k(\lambda) = \sum_{p=0}^{k-1} (-1)^p \binom{k-1-p}{p} \lambda^{k-2p-1}. \quad (\text{A.63})$$

Then, the expression for $f_k(\lambda)$ for any $k \geq 3$ is given by

$$\begin{aligned} f_k &= \sum_{p=0}^{k-1} (-1)^p \lambda^{k-2p-1} \binom{k-1-p}{p} + \sum_{p=0}^{k-2} (-1)^{p+1} \lambda^{k-2p-1} \binom{k-2-p}{p} \\ &\quad + \sum_{p=0}^{k-3} (-1)^p \lambda^{k-2p-3} \binom{k-3-p}{p}. \end{aligned} \quad (\text{A.64})$$

The last term can be rewritten in a more convenient way if we change the summation variable to $p+1$:

$$\sum_{p=0}^{k-3} (-1)^p \lambda^{k-2p-3} \binom{k-3-p}{p} = \sum_{p=1}^{k-2} (-1)^{p+1} \lambda^{k-2p-1} \binom{k-2-p}{p-1} \quad (\text{A.65})$$

This term is essentially the same as the second term in the sum (A.64), except for the binomial coefficients. Using the Pascal identity

$$\binom{k-p-2}{p} + \binom{k-p-2}{p-1} = \binom{k-p-1}{p}, \quad (\text{A.66})$$

we obtain that

$$\begin{aligned} f_k &= \sum_{p=0}^{k-1} (-1)^p \lambda^{k-2p-1} \binom{k-1-p}{p} + \sum_{p=0}^{k-2} (-1)^{p+1} \lambda^{k-2p-1} \binom{k-2-p}{p} \\ &= (-1)^{k-1} \binom{0}{k-1} \lambda^{1-k} \\ &= (-\lambda)^{1-k} \delta_{k,1} = 0, \end{aligned} \quad (\text{A.67})$$

which is zero because we are assuming that $k \geq 3$. This completes the proof. \square

Now we are ready to prove the main result (3.43a):

Theorem A.10 *For any integer $k \geq 1$ let us define the quantity [cf. (3.34)]*

$$\begin{aligned} a_k^F(k) &= \sum_{p=0}^k (-1)^p \binom{k-1-p}{p} \sum_{r=0}^{k-p} 3^r \binom{k-1-2p}{r} \binom{p+1}{k-p-r} \\ &\quad + \sum_{p=1}^k (-1)^p \binom{k-1-p}{p-1} \sum_{r=0}^{k-p} 3^r \binom{k-2p}{r} \binom{p-1}{k-p-r}. \end{aligned} \quad (\text{A.68})$$

Then for any $k \geq 1$, $a_k^F(k) = F_{2k}$, where F_{2k} is the $(2k)$ -th Fibonacci number [30, sequences A001906/A088305].

PROOF. The quantity $a_k^F(k)$ can be written as

$$a_k^F(k) = C_k(3), \quad (\text{A.69})$$

where C_k is given in Lemma A.9 (see also Lemmas A.7 and A.8). For any $k \geq 3$, the quantities $a_k^F(k)$ satisfy the recurrence (A.62) for $\lambda = 3$, i.e.

$$a_k^F(k) - 3a_{k-1}^F(k-1) + a_{k-2}^F(k-2) = 0, \quad (\text{A.70})$$

which is the same recurrence as the Fibonacci numbers F_{2n} [30]. Furthermore, a direct computation shows that the initial conditions for the two sequences are the same: $a_1^F(1) = 1 = F_2$ and $a_2^F(2) = 3 = F_4$. Therefore, the sequences $a_k^F(k)$ and F_{2k} coincide. \square

B Upper zero-free interval for bipartite planar graphs

Let G be a loopless planar graph. Then it is not hard to prove that $P_G(q) > 0$ for all *integers* $q \geq 5$;³⁴ moreover, one of the most famous theorems of graph theory — the Four-Color Theorem [82–86] — asserts that $P_G(q) > 0$ holds in fact for all integers $q \geq 4$.

It is natural to ask whether these results can be extended from integer q to *real* q . The answer is yes, at least in part: Birkhoff and Lewis [87] proved in 1946 that if G is a loopless planar graph, then $P_G(q) > 0$ for all real numbers $q \geq 5$.³⁵ Furthermore, they conjectured that $P_G(q) > 0$ also for $4 < q < 5$; and while no one has yet found a proof, no one has found a counterexample either, so it seems plausible (in the light of the Four-Color Theorem) that the conjecture is true.

Now, some planar graphs can be colored with three or even two colors; this means that their chromatic polynomials $P_G(q)$ are strictly positive for *integers* $q \geq 3$ or $q \geq 2$, respectively. Can *these* bounds can be extended to real q ? That is, if G is a k -colorable planar graph, do we have $P_G(q) > 0$ for all real $q \geq k$? Woodall [88, p. 142] conjectured that the answer is yes. For $k = 4$, this is the conjecture of Birkhoff and Lewis mentioned above. For $k = 3$, however, Thomassen [89, pp. 505–506] has shown that Woodall’s conjecture is false: there exist 3-colorable (and in fact 2-degenerate³⁶) planar graphs with real chromatic roots greater than 3. Indeed, by

³⁴This is the Five-Color Theorem, which goes back to Heawood in 1890. For a proof, see e.g. [81, Theorem V.8, pp. 154–155]; or for an elegant alternate proof of an even stronger result, see [81, Theorem V.12, pp. 161–163].

³⁵See also Woodall [88, Theorem 1] and Thomassen [89, Theorem 3.1 ff.] for alternate proofs of a more general result. These theorems are, in turn, consequences of a stronger and even more general result for matroids that was proved but not stated (!) twenty years earlier by Oxley [90]; see Jackson [91, Theorem 38].

³⁶A graph G is said to be *k-degenerate* if every subgraph $H \subseteq G$ has at least one vertex of degree $\leq k$. It is not difficult to prove [81, Theorem V.1, p. 148] that every k -degenerate graph is $(k+1)$ -colorable.

combining Thomassen’s construction [89, proof of Theorem 3.9] with Royle’s [92] recent construction of planar graphs with real chromatic roots arbitrarily close to 4, we see that there exist 3-colorable (and in fact 2-degenerate) planar graphs with real chromatic roots arbitrarily close to 4.

In Ref. [6] we showed that Woodall’s conjecture is false also for $k = 2$: there exist 2-colorable (i.e. bipartite) planar graphs with real chromatic roots greater than 2. For example, the $4_P \times 6_F$ square lattice has chromatic roots at $q \approx 2.009978$ and $q \approx 2.168344$. For the cases $8_F \times n_F$ and $8_P \times n_F$, we also observed numerically [6] that there are real chromatic roots tending to $B_5 = (3 + \sqrt{5})/2 \approx 2.618034$ from below as $n \rightarrow \infty$. This led us to modify Woodall’s conjecture as follows [6, Conjecture 7.5]:

Conjecture B.1 [6] *Let G be a bipartite planar graph. Then $P_G(q) > 0$ for real $q \geq B_5 = (3 + \sqrt{5})/2$.*

However, the numerical results reported in the present paper (see Tables 15 and 16) now show that this conjecture is also false. Indeed, it appears that all strip graphs $9_F \times n_F$ (with *odd* $n \geq 39$) and $11_F \times n_F$ (with *odd* $n \geq 23$) have *two* real roots greater than B_5 .

So, not only is Conjecture B.1 false; it is actually false for *two distinct reasons*. First of all, the real roots converging to the isolated limiting point B_5 need not do so only from below. (Empirically we find that, for $m = 9$ and 11 , these roots converge to B_5 with parity $(-1)^{n+1}$.) Secondly, real roots can converge to the real crossing point $q_0(m) > B_5$ when one exists.³⁷ (Empirically we find that such a crossing point exists at least for *odd* widths m and that the real roots converging to it exist for sufficiently large *odd* lengths n .)

We expect both of these behaviors to persist for all larger *odd* widths m . In particular, since we expect that $q_0(m) \uparrow 3$ as $m \rightarrow \infty$ (see Section 6.2), we expect that $m_F \times n_F$ square-lattice strips with m, n both odd and large can have real chromatic roots arbitrarily close to 3. However, in most cases of which we are aware [6–10, 92], the convergence of real chromatic roots to $q_0(m)$ occurs only *from below*.³⁸ Therefore, the following weakened version of Conjecture B.1 is plausible:

³⁷A similar phenomenon was exploited recently by Royle [92] to provide examples of plane triangulations with real chromatic roots converging to 4 from below. His graphs are $4_P \times n_F$ triangular lattices with carefully chosen endgraphs adjoined at top and bottom (see [93] for a general analysis of such strips-with-endgraphs). The key fact underlying this construction is that $q_0(\text{tri}, 4_P) = 4$.

³⁸The only exceptions we know are as follows:

- (a) For square-lattice strips of width $m = 2$ with cyclic boundary conditions [94], and triangular-lattice strips of width $m = 2, 3$ with cyclic and toroidal boundary conditions [9, 10], it appears that there exists an infinite sequence of lengths n with real zeros converging to $q_0(m)$ *from above*.
- (b) For triangular-lattice strips of width $m = 4, 5$ with cyclic boundary conditions [9] and width $m = 5, 7$ with toroidal boundary conditions [10], and for square-lattice strips of width $m = 3$ with cyclic boundary conditions [9], there are real zeros $q > q_0(m)$ for some small lengths n , but the ultimate convergence of real zeros to $q_0(m)$ appears to be only from below.

There are also some cases in which the maximal real zero is exactly equal to $q_0(m)$. Finally, in some cases (e.g., triangular-lattice strips of width $m = 4, 5, 6, 7$ with toroidal boundary conditions [10])

Conjecture B.2 *Let G be a bipartite planar graph. Then $P_G(q) > 0$ for real $q \geq 3$.*

(Note that the honeycomb lattice, which is bipartite and planar, has $q_c = B_5 < 3$.)

We can also give some plausible “physics” considerations that provide additional support for a slightly weakened version of Conjecture B.2. Some two-dimensional antiferromagnetic models at zero temperature have the remarkable property that they can be mapped onto a “height” (or “interface” or “SOS-type”) model (see e.g. [74] and the references cited there). Experience tells us that when such a representation exists, the corresponding zero-temperature spin model is most often critical.³⁹ In particular, when the q -state zero-temperature Potts antiferromagnet on a lattice \mathcal{L} admits a height representation, one expects that $q = q_c(\mathcal{L})$.⁴⁰ This prediction is confirmed in all heretofore-studied cases: 3-state square-lattice [71, 73, 74, 96], 3-state kagomé [97, 98], 4-state triangular [99], and 4-state on the line graph (= covering lattice) of the square lattice [98, 100]. Now, the height representation of the square-lattice zero-temperature 3-state Potts antiferromagnet (i.e., the square-lattice chromatic polynomial at $q = 3$), as presented in [74], generalizes immediately from the square lattice to an arbitrary finite or infinite plane quadrangulation G . This suggests that $q_c(\mathcal{L}) = 3$ for all infinite periodic lattices that are plane quadrangulations. It in turn provides some support for the following weakened version of Conjecture B.2:

Conjecture B.3 *Let G be a plane quadrangulation. Then $P_G(q) > 0$ for real $q \geq 3$.*

Surprisingly, however, we know of a potential counterexample to Conjectures B.2 and B.3! Consider the diced lattice [101, Figure 15], which is the dual of the kagomé lattice and is a plane quadrangulation. Even though there exists a height representation for the 3-state Potts antiferromagnet on the diced lattice, this model is in a non-critical ordered phase at zero temperature. Indeed, Feldmann *et al.* [102] found (by dualizing the numerical data of Ref. [103] for the kagomé-lattice Potts model) that the 3-state diced-lattice Potts model has a critical point at $v_c = -0.8607 \pm 0.0008$, which lies at *nonzero* temperature in the physical antiferromagnetic region $-1 \leq v \leq 0$. (By contrast, the 4-state model was found to have its antiferromagnetic critical point in the unphysical region at $v_c = -1.18 \pm 0.02$, so that the 4-state antiferromagnet

there are sequences of *complex* zeros converging to $q_0(m)$ but apparently *no* sequences of real zeros converging to $q_0(m)$.

Let us remark that the tables of real chromatic roots in Refs. [6–9] show only the cases of strips $m \times (km)$ with $k = 1, \dots, 10$. Moreover, in Ref. [10] such tables are absent. Therefore, we have here used the transfer matrices reported in those papers to recompute all the chromatic polynomials for strips $m \times n$ with $1 \leq n \leq 10m$ (and in some cases for even larger lengths) and their corresponding chromatic roots.

³⁹Some exceptions are the constrained square-lattice 4-state antiferromagnetic Potts model [73] and the triangular-lattice antiferromagnetic spin- s Ising model for large enough s [95], both of which appear to lie in a non-critical ordered phase at zero temperature.

⁴⁰Here $q_c(\mathcal{L})$ is the value (which is conjectured to exist) such that for $q > q_c(\mathcal{L})$ the antiferromagnetic Potts model has exponential decay of correlations uniformly at all temperatures, including zero temperature, while for $q = q_c(\mathcal{L})$ the model has a zero-temperature critical point.

is disordered for all temperatures, including zero temperature.) We have very recently [79] confirmed this scenario by Monte Carlo simulations: for $q = 3$ we find a critical point at $v_c = -0.860599 \pm 0.000004$, while for $q = 4$ we find a finite correlation length uniformly in the region $-1 \leq v \leq 0$. Furthermore, for $q = 3$ we are able to give a mathematically rigorous proof of the existence of a phase transition at nonzero temperature, using a (computer-assisted) Peierls argument. These results indicate that $3 < q_c(\text{diced}) < 4$, contrary to our prediction that $q_c = 3$ for all (regular) plane quadrangulations. Indeed, linear interpolation from the predictions of [102] would suggest $q_c(\text{diced}) \approx 3.44$.

Now, one strongly expects that finite pieces of the diced lattice with free or cylindrical boundary conditions will have chromatic roots tending to $q_c(\text{diced})$ in the infinite-volume limit. What is less clear, however, is whether the roots converging to q_c will necessarily be *real* roots. If they are, then a sufficiently large finite piece of the diced lattice, with boundary conditions arranged so that the graph is a plane quadrangulation (or at least planar and bipartite), would provide a counterexample to Conjecture B.3 (or at least to Conjecture B.2). But if they are not, then the fact that $q_c > 3$ is in no way incompatible with Conjectures B.2 and B.3. Please note also that the roots converging to q_c can be complex for some choices of endgraphs and real for others; this possibility was recently exploited by Royle [92] to provide examples of plane triangulations (based on $4_P \times n_F$ triangular-lattice strips with suitable endgraphs [93]) having real chromatic roots converging from below to $q_c(\text{tri}) = 4$. It would be very interesting to undertake a transfer-matrix study of the diced-lattice chromatic polynomial along the lines of [6–10, 92, 93], in order to test whether the roots converging to q_c can be real, at least for *some* choices of planar bipartite endgraphs.

Acknowledgments

We wish to thank Jesper Jacobsen for many helpful conversations, Chris Henley for correspondence concerning height representations, Tony Guttmann for help with series analysis, and Roman Kotecký and Charles Pfister for discussions concerning the nature of complex phase boundaries. We also thank two anonymous referees for many helpful suggestions that strongly influenced the revised version of this paper.

J.S. is grateful for the kind hospitality of the Physics Department of New York University and the Mathematics Department of University College London, where part of this work was done. Likewise, A.D.S. is grateful for the kind hospitality of the M.S.M.I. group of the Universidad Carlos III de Madrid. Both authors also thank the Isaac Newton Institute for Mathematical Sciences, University of Cambridge, for hospitality during the programme on Combinatorics and Statistical Mechanics (January–June 2008); and A.D.S. thanks the Institut Henri Poincaré for hospitality during the programme on Interacting Particle Systems, Statistical Mechanics and Probability Theory (September–December 2008).

The authors' research was supported in part by U.S. National Science Foundation grants PHY-0116590 and PHY-0424082 (A.D.S.), and by Spanish MEC grants

MTM2005–08618, MTM2008-03020, and FIS2004-03767 (J.S.).

References

- [1] R.B. Potts, Proc. Cambridge Philos. Soc. **48**, 106 (1952).
- [2] F.Y. Wu, Rev. Mod. Phys. **54**, 235 (1982).
- [3] F.Y. Wu, Rev. Mod. Phys. **55**, 315 (E) (1983).
- [4] F.Y. Wu, J. Appl. Phys. **55**, 2421 (1984).
- [5] C.N. Yang and T.D. Lee, Phys. Rev. **87**, 404 (1952).
- [6] J. Salas and A.D. Sokal, J. Stat. Phys. **104**, 609 (2001), cond-mat/0004330.
- [7] J.L. Jacobsen and J. Salas, J. Stat. Phys. **104**, 701 (2001), cond-mat/0011456.
- [8] J.L. Jacobsen, J. Salas and A.D. Sokal, J. Stat. Phys. **112**, 921 (2003), cond-mat/0204587.
- [9] J.L. Jacobsen and J. Salas, J. Stat. Phys. **122**, 705 (2006), cond-mat/0407444.
- [10] J.L. Jacobsen and J. Salas, Nucl. Phys. B **783**, 238 (2007), cond-mat/0703228.
- [11] R. Shrock, Discrete Math. **231**, 421 (2001), cond-mat/9908387.
- [12] A.V. Bakaev and V.I. Kabanovich, J. Phys. A **27**, 6731 (1994).
- [13] P.W. Kasteleyn and C.M. Fortuin, J. Phys. Soc. Japan **26** (Suppl.), 11 (1969).
- [14] C.M. Fortuin and P.W. Kasteleyn, Physica **57**, 536 (1972).
- [15] H.W.J. Blöte and M.P. Nightingale, Physica **112A**, 405 (1982).
- [16] S. Beraha, J. Kahane and N.J. Weiss, Proc. Nat. Acad. Sci. USA **72**, 4209 (1975).
- [17] S. Beraha, J. Kahane and N.J. Weiss, in *Studies in Foundations and Combinatorics* (Advances in Mathematics Supplementary Studies, Vol. 1), ed. G.-C. Rota (Academic Press, New York, 1978).
- [18] S. Beraha and J. Kahane, J. Combin. Theory B **27**, 1 (1979).
- [19] S. Beraha, J. Kahane and N.J. Weiss, J. Combin. Theory B **28**, 52 (1980).
- [20] A.D. Sokal, Combin. Probab. Comput. **13**, 221 (2004), cond-mat/0012369.
- [21] G.D. Birkhoff, Ann. Math. **14**, 42 (1912).
- [22] H. Whitney, Bull. Amer. Math. Soc. **38**, 572 (1932).

- [23] W.T. Tutte, Proc. Cambridge Philos. Soc. **43**, 26 (1947).
- [24] W.T. Tutte, Canad. J. Math. **6**, 80 (1954).
- [25] R.G. Edwards and A.D. Sokal, Phys. Rev. D **38**, 2009 (1988).
- [26] A.D. Sokal, The multivariate Tutte polynomial (alias Potts model) for graphs and matroids, in Bridget S. Webb (editor), *Surveys in Combinatorics, 2005*, pp. 173–226 (Cambridge University Press, Cambridge–New York, 2005), math.CO/0503607.
- [27] R.P. Stanley, *Enumerative Combinatorics*, vol. 1 (Wadsworth & Brooks/Cole, Monterey, CA, 1986). Reprinted by Cambridge University Press, 1999.
- [28] R.P. Stanley, *Enumerative Combinatorics*, vol. 2 (Cambridge University Press, Cambridge–New York, 1999).
- [29] N.G. De Bruijn, *Asymptotic Methods in Analysis*, 2nd ed. (North-Holland, Amsterdam, 1961).
- [30] N.J.A. Sloane, Sloane’s On-Line Encyclopedia of Integer Sequences, <http://www.research.att.com/~njas/sequences/index.html>
- [31] R. Simion and D. Ullman, Discrete Math. **98**, 193 (1991).
- [32] M. Klazar, Discrete Appl. Math. **82**, 263 (1998).
- [33] J. Riordan, J. Combin. Theory A **19**, 214 (1975).
- [34] R. Donaghey and L.W. Shapiro, J. Combin. Theory A **23**, 291 (1977).
- [35] D. Gouyou-Beauchamps and G. Viennot, Adv. Appl. Math. **9**, 334 (1988).
- [36] F.R. Bernhart, Discrete Math. **204**, 73 (1999).
- [37] S.-C. Chang, J. Salas and R. Shrock, J. Stat. Phys. **107**, 1207 (2002), cond-mat/0108144.
- [38] J. Salas and A.D. Sokal, Transfer matrices and partition-function zeros for antiferromagnetic Potts models. VI. Square lattice with special boundary conditions, in preparation.
- [39] S.-C. Chang, J. Jacobsen, J. Salas and R. Shrock, J. Stat. Phys. **114**, 763 (2004), cond-mat/0211623.
- [40] S.-C. Chang and R. Shrock, Physica A **296**, 131 (2001), cond-mat/0005232.
- [41] T. Kato, *Perturbation Theory for Linear Operators*, 2nd ed., corrected printing (Springer-Verlag, Berlin–New York, 1980).

- [42] R.L. Graham, D.E. Knuth and O. Patashnik, *Concrete Mathematics: A Foundation for Computer Science*, 2nd ed. (Addison-Wesley, Reading, Mass., 1994).
- [43] G.H. Golub and C.F. Van Loan, *Matrix Computations*, 3rd ed. (Johns Hopkins University Press, Baltimore, 1996).
- [44] T. de Neef and I.G. Enting, J. Phys. A **10**, 801 (1977).
- [45] I.G. Enting, J. Phys. A **11**, 563 (1978).
- [46] D. Kim and I.G. Enting, J. Combin. Theory B **26**, 327 (1979).
- [47] I.G. Enting, Nucl. Phys. B (Proc. Suppl.) **47**, 180 (1996).
- [48] I.G. Enting, J. Stat. Mech. (2005), P12007.
- [49] I.G. Enting, J. Phys.: Conf. Ser. **42**, 83 (2006).
- [50] A.D. Sokal, Combin. Probab. Comput. **10**, 41 (2001), cond-mat/9904146.
- [51] R. Fernández and A. Procacci, Combin. Probab. Comput. **17**, 225 (2008), arXiv:0704.2617.
- [52] B. Jackson, A. Procacci and A.D. Sokal, Complex zero-free regions at large $|q|$ for multivariate Tutte polynomials (alias Potts-model partition functions) with general complex edge weights, preprint (October 2008), arXiv:0810.4703 [math.CO].
- [53] R.M. Corless, G.H. Gonnet, D.E.G. Hare, D.J. Jeffrey and D.E. Knuth, Adv. Comput. Math. **5**, 329–359 (1996).
- [54] A. Procacci, B. Scoppola and V. Gerasimov, Commun. Math. Phys. **235**, 215 (2003), cond-mat/0201183.
- [55] V. Privman, in *Finite Size Scaling and Numerical Simulation of Statistical Physics*, V. Privman (editor), pp. 1–98 (World Scientific, Singapore, 1990).
- [56] N. Biggs, *Algebraic Graph Theory*, 2nd ed. (Cambridge University Press, Cambridge–New York–Melbourne, 1993).
- [57] A.J. Guttmann and I.G. Enting, J. Phys. A **21**, L467 (1988).
- [58] S.N. Isakov, Commun. Math. Phys. **95**, 427 (1984).
- [59] S. Friedli and C.-E. Pfister, Commun. Math. Phys. **245**, 69 (2004), cond-mat/0212015.
- [60] S. Friedli and C.-E. Pfister, J. Stat. Phys. **114**, 665 (2004), cond-mat/0302480.
- [61] C.-E. Pfister, Ensaios Mat. **9** (2005).

- [62] M. Biskup, C. Borgs, J.T. Chayes, L.J. Kleinwaks, and R. Kotecký, Commun. Math. Phys. **251**, 79 (2004), math-ph/0304007.
- [63] M. Biskup, C. Borgs, J.T. Chayes, and R. Kotecký, J. Stat. Phys. **116**, 97 (2004), math-ph/0312041.
- [64] A.J. Guttmann, in *Phase Transitions and Critical Phenomena*, Vol. 13, pp. 1..234. C. Domb and J.L. Lebowitz, eds. (Academic Press, New York, 1989).
- [65] D.A. Bini and G. Fiorentino, Numerical computation of polynomial roots using MPSolve version 2.2 (January 2000). Software package and documentation available for download at http://fibonacci.dm.unipi.it/pages/bini/public_html/ric.html
- [66] D.A. Bini and G. Fiorentino, Num. Algorithms **23**, 127 (2000).
- [67] J. Jacobsen, J. Salas, and A.D. Sokal, J. Stat. Phys. **119**, 1153 (2005), cond-mat/0401026.
- [68] A. Lenard, cited in E.H. Lieb, Phys. Rev. **162**, 162 (1967) at pp. 169–170.
- [69] R.J. Baxter, J. Math. Phys. **11**, 3116 (1970).
- [70] R.J. Baxter, Proc. Roy. Soc. London A **383**, 43 (1982).
- [71] M. den Nijs, M.P. Nightingale and M. Schick, Phys. Rev. B **26**, 2490 (1982).
- [72] H. Park and M. Widom, Phys. Rev. Lett. **63**, 1193 (1989).
- [73] J.K. Burton Jr. and C.L. Henley, J. Phys. A **30**, 8385 (1997), cond-mat/9708171.
- [74] J. Salas and A.D. Sokal, J. Stat. Phys. **92**, 729 (1998), cond-mat/9801079.
- [75] S.J. Ferreira and A.D. Sokal, J. Stat. Phys. **96**, 461 (1999), cond-mat/9811345.
- [76] R.B. Lehoucq, D.C. Sorensen and C. Yang, *ARPACK Users' Guide: Solution of Large-Scale Eigenvalue Problems with Implicitly Restarted Arnoldi Methods* (SIAM, Philadelphia, 1998). The ARPACK package (written in Fortran 77) and its documentation can be obtained on-line at <http://www.caam.rice.edu/software/ARPACK/>
- [77] R.J. Baxter, J. Phys. A **19**, 2821 (1986).
- [78] R.J. Baxter, J. Phys. A **20**, 5241 (1987).
- [79] R. Kotecký, J. Salas and A.D. Sokal, Phys. Rev. Lett. **101**, 030601 (2008), arXiv:0802.2270 [cond-mat.stat-mech].
- [80] L. Comtet, *Advanced Combinatorics* (D. Reidel Publishing Company, Dordrecht–Boston, 1974).

- [81] B. Bollobas, *Modern Graph Theory* (Springer-Verlag, New York–Berlin–Heidelberg, 1998).
- [82] K. Appel and W. Haken, Illinois J. Math. **21**, 429 (1977).
- [83] K. Appel, W. Haken and J. Koch, Illinois J. Math. **21**, 491 (1977).
- [84] K. Appel and W. Haken, *Every Planar Map is Four Colorable*, Contemporary Mathematics #98 (American Mathematical Society, Providence RI, 1989).
- [85] N. Robertson, D.P. Sanders, P.D. Seymour and R. Thomas, J. Combin. Theory B **70**, 2 (1997).
- [86] R. Thomas, Notices Amer. Math. Soc. **45**, 848 (1998).
- [87] G.D. Birkhoff and D.C. Lewis, Trans. Amer. Math. Soc. **60**, 355 (1946).
- [88] D.R. Woodall, Discrete Math. **172**, 141 (1997).
- [89] C. Thomassen, Combin. Probab. Comput. **6**, 497 (1997).
- [90] J.G. Oxley, Quart. J. Math. Oxford **29**, 11 (1978).
- [91] B. Jackson, J. Geom. **76**, 95 (2003), math.CO/0205047.
- [92] G.F. Royle, Ann. Combinatorics **12**, 195 (2008), math.CO/0511304.
- [93] M. Roček, R. Shrock and S.-H. Tsai, Physica A **259**, 367 (1998), cond-mat/9807106.
- [94] R. Shrock and S.-H. Tsai, Phys. Rev. E **55**, 5165 (1997), cond-mat/9612249.
- [95] C. Zeng and C.L. Henley, Phys. Rev. B **55**, 14935 (1997), cond-mat/9609007.
- [96] J. Kolafa, J. Phys. A: Math. Gen. **17**, L777 (1984).
- [97] D.A. Huse and A.D. Rutenberg, Phys. Rev. B **45**, 7536 (1992).
- [98] J. Kondev and C.L. Henley, Nucl. Phys. B **464**, 540 (1996).
- [99] C.L. Henley, private communications.
- [100] J. Kondev and C.L. Henley, Phys. Rev. B **52**, 6628 (1995).
- [101] I. Syozi, Transformations of Ising models, in C. Domb and M.S. Green (editors), *Phase Transitions and Critical Phenomena*, Vol. 1, pp. 269–329 (Academic Press, London–New York, 1972).
- [102] H. Feldmann, R. Shrock, and S.-H. Tsai, J. Phys. A **30**, L663 (1997), cond-mat/9710018.
- [103] I. Jensen, A.J. Guttmann, and I.G. Enting, J. Phys. A **30**, 8067 (1997).

m	b_0^F	b_1^F	b_2^F	b_3^F	b_4^F	b_5^F	b_6^F	b_7^F	b_8^F	b_9^F	b_{10}^F	b_{11}^F	b_{12}^F	b_{13}^F	b_{14}^F	b_{15}^F
1	1	1	0	0	0	0	0	0	0	0	0	0	0	0	0	0
2	1	3	3	0	0	0	0	0	0	0	0	0	0	0	0	0
3	1	5	10	8	1	-1	1	-2	6	-16	35	-61	69	42	-583	2371
4	1	7	21	32	23	3	-2	-1	6	-14	28	-54	102	-172	145	695
5	1	9	36	80	102	66	10	-9	6	-6	14	-38	97	-218	361	-75
6	1	11	55	160	290	322	192	26	-19	2	15	-35	77	-160	241	-5
7	1	13	78	280	655	1017	1011	556	75	-59	21	-6	32	-84	103	107
8	1	15	105	448	1281	2541	3486	3153	1617	201	-151	22	64	-73	24	132
9	1	17	136	672	2268	5460	9492	11741	9785	4697	550	-436	96	103	-97	67
10	1	19	171	960	3732	10548	22128	34468	39006	30223	13652	1461	-1190	229	316	-221
11	1	21	210	1320	5805	18819	46149	86346	122436	128142	92975	39640	3874	-3318	650	881
12	1	23	253	1760	8635	31559	88462	192787	327120	427276	417066	284954	115022	10141	-9225	1865

Table 1: Coefficients $b_k^F(m)$ of the large- q expansion of the dominant eigenvalue λ_\star^F for free boundary conditions. For each $1 \leq m \leq 12$, we include all coefficients $b_k^F(m)$ up to $k = 15$. For the whole data set up to $k = 40$, see the MATHEMATICA file `data_FREE.m` included in the on-line version of the paper at arXiv.org. Those data points below the stair-case-like line satisfy $m \geq m_{\min}^F(k)$ [cf. (4.11)].

m	c_1^F	$2c_2^F$	$3c_3^F$	$4c_4^F$	$5c_5^F$	$6c_6^F$	$7c_7^F$	$8c_8^F$	$9c_9^F$	$10c_{10}^F$	$11c_{11}^F$	$12c_{12}^F$	$13c_{13}^F$	$14c_{14}^F$	$15c_{15}^F$
1	-1	-1	-1	-1	-1	-1	-1	-1	-1	-1	-1	-1	-1	-1	-1
2	-3	-3	0	9	27	54	81	81	0	-243	-729	-1458	-2187	-2187	0
3	-5	-5	1	19	55	109	170	243	496	1685	5957	17449	39463	57430	-21119
4	-7	-7	2	29	83	164	259	405	1001	3743	13688	42548	111078	240401	393557
5	-9	-9	3	39	111	219	348	567	1506	5801	21430	67839	184617	437890	898368
6	-11	-11	4	49	139	274	437	729	2011	7859	29172	93130	258169	635645	1406389
7	-13	-13	5	59	167	329	526	891	2516	9917	36914	118421	331721	833400	1914425
8	-15	-15	6	69	195	384	615	1053	3021	11975	44656	143712	405273	1031155	2422461
9	-17	-17	7	79	223	439	704	1215	3526	14033	52398	169003	478825	1228910	2930497
10	-19	-19	8	89	251	494	793	1377	4031	16091	60140	194294	552377	1426665	3438533
11	-21	-21	9	99	279	549	882	1539	4536	18149	67882	219585	625929	1624420	3946569
12	-23	-23	10	109	307	604	971	1701	5041	20207	75624	244876	699481	1822175	4454605

Table 2: Coefficients $kc_k^F(m)$ of the large- q expansion of $\log(q^{-m}\lambda_\star^F)$ where λ_\star^F is the dominant eigenvalue for free boundary conditions. For each $1 \leq m \leq 12$, we include all coefficients $c_k^F(m)$ up to $k = 15$. For the whole data set up to $k = 40$, see the MATHEMATICA file `data_FREE.m` included in the on-line version of the paper at arXiv.org. Those data points below the stair-case-like line satisfy $m \geq m_{\min}^F(k)$ [cf. (4.11)].

m	Δ_6^F	Δ_7^F	Δ_8^F	Δ_9^F	Δ_{10}^F	Δ_{11}^F	Δ_{12}^F	Δ_{13}^F	Δ_{14}^F	Δ_{15}^F	Δ_{16}^F	Δ_{17}^F	Δ_{18}^F	Δ_{19}^F	Δ_{20}^F	Δ_{21}^F
1	0	1	10	57	243	867	2777	8430	$\frac{50447}{2}$	75586	224939	650699	$\frac{3583917}{2}$	4637373	$\frac{22526941}{2}$	$\frac{78375472}{3}$
2	0	0	0	1	13	97	548	2604	10942	41717	146333	476291	$\frac{2896101}{2}$	4142266	$\frac{22531163}{2}$	29609731
3	0	0	0	0	0	1	16	150	1075	6440	33513	154727	643296	2438443	8522559	27772788
4	0	0	0	0	0	0	0	1	19	216	1883	13595	84238	458660	2235421	9900665
5	0	0	0	0	0	0	0	0	0	1	22	295	3031	25574	183804	1155646
6	0	0	0	0	0	0	0	0	0	0	0	1	25	387	4578	44167
7	0	0	0	0	0	0	0	0	0	0	0	0	0	1	28	492
8	0	0	0	0	0	0	0	0	0	0	0	0	0	0	0	1
9	0	0	0	0	0	0	0	0	0	0	0	0	0	0	0	0
10	0	0	0	0	0	0	0	0	0	0	0	0	0	0	0	0
11	0	0	0	0	0	0	0	0	0	0	0	0	0	0	0	0
12	0	0	0	0	0	0	0	0	0	0	0	0	0	0	0	0

Table 3: Coefficients $\Delta_k^F(m)$ for free boundary conditions [cf. (4.16)] for $6 \leq k \leq 21$ and $1 \leq m \leq 12$. For $0 \leq k \leq 6$ and $1 \leq m \leq 12$, the coefficients $\Delta_k^F(m)$ vanish. For the whole data set up to $k = 33$, see the MATHEMATICA file `data_FREE.m` included in the on-line version of the paper at arXiv.org. Those data points below the stair-case-like line satisfy $m \geq m_{\min}^F(k)$ [cf. (4.11)] and are therefore zero.

m	b_0^P	b_1^P	b_2^P	b_3^P	b_4^P	b_5^P	b_6^P	b_7^P	b_8^P	b_9^P	b_{10}^P	b_{11}^P	b_{12}^P	b_{13}^P	b_{14}^P	b_{15}^P
1	0	0	0	0	0	0	0	0	0	0	0	0	0	0	0	0
2	1	3	3	0	0	0	0	0	0	0	0	0	0	0	0	0
3	1	6	14	13	0	0	0	0	0	0	0	0	0	0	0	0
4	1	8	28	51	45	2	-8	10	2	2	-192	980	-2942	6164	-7566	-9986
5	1	10	45	115	174	141	20	-45	20	50	15	-400	670	930	-8155	27400
6	1	12	66	214	441	575	428	81	-119	-45	210	35	-396	-122	1075	2106
7	1	14	91	357	924	1617	1868	1275	273	-287	-210	294	532	-679	-539	-609
8	1	16	120	552	1716	3744	5748	5991	3777	812	-636	-634	280	1096	724	-3022
9	1	18	153	807	2925	7623	14505	19962	19034	11140	2313	-1497	-1374	-360	1662	4377
10	1	20	190	1130	4675	14144	32005	54340	68085	59999	32790	6375	-3660	-2760	-1792	215
11	1	22	231	1529	7106	24453	64009	128777	198330	228866	187901	96306	17336	-9537	-5093	-4367
12	1	24	276	2012	10374	39984	118702	275460	501213	708868	760164	585131	282358	46638	-25822	-9177
13	1	26	325	2587	14651	62491	207285	544232	1139450	1899300	2490423	2499471	1813122	826359	124540	-71760

Table 4: Coefficients $b_k^P(m)$ of the large- q expansion of the dominant eigenvalue λ_\star^P for cylindrical boundary conditions. For each $1 \leq m \leq 13$, we include all coefficients $b_k^F(m)$ up to $k = 15$. For the whole data set up to $k = 40$, see the MATHEMATICA file `data_CYL.m` included in the on-line version of the paper at arXiv.org. Those data points below the stair-case-like line satisfy $m \geq m_{\min}^P(k) = k + 2$.

m	c_1^P	$2c_2^P$	$3c_3^P$	$4c_4^P$	$5c_5^P$	$6c_6^P$	$7c_7^P$	$8c_8^P$	$9c_9^P$	$10c_{10}^P$	$11c_{11}^P$	$12c_{12}^P$	$13c_{13}^P$	$14c_{14}^P$	$15c_{15}^P$
2	-3	-3	0	9	27	54	81	81	0	-243	-729	-1458	-2187	-2187	0
3	-6	-8	-3	16	34	-59	-622	-2464	-6843	-14648	-24118	-28595	-24342	-59256	-386483
4	-8	-8	7	52	162	493	1595	4764	11383	15722	-31303	-360503	-1801119	-6704573	-19871718
5	-10	-10	5	46	120	155	-325	-2914	-10984	-27430	-37245	62971	649587	2559421	6057120
6	-12	-12	6	60	173	360	765	2644	11922	49003	170840	505212	1251225	2440055	2788766
7	-14	-14	7	70	196	379	581	742	385	-4074	-32123	-167537	-694721	-2340051	-6229223
8	-16	-16	8	80	224	440	719	1352	4652	21864	96762	384848	1421716	4975913	16390643
9	-18	-18	9	90	252	495	801	1450	4473	17622	61032	166635	307107	-34941	-3730356
10	-20	-20	10	100	280	550	890	1620	5059	20670	78685	266050	836335	2622628	8719855
11	-22	-22	11	110	308	605	979	1782	5555	22628	85052	276485	789910	2016223	4478441
12	-24	-24	12	120	336	660	1068	1944	6060	24696	92915	303624	884886	2400080	6337977
13	-26	-26	13	130	364	715	1157	2106	6565	26754	100646	328771	956020	2567903	6567418

Table 5: Coefficients $kc_k^P(m)$ of the large- q expansion of $\log(q^{-m}\lambda_\star^P)$ where λ_\star^P is the dominant eigenvalue for cylindrical boundary conditions. For each $2 \leq m \leq 13$, we include all coefficients $c_k^P(m)$ up to $k = 15$. For the whole data set up to $k = 40$, see the MATHEMATICA file `data_CYL.m` included in the on-line version of the paper at arXiv.org. Those data points below the stair-case-like line satisfy $m \geq m_{\min}^P(k) = k + 2$.

m	\tilde{b}_0^P	\tilde{b}_1^P	\tilde{b}_2^P	\tilde{b}_3^P	\tilde{b}_4^P	\tilde{b}_5^P	\tilde{b}_6^P	\tilde{b}_7^P	\tilde{b}_8^P	\tilde{b}_9^P	\tilde{b}_{10}^P	\tilde{b}_{11}^P	\tilde{b}_{12}^P	\tilde{b}_{13}^P	\tilde{b}_{14}^P	\tilde{b}_{15}^P
0	1	0	0	0	0	0	0	0	0	0	0	0	0	0	0	0
1	1	2	0	0	0	0	0	0	0	0	0	0	0	0	0	0
2	1	4	6	0	0	0	0	0	0	0	0	0	0	0	0	0
3	1	6	15	17	0	0	0	0	0	0	0	0	0	0	0	0
4	1	8	28	52	50	2	-8	10	2	2	-192	980	-2942	6164	-7566	-9986
5	1	10	45	115	175	147	20	-45	20	50	15	-400	670	930	-8155	27400
6	1	12	66	214	441	576	435	81	-119	-45	210	35	-396	-122	1075	2106
7	1	14	91	357	924	1617	1869	1283	273	-287	-210	294	532	-679	-539	-609
8	1	16	120	552	1716	3744	5748	5992	3786	812	-636	-634	280	1096	724	-3022
9	1	18	153	807	2925	7623	14505	19962	19035	11150	2313	-1497	-1374	-360	1662	4377
10	1	20	190	1130	4675	14144	32005	54340	68085	60000	32801	6375	-3660	-2760	-1792	215
11	1	22	231	1529	7106	24453	64009	128777	198330	228866	187902	96318	17336	-9537	-5093	-4367
12	1	24	276	2012	10374	39984	118702	275460	501213	708868	760164	585132	282371	46638	-25822	-9177
13	1	26	325	2587	14651	62491	207285	544232	1139450	1899300	2490423	2499471	1813123	826373	124540	-71760

Table 6: Coefficients $\tilde{b}_k^P(m)$ of the large- q expansion of the dominant eigenvalue λ_\star^P for cylindrical boundary conditions. For each $1 \leq m \leq 13$, we include all coefficients $\tilde{b}_k^P(m)$ up to $k = 15$. For the whole data set up to $k = 40$, see the MATHEMATICA file `data_CYL.m` included in the on-line version of the paper at arXiv.org. Those data points below the stair-case-like line satisfy $m \geq k$.

m	\tilde{c}_1^P	$2\tilde{c}_2^P$	$3\tilde{c}_3^P$	$4\tilde{c}_4^P$	$5\tilde{c}_5^P$	$6\tilde{c}_6^P$	$7\tilde{c}_7^P$	$8\tilde{c}_8^P$	$9\tilde{c}_9^P$	$10\tilde{c}_{10}^P$	$11\tilde{c}_{11}^P$	$12\tilde{c}_{12}^P$	$13\tilde{c}_{13}^P$	$14\tilde{c}_{14}^P$	$15\tilde{c}_{15}^P$
2	-4	-4	8	56	176	368	416	-544	-4672	-15424	-33664	-42112	33536	386816	1346048
3	-6	-6	3	6	-111	-705	-2463	-6090	-11580	-20001	-49836	-195861	-767643	-2515155	-6905922
4	-8	-8	4	40	182	880	3674	12096	30586	51852	-5024	-534920	-3020324	-12012568	-38506486
5	-10	-10	5	50	140	125	-1130	-8030	-32125	-92520	-188000	-169195	584925	3408080	8106710
6	-12	-12	6	60	168	330	807	4148	23001	101778	360304	1038354	2394614	3965607	1844286
7	-14	-14	7	70	196	385	623	686	-2198	-25704	-148624	-642719	-2239797	-6350183	-13989773
8	-16	-16	8	80	224	440	712	1296	4724	26024	135790	619232	2490264	8897768	28169498
9	-18	-18	9	90	252	495	801	1458	4545	17532	54663	100467	-131058	-2239899	-12715191
10	-20	-20	10	100	280	550	890	1620	5050	20580	78795	275410	943000	3394462	12965290
11	-22	-22	11	110	308	605	979	1782	5555	22638	85162	276353	776611	1851289	3184016
12	-24	-24	12	120	336	660	1068	1944	6060	24696	92904	303492	885042	2418448	6584247
13	-26	-26	13	130	364	715	1157	2106	6565	26754	100646	328783	956176	2567721	6542653

Table 7: Coefficients $k\tilde{c}_k^P(m)$ defined in (4.10). For each $2 \leq m \leq 13$, we include all coefficients $c_k^P(m)$ up to $k = 15$. For the whole data set up to $k = 40$, see the MATHEMATICA file `data_CYL.m` included in the on-line version of the paper at arXiv.org. Those data points below the stair-case-like line satisfy $m \geq \tilde{m}_{\min}^P(k) = \max(k, 2)$.

m	Δ_2^P	Δ_3^P	Δ_4^P	Δ_5^P	Δ_6^P	Δ_7^P	Δ_8^P	Δ_9^P	Δ_{10}^P	Δ_{11}^P	Δ_{12}^P	Δ_{13}^P	Δ_{14}^P	Δ_{15}^P	Δ_{16}^P
2	0	2	9	24	43	34	$-\frac{217}{2}$	$-\frac{1894}{3}$	-1954	-4468	$-\frac{15449}{2}$	-8736	-621	$\frac{109992}{5}$	$\frac{133695}{4}$
3	0	0	-6	-39	-145	-390	-822	-1455	$-\frac{5235}{2}$	-6642	$-\frac{45289}{2}$	-76023	-222030	-562002	-1284432
4	0	0	0	14	110	474	1431	3174	4362	-3272	-53007	-254964	-914542	$-\frac{8107726}{3}$	$-\frac{12999385}{2}$
5	0	0	0	0	-25	-225	-1105	-3850	-10281	-20610	$-\frac{49275}{2}$	16705	$\frac{345615}{2}$	371102	$-\frac{916875}{2}$
6	0	0	0	0	0	39	397	2219	8943	28532	73884	150254	$\frac{397011}{2}$	-80262	$-\frac{3442249}{2}$
7	0	0	0	0	0	0	-56	-637	-4011	-18438	-68313	-211897	-552462	-1169735	-1737302
8	0	0	0	0	0	0	0	76	956	6714	34742	146296	522552	1607014	4237541
9	0	0	0	0	0	0	0	0	-99	-1365	-10596	-61002	-287121	-1152501	-4024251
10	0	0	0	0	0	0	0	0	0	125	1875	15960	101208	525662	2333070
11	0	0	0	0	0	0	0	0	0	0	-154	-2497	-23144	-160292	-909502
12	0	0	0	0	0	0	0	0	0	0	0	186	3242	32521	244227
13	0	0	0	0	0	0	0	0	0	0	0	0	-221	-4121	-44499

Table 8: Modified coefficients $\Delta_k^P(m)$ for cylindrical boundary conditions for $2 \leq k \leq 16$ and $2 \leq m \leq 13$. For $k = 1$ and $2 \leq m \leq 13$, the coefficients $\Delta_k^P(m)$ vanish. Those data points below the stair-case-like line satisfy $m \geq \tilde{m}_{\min}^P(k) = \max(k, 2)$ and are therefore zero.

k	α_k	β_k	γ_k
0	1	1	1
1	0	1	0
2	0	0	0
3	1	-1	1
4	0	-1	0
5	0	0	0
6	0	1	0
7	1	-1	4
8	3	-8	12
9	4	-16	20
10	3	-16	28
11	3	-12	67
12	11	-41	208
13	24	-138	484
14	8	-210	753
15	-91	47	750
16	-261	849	679
17	-290	1471	2320
18	254	-493	10020
19	1671	-8052	30548
20	3127	-19901	68832
21	786	-19966	108744
22	-13939	37556	65229
23	-49052	223807	-236055
24	-80276	508523	-739289
25	21450	321314	101404
26	515846	-2052462	7201383
27	1411017	-8417723	26255714
28	1160761	-13374892	43505098
29	-4793764	10841423	-17552274
30	-20340586	112595914	-291420026
31	-29699360	260687001	-674637832
32	33165914	70989018	27442
33	256169433	-1341964856	4426763291
34	495347942	-4108283969	12910062402
35	-127736296	-3304416038	9737827437
36	-3068121066	14960606999	-49131891078
37	-7092358808	58237169596	-184470253912
38	-1024264966	65268280922	-183956055539
39	35697720501	-162368154719	621518352427
40	91243390558	-767619757924	2660084937207
41	25789733672	-975329692910	3075466954690
42	-420665229170	1872486336165	-7500763944932
43	-1089052872105	9701425034093	-34822638005931
44	-238516756366	12262136381593	-38841312202313
45	5101697398582	-24192583755347	104412348649015
46	12146149238921	-118764516172484	448320847685638
47	-598931311074	-130312353695974	

Table 9: Large- q series expansions for the bulk, surface and corner free energies of the square-lattice zero-temperature Potts antiferromagnet, in terms of the variable $z = 1/(q - 1)$. The coefficients are defined by $e^{f_{\text{bulk}}} = [(q - 1)^2/q] \sum_{k=0}^{\infty} \alpha_k z^k$, $e^{f_{\text{surf}}} = \sum_{k=0}^{\infty} \beta_k z^k$ and $e^{f_{\text{corner}}} = \sum_{k=0}^{\infty} \gamma_k z^k$. The coefficients α_k for $k \leq 36$ were obtained in Ref. [12]; all the other coefficients are new. The coefficient β_{47} is conjectural.

N	z_1	z_2	z_3
30	$-0.27(1) \pm 0.773(7) i$ 0.6(2)		$0.502(3) \pm 0.292(5) i$ 0.2(2)
40	$-0.2811(5) \pm 0.7757(7) i$ 0.47(3)	$0.45(2) \pm 0.53(1) i$ 0.4(5)	$0.501(2) \pm 0.289(2) i$ 0.4(1)
50	$-0.2811(2) \pm 0.7752(1) i$ 0.50(1)	$0.452(6) \pm 0.538(5) i$ 0.3(2)	$0.49999(2) \pm 0.28868(2) i$ 0.501(5)
60	$-0.28112(3) \pm 0.77520(2) i$ 0.500(3)	$0.4480(9) \pm 0.538(1) i$ 0.48(7)	$0.499997(5) \pm 0.288676(6) i$ 0.501(2)
70	$-0.281118(3) \pm 0.775201(4) i$ 0.4999(6)	$0.44778(4) \pm 0.53827(8) i$ 0.500(4)	$0.499999(2) \pm 0.288675(1) i$ 0.5001(5)
80	$-0.281118(2) \pm 0.775201(2) i$ 0.5000(3)	$0.447783(5) \pm 0.538251(8) i$ 0.5000(7)	$0.500000(1) \pm 0.2886751(1) i$ 0.5001(4)
90	$-0.281118(2) \pm 0.775201(2) i$ 0.5000(3)	$0.447784(1) \pm 0.538250(2) i$ 0.4999(3)	$0.4999997(9) \pm 0.2886752(8) i$ 0.5001(3)
100	$-0.2811174(5) \pm 0.7752009(6) i$ 0.5000(1)	$0.447784(1) \pm 0.538249(2) i$ 0.5000(2)	$0.4999998(8) \pm 0.2886752(8) i$ 0.5000(2)
Exact	$-0.2811172691 \pm 0.7752009092 i$ 0.5	$0.44778393657 \pm 0.5382490441 i$ 0.5	$0.5 \pm 0.2886751346 i$ 0.5
$ z_i $	0.8245989138	0.7001589015	0.5773502692

Table 10: Estimates of the position and exponent of the “correct” singularities for the square-lattice strip of width $L = 3$ and free boundary conditions. The column N indicates the maximum order of the series in $z = 1/(q - 1)$ that was used in the analysis. The row marked ‘Exact’ shows the known exact results. The last row (marked $|z_i|$) shows the absolute value of the corresponding exact singularity. Blank entries mean that we were unable to obtain the corresponding estimates.

N	z_4	z_5	z_6	z_7
30	$0.36(1) \pm 0.66(2) i$ $0.4(5)$	$-1.000(5)$ $-0.1(2)$		
40	$0.368(7) \pm 0.654(8) i$ $0.0(2)$	$-1.0000(1)$ $-0.001(6)$		
50	$0.3695(6) \pm 0.6524(1) i$ $-0.03(5)$	$-1.0000(1)$ $0.000(6)$		
60	$0.3695(2) \pm 0.6516(4) i$ $-0.01(3)$	$-1.00000(6)$ $0.000(4)$		
70	$0.3695(1) \pm 0.6514(2) i$ $0.00(1)$	$-1.00000(2)$ $0.000(2)$		$0.487(5) \pm 0.427(4) i$ $2.03(9)$
80	$0.36947(2) \pm 0.65136(2) i$ $-0.001(3)$	$-1.00000(2)$ $0.000(2)$	$0.59(5)$ $0.0(6)$	$0.488(2) \pm 0.428(1) i$ $2.01(4)$
90	$0.369460(3) \pm 0.651363(2) i$ $0.0001(6)$	$-1.00000(2)$ $0.000(2)$	$0.595(1)$ $0.001(1)$	$0.4878(5) \pm 0.4277(2) i$ $2.000(2)$
100	$0.369460(3) \pm 0.651363(3) i$ $0.0000(6)$	$-1.000000(9)$ $0.0000(9)$	$0.5945(4)$ $0.000(8)$	$0.4877(4) \pm 0.4277(2) i$ $2.000(2)$

Table 11: Estimates of the position and exponent of the spurious singularities for the square-lattice strip of width $L = 3$ and free boundary conditions. The column N indicates the maximum order of the series in $z = 1/(q - 1)$ that was used in the analysis. Blank entries mean that we were unable to obtain the corresponding estimates.

N	z_1	z_2	z_3	z_4	z_5
30	$0.331(2) \pm 0.238(2) i$ 0.5(2)	$-0.068(1) \pm 0.4795(8) i$ 0.53(8)	$0.29(2) \pm 0.49(3) i$ -0.3(3)		
40	$0.3315(4) \pm 0.2370(4) i$ 0.53(8)	$-0.0682(2) \pm 0.4798(2) i$ 0.51(3)	$0.30(2) \pm 0.48(2) i$ -0.4(6)		
50	$0.33162(6) \pm 0.23712(5) i$ 0.50(2)	$-0.068171(3) \pm 0.479859(4) i$ 0.5005(9)	$0.30(1) \pm 0.48(3) i$ -0.2(6)		
60	$0.331635(2) \pm 0.237117(2) i$ 0.4995(9)	$-0.0681711(4) \pm 0.4798607(9) i$ 0.5001(3)	$0.30(2) \pm 0.46(3) i$ 0.3(13)		
70	$0.3316353(8) \pm 0.237116(1) i$ 0.4998(4)	$-0.0681712(2) \pm 0.4798609(5) i$ 0.5000(1)	$0.29(2) \pm 0.46(3) i$ 0.4(12)		
80	$0.3316354(7) \pm 0.2371156(1) i$ 0.4998(4)	$-0.0681712(2) \pm 0.4798609(2) i$ 0.50000(6)	$0.29(1) \pm 0.45(2) i$ 0.6(10)	$0.76(3)$ -0.9(6)	
90	$0.3316354(6) \pm 0.2371155(9) i$ 0.4999(3)	$-0.0681712(2) \pm 0.4798609(2) i$ 0.50001(7)	$0.28144(4) \pm 0.45208(5) i$ 0.503(6)	$0.75(1)$ -0.7(4)	
100	$0.3316354(7) \pm 0.237116(1) i$ 0.4999(4)	$-0.0681712(1) \pm 0.4798609(3) i$ 0.50000(9)	$0.281427(4) \pm 0.452108(3) i$ 0.5000(4)	$0.754(9)$ -0.7(3)	
Exact	$0.3316354418 \pm 0.2371152471 i$ 0.5	$-0.0681712693 \pm 0.4798609413 i$ 0.5	$0.2814289723 \pm 0.4521062477 i$ 0.5	0.7398155434 0.5	0.7978491474 0.5
$ z_i $	0.4076833412	0.4846791154	0.5325432618	0.7398155434	0.7978491474

Table 12: Estimates of the position and exponent of the “correct” singularities for the square-lattice strip of width $L = 4$ and periodic boundary conditions. The column N indicates the maximum order of the series in $z = 1/(q - 1)$ that was used in the analysis. The row marked ‘Exact’ shows the known exact results. The last row (marked $|z_i|$) shows the absolute value of the corresponding exact singularity.

N	z_6	z_7
30	$-0.999(4)$ $0.0(1)$	
40	$-1.000(1)$ $0.00(3)$	
50	$-1.00000(4)$ $0.000(2)$	$0.30(2) \pm 0.47(2) i$ $0.3(12)$
60	$-1.00000(1)$ $0.0002(9)$	$0.29(1) \pm 0.46(2) i$ $0.5(10)$
70	$-0.999999(9)$ $0.0001(5)$	$0.29(2) \pm 0.46(3) i$ $0.3(10)$
80	$-1.00000(1)$ $0.0001(7)$	$0.286(2) \pm 0.517(2) i$ $0.0(1)$
90	$-1.000000(2)$ $0.0000(2)$	$0.2854(4) \pm 0.5180(4) i$ $0.00(3)$
100	$-1.000000(4)$ $0.0000(4)$	$0.28528(4) \pm 0.51814(6) i$ $0.000(4)$

Table 13: Estimates of the position and exponent of the spurious singularities for the square-lattice strip of width $L = 4$ and periodic boundary conditions. The column N indicates the maximum order of the series in $z = 1/(q - 1)$ that was used in the analysis. Blank entries mean that we were unable to obtain the corresponding estimates.

m_F	$\text{Re } q_0$	$ \text{Im } q_0 $	Type
3 _F	2	0	S
4 _F	2.2283590792	0	+
5 _F	2.4284379020	0	S
6 _F	2.5286467909	0	+
7 _F	2.6062482130	0	S
8 _F	2.6602596967	0.0007413717	D
9 _F	2.7016599568	0	S
10 _F	2.7343903604	0.0003924978	D
11 _F	2.7608973951	0	S
12 _F	2.782817590	0.00018700	D

Table 14: Values of $q_0(m)$ for square-lattice strips with free boundary conditions. Type “S” means that the limiting curve \mathcal{B}_m crosses the real axis at a single point, “D” means that the limiting curve does not cross the real q -axis but has two complex-conjugate endpoints nearby, and “+” means that the limiting curve contains a segment on the real q -axis (we define q_0 to be the lower end of that segment). For points of type “D”, we also show the imaginary part. The data for $m \leq 7$ are taken from [6]. Notice that the value for $m = 8$ reported in [6] is wrong; the correct value is displayed here.

n	4th Zero - B_5	5th Zero
30	$-8.9459389900 \times 10^{-3}$	
32	$-5.6487223660 \times 10^{-3}$	
34	$-3.1962919070 \times 10^{-3}$	
36	$-1.5712164060 \times 10^{-3}$	
38	$-6.6617400470 \times 10^{-4}$	
39	$5.8575529850 \times 10^{-4}$	2.6298556468
40	$-2.5161135990 \times 10^{-4}$	
41	$1.7270275260 \times 10^{-4}$	2.6345567384
42	$-8.8890257250 \times 10^{-5}$	
43	$5.5346483490 \times 10^{-5}$	2.6384105545
44	$-3.0434570840 \times 10^{-5}$	
45	$1.8199961300 \times 10^{-5}$	2.6417380816
46	$-1.0281765140 \times 10^{-5}$	
47	$6.0420071920 \times 10^{-6}$	2.6446771074
48	$-3.4539716110 \times 10^{-6}$	
49	$2.0135551740 \times 10^{-6}$	2.6473078802
50	$-1.1574596530 \times 10^{-6}$	
51	$6.7216127470 \times 10^{-7}$	2.6496845069
52	$-3.8744221380 \times 10^{-7}$	
53	$2.2455458550 \times 10^{-7}$	2.6518466022
54	$-1.2962041990 \times 10^{-7}$	
55	$7.5047689080 \times 10^{-8}$	2.6538246782
56	$-4.3353170180 \times 10^{-8}$	
57	$2.5086443380 \times 10^{-8}$	2.6556430336
58	$-1.4497910190 \times 10^{-8}$	
59	$8.3866240660 \times 10^{-9}$	2.6573214747
60	$-4.8479232330 \times 10^{-9}$	
61	$2.8038883660 \times 10^{-9}$	2.6588764247
62	$-1.6210151380 \times 10^{-9}$	
63	$9.3745081850 \times 10^{-10}$	2.6603216811
64	$-5.4201053100 \times 10^{-10}$	
65	$3.1343270220 \times 10^{-10}$	2.6616689582
66	$-1.8122675760 \times 10^{-10}$	
67	$1.0479599710 \times 10^{-10}$	2.6629282884
68	$-6.0594535690 \times 10^{-11}$	
69	$3.5038676450 \times 10^{-11}$	2.6641083276
70	$-2.0260148680 \times 10^{-11}$	
∞	0	2.7016599568

Table 15: Fourth and fifth real chromatic zeros for a strip $9_F \times n_F$ with free boundary conditions. As the fourth zero converges rapidly to B_5 , we show their difference. The last row (labelled with $n = \infty$) shows the infinite-length limit; in particular, the value of $q_0(9)$.

n	4th Zero - B_5	5th Zero
14	$-3.6516138320 \times 10^{-2}$	
16	$-1.9375298640 \times 10^{-2}$	
18	$-8.1115634110 \times 10^{-3}$	
20	$-2.2141892360 \times 10^{-3}$	
22	$-3.6952234840 \times 10^{-4}$	
23	$2.7283542170 \times 10^{-4}$	2.6360127941
24	$-4.7440730960 \times 10^{-5}$	
25	$2.3461500250 \times 10^{-5}$	2.6467690175
26	$-5.5660625770 \times 10^{-6}$	
27	$2.2973640450 \times 10^{-6}$	2.6554417441
28	$-6.2842068380 \times 10^{-7}$	
29	$2.3500000310 \times 10^{-7}$	2.6628475620
30	$-6.9454825890 \times 10^{-8}$	
31	$2.4549166270 \times 10^{-8}$	2.6693333011
32	$-7.5798800910 \times 10^{-9}$	
33	$2.5935418370 \times 10^{-9}$	2.6750988717
34	$-8.2103756740 \times 10^{-10}$	
35	$2.7571779370 \times 10^{-10}$	2.6802756665
36	$-8.8542077070 \times 10^{-11}$	
37	$2.9415010300 \times 10^{-11}$	2.6849567990
38	$-9.5240493620 \times 10^{-12}$	
39	$3.1444559750 \times 10^{-12}$	2.6892116307
40	$-1.0229343110 \times 10^{-12}$	
41	$3.3652761350 \times 10^{-13}$	2.6930937453
42	$-1.0977435000 \times 10^{-13}$	
43	$3.6039742950 \times 10^{-14}$	2.6966457592
44	$-1.1774405610 \times 10^{-14}$	
45	$3.8610612020 \times 10^{-15}$	2.6999024444
46	$-1.2625636940 \times 10^{-15}$	
47	$4.1373846520 \times 10^{-16}$	2.7028928687
48	$-1.3536187010 \times 10^{-16}$	
49	$4.4340363840 \times 10^{-17}$	2.7056419158
50	$-1.4511035420 \times 10^{-17}$	
51	$4.7522986580 \times 10^{-18}$	2.7081713766
52	$-1.5555245880 \times 10^{-18}$	
53	$5.0936147060 \times 10^{-19}$	2.7105007206
54	$-1.6674076830 \times 10^{-19}$	
∞	0	2.7608973951

Table 16: Fourth and fifth real chromatic zeros for a strip $11_F \times n_F$ with free boundary conditions. As the third zero converges rapidly to B_5 , we show their difference. The last row (labelled with $n = \infty$) shows the infinite-length limit; in particular, the value of $q_0(11)$.

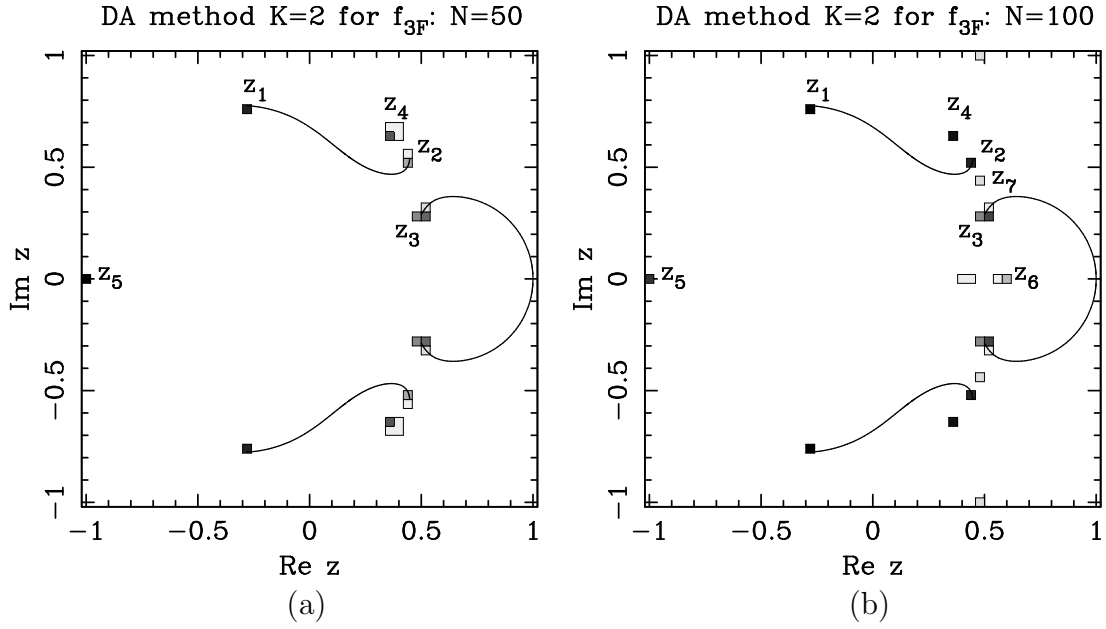


Figure 1: Histograms of the non-defective zeros for the square lattice strip of width $L = 3_F$ using $K = 2$ differential approximants with $N = 50$ (a) and $N = 100$ (b) coefficients of the free-energy series expansion. Each cell is a square of size 0.04, and the bin count is indicated with a gray-scale code: there are 16 gray tones ranging from black (largest counts) to white (smallest counts). We also show the limiting curve \mathcal{B}_{3_F} .

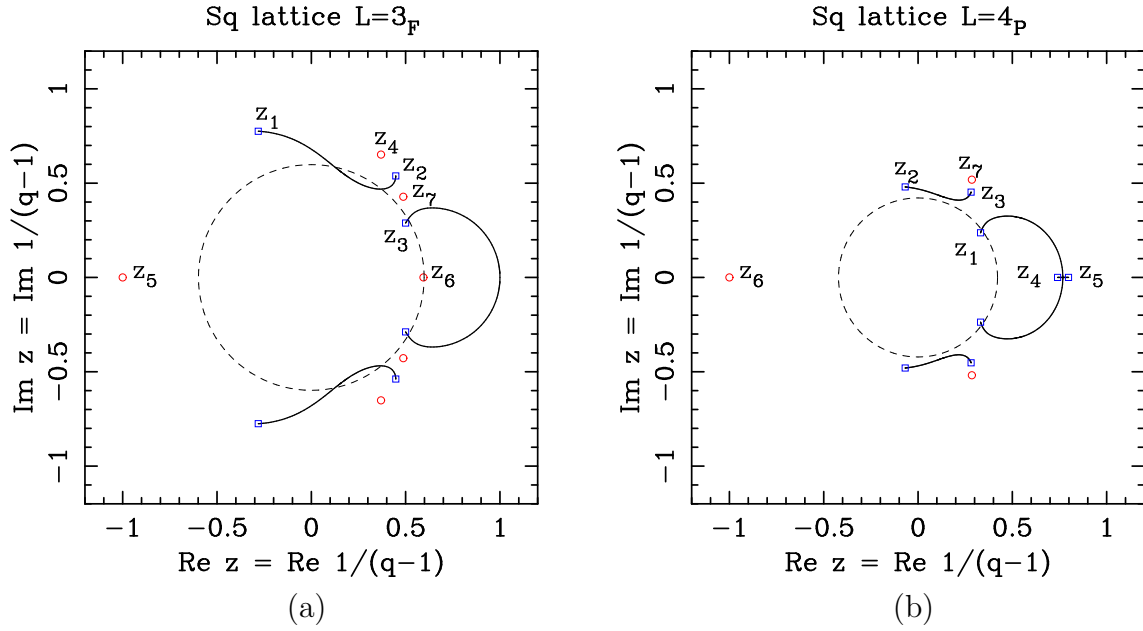


Figure 2: Plot of the limiting curves for the square-lattice strips of widths 3_F (a) and 4_P (b) in the complex $z = 1/(q-1)$ plane. We also show the location of the physical singularities (i.e., the endpoints of the limiting curve, depicted in blue \square) and of the spurious ones (red \circ). The dashed line shows the circle with the radius of convergence obtained by a raw fit using $r_{\text{conv}} = \liminf_{n \rightarrow \infty} |a_n|^{-1/n}$. The point labels correspond to those of the tables.

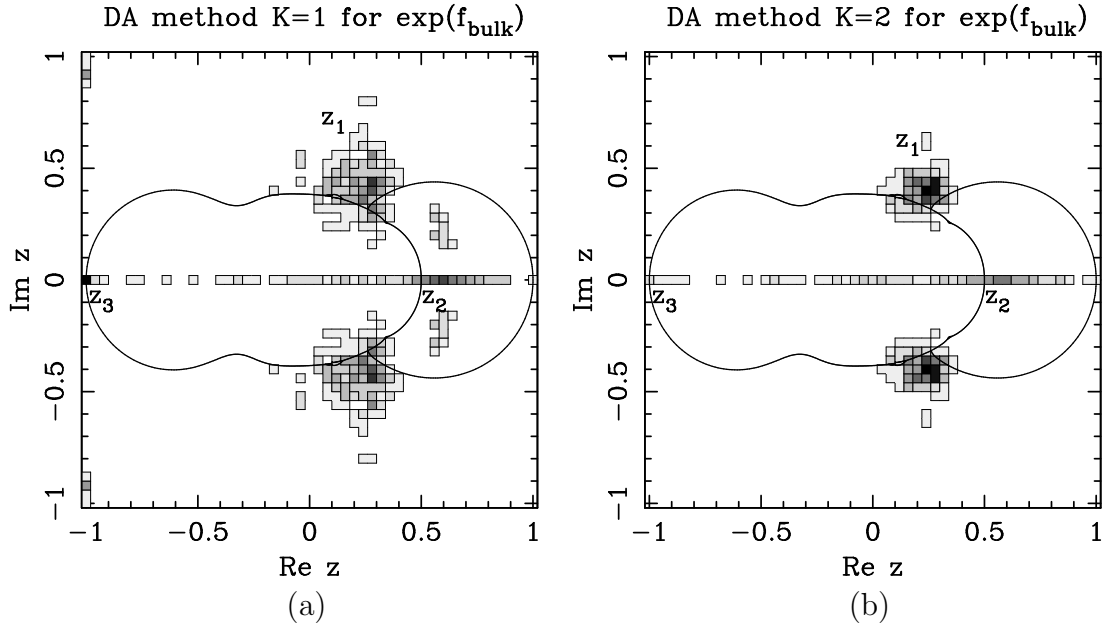


Figure 3: Histograms of the non-defective zeros for the bulk-free-energy series (5.23) using $K = 1$ (a) and $K = 2$ (b) differential approximants with $N = 47$ coefficients. Gray-scale codes are as in Figure 1. For comparison, we show the limiting curve \mathcal{B}_m for the square-lattice strip of width $m = 7$ with toroidal boundary conditions [10].

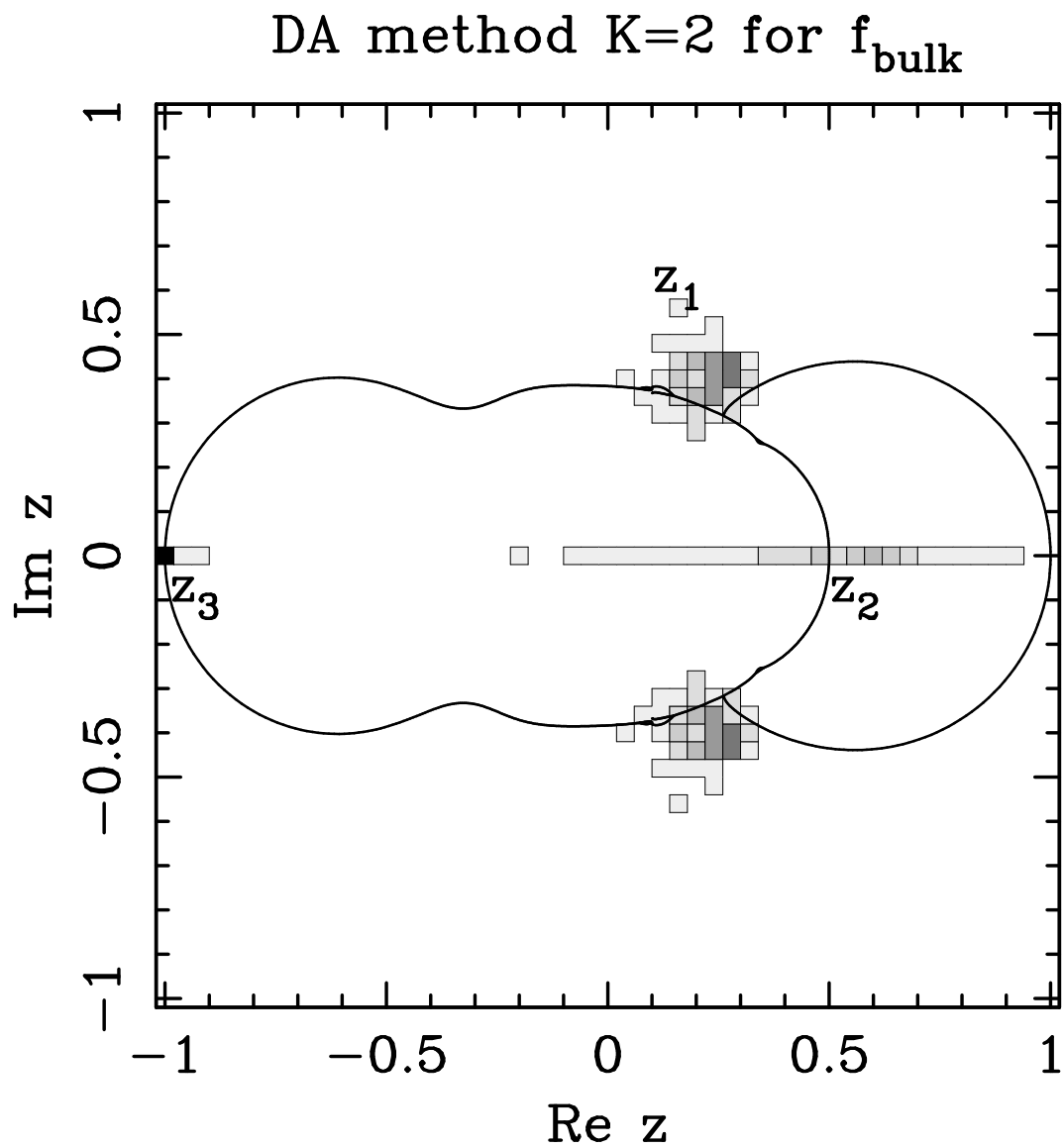


Figure 4: Histogram of the non-defective zeros for the unexponentiated bulk-free-energy series (5.25) using $K = 2$ differential approximants with $N = 47$ coefficients.

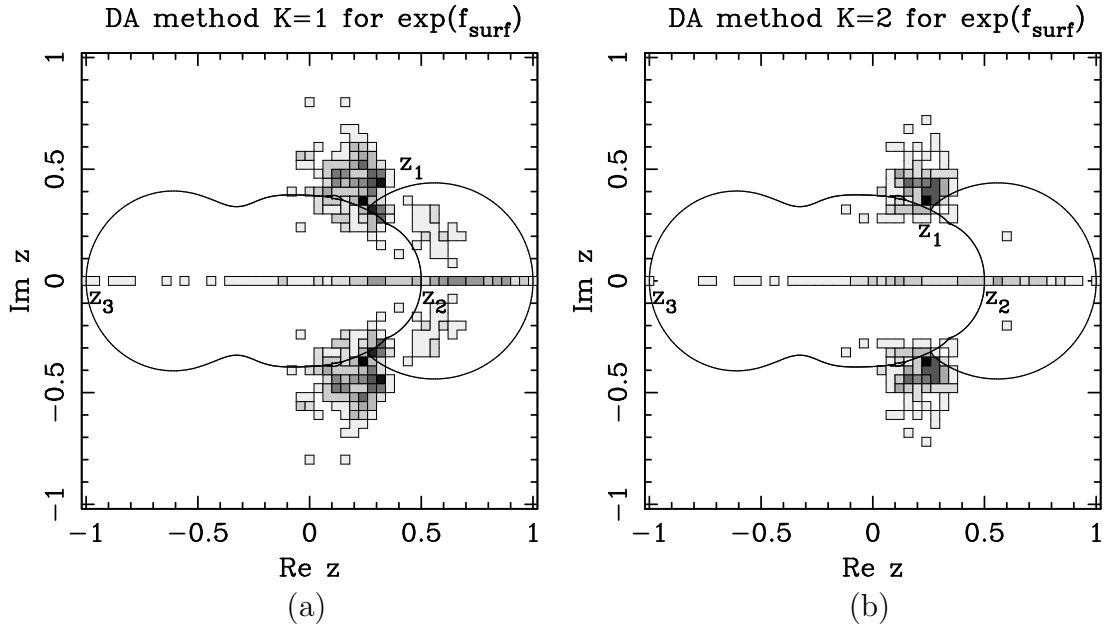


Figure 5: Histograms of the non-defective zeros for the surface-free-energy series (5.33) using $K = 1$ (a) and $K = 2$ (b) differential approximants with $N = 47$ coefficients. Codes are as in Figure 1. We show the limiting curve \mathcal{B}_m for the square-lattice strip of width $L = 11$ with toroidal boundary conditions as a solid black curve.

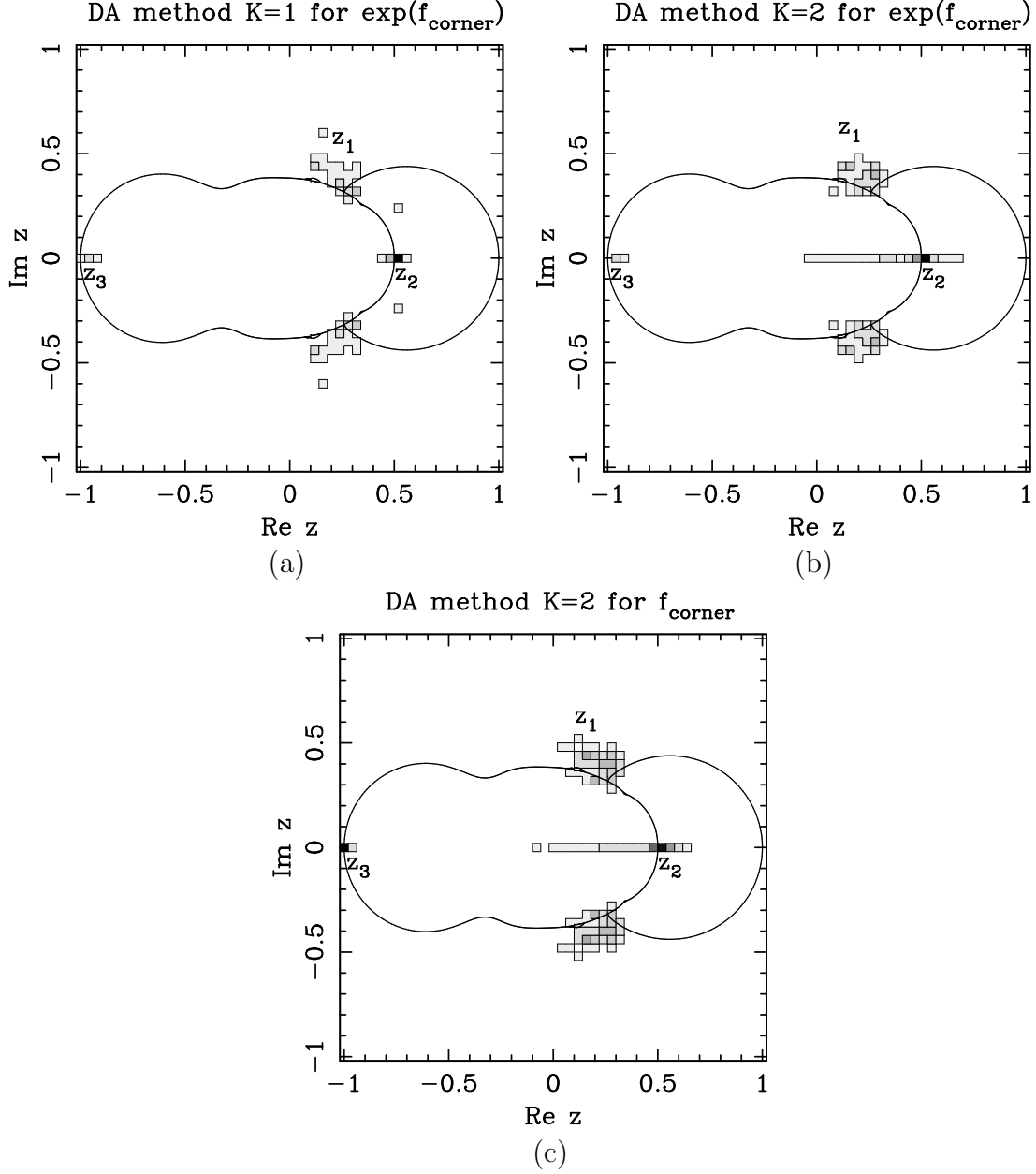


Figure 6: Histograms of the non-defective zeros for the corner-free-energy series (5.32) using $K = 1$ (a) and $K = 2$ (b) differential approximants with $N = 46$ coefficients. Panel (c) shows the analogous $K = 2$ histogram for the unexponentiated series (5.34). Codes are as in Figure 1. We show the limiting curve \mathcal{B}_m for the square-lattice strip of width $L = 11$ with toroidal boundary conditions as a solid black curve.

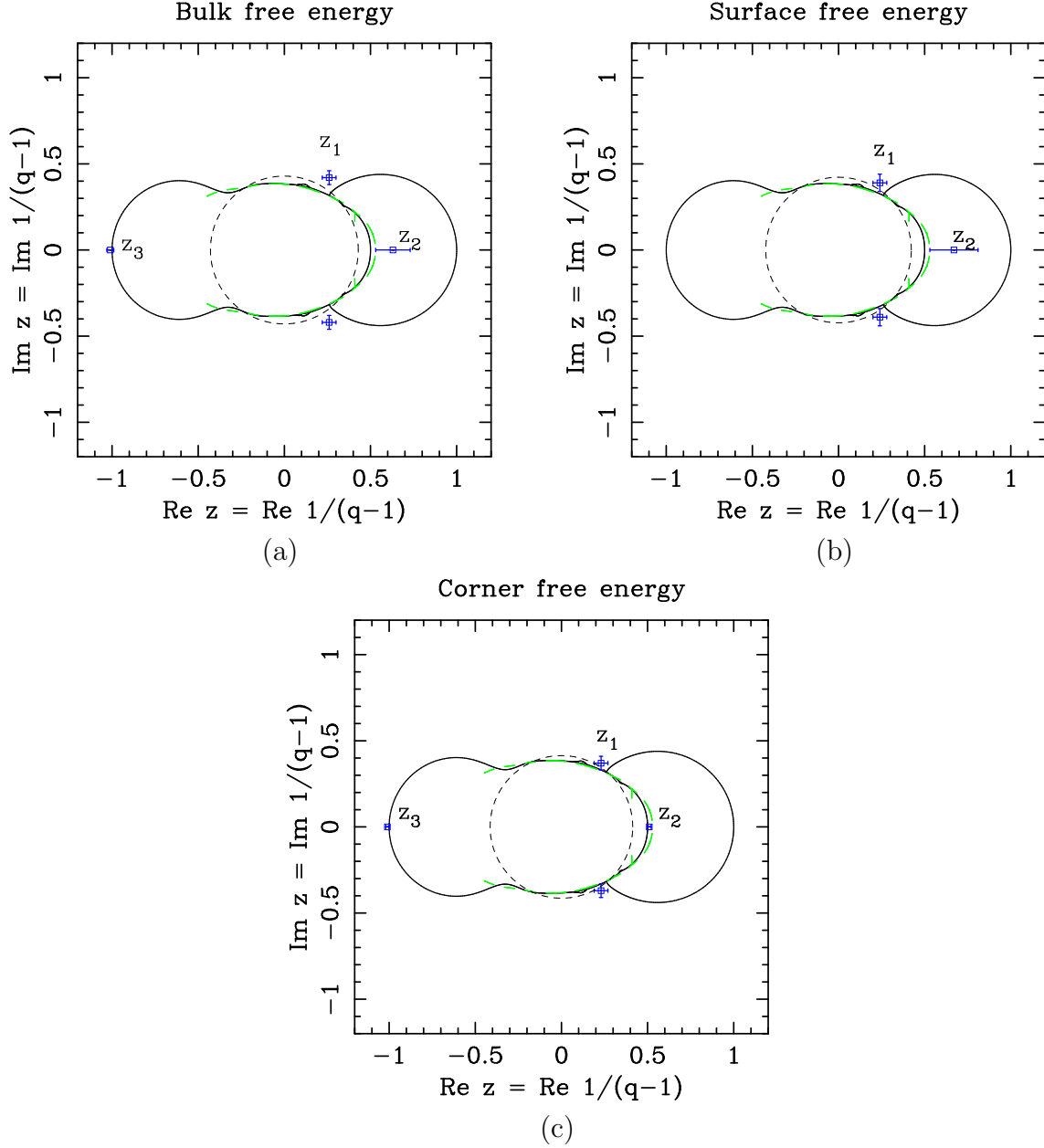


Figure 7: Singularities for the bulk (a), surface (b), and corner (c) free energies in the complex plane of $z = 1/(q-1)$. In each panel, we show the limiting curve \mathcal{B}_m for the square-lattice strip of width $L = 7$ (resp. $L = 11$) with toroidal (resp. cylindrical) boundary conditions as a solid black (resp. dashed green) curve. We also show the location of the singularities found in the series analysis (blue \square). The dashed black line shows the circle with the radius of convergence estimated from $r_{\text{conv}} = \liminf_{n \rightarrow \infty} |a_n|^{-1/n}$.

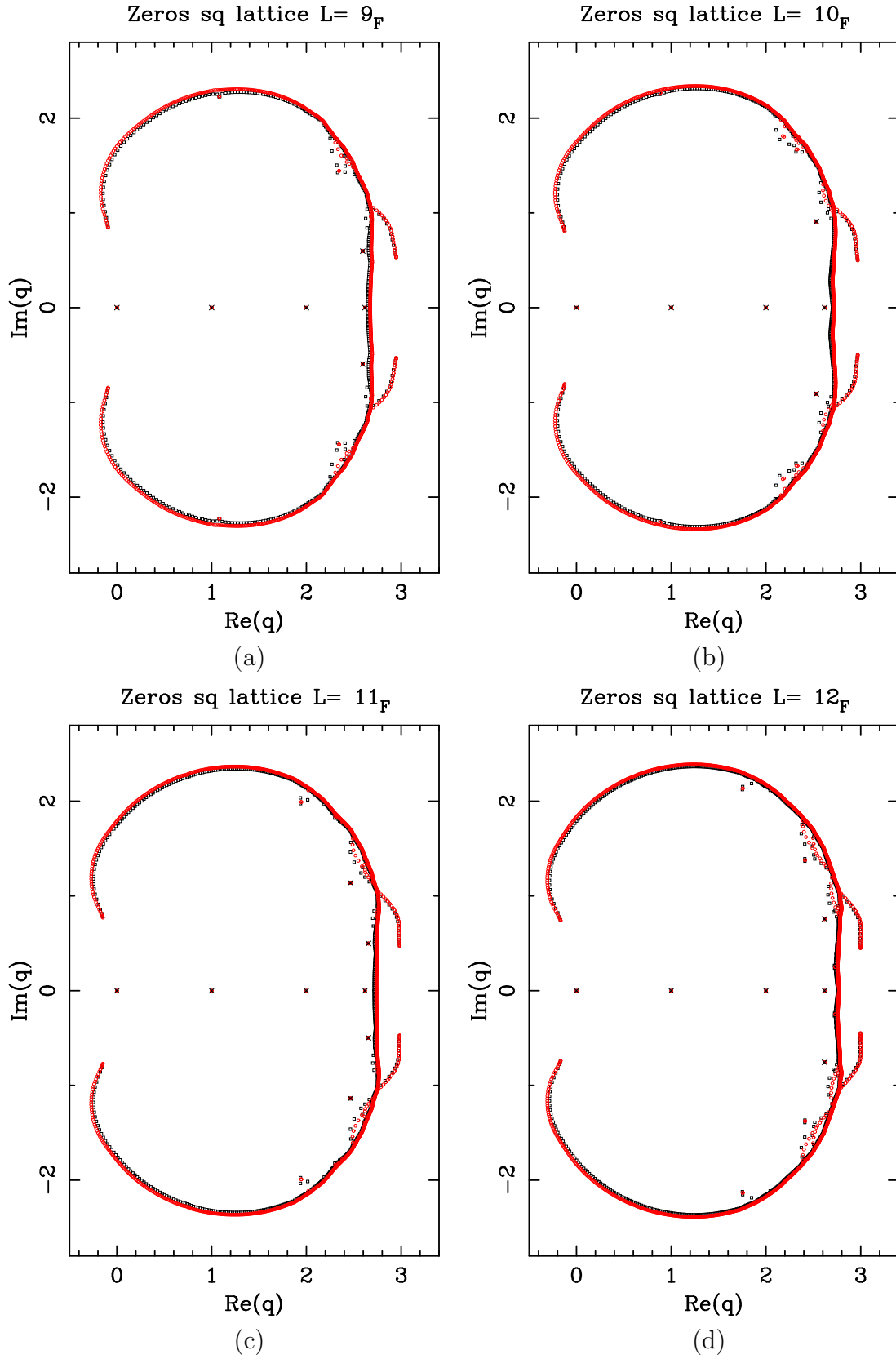


Figure 8: Zeros of the chromatic polynomial for the square lattices of widths 9_F (a), 10_F (b), 11_F (c), and 12_F (d). For each width L , we show the chromatic zeros of the strips $L_F \times (5L)_F$ (\square black) and $L_F \times (10L)_F$ (\circ red).